

# Chemical Reviews

Volume 93, Number 6

September/October 1993

## Nonequilibrium Thermodynamics of Electrokinetic Phenomena

R. P. Rastogi\* and R. C. Srivastava

*Department of Chemistry, Banaras Hindu University, Varanasi-221005, India*

S. N. Singh

*Department of Chemistry, Uda Pratap College, Varanasi, India*

*Received August 26, 1991 (Revised Manuscript Received April 19, 1993)*

### Contents

I. Introduction	1945
II. General Formalism	1947
A. Thermodynamic Formalism for Steady States in the Linear Region	1947
B. The Composite Membrane System	1950
C. Double-Layer Considerations	1951
D. The Frictional Formalism	1953
E. Relaxation Times	1954
F. Electrokinetic Energy Conversion	1956
III. Studies in the Linear Region	1958
A. Electroosmotic Studies	1958
B. Electroosmotic Effects in the Context of Water Desalination	1962
C. Studies on Soil Systems	1963
D. Studies on Biologically Relevant Systems	1964
1. Model Membrane and Related Systems	1964
2. Photoelectroosmosis	1966
3. Electroosmosis in Plant Physiology	1968
4. Electroosmosis in Animal Physiology	1970
5. Iontophoresis	1970
E. Electrophoretic Effects	1970
IV. Nonlinear Region Studies	1973
A. Nonlinear Flux Equations	1973
B. Ion-Exchange Membranes	1976
C. Studies on Soil Systems	1980
D. Studies on Systems of Biological Relevance	1980
V. Far-from-Equilibrium Region	1982
A. Electrokinetic Oscillations—Introductory	1982
B. Bistability	1982
C. Indications of Electrokinetic Mechanism in Cellular Excitability	1983
D. Teorell's Oscillator	1984
VI. Concluding Remarks and Future Projections	1986

VII. List of Symbols	1987
VIII. Acknowledgments	1987
IX. References	1987

### I. Introduction

The scientific study of equilibrium phenomena has attained a state of considerable maturity. Well-developed experimental procedures and unambiguous theoretical frameworks (equilibrium thermodynamics, statistical mechanics, quantum mechanics) permit a greater understanding of equilibrium phenomena. Consequently such phenomena are now well understood. However, in natural processes an equilibrium is the exception rather than the rule. Living systems and biological processes are typical examples of nonequilibrium phenomena. During the latter half of this century thanks to the contribution of people such as Onsager,<sup>5</sup> Meixner,<sup>6</sup> Casimir,<sup>7</sup> deGroot,<sup>8</sup> and Prigogine,<sup>9</sup> nonequilibrium thermodynamics has evolved as a discipline<sup>1-4</sup> for the treatment of nonequilibrium phenomena. It has proven most useful in the study of coupled phenomena in the steady state when the phenomenological relations between fluxes and forces are linear. In spite of its limitations, it has given new direction on how to go beyond the linear range as well as stimulated understanding of the far equilibrium region. New knowledge accumulated in this process has visibly influenced physics, chemistry, mathematics, applied sciences, engineering, and medicine. Dynamics and stability theory, together with the subservient role of the thermodynamics of irreversible processes has helped in exploring the far-from equilibrium region. It can be predicted that future developments in nonlinear dynamics will be far reaching.

\* Present address: Emeritus Scientist, Medicinal Chemistry Division (2nd floor), Central Drug Research Institute, Lucknow-226 001, India.



R. P. Rastogi (born 1926) received his doctorate degree in 1952 from the University of Lucknow where he started his career as a Lecturer in the Department of Chemistry. In 1959 he moved to Panjab University as a Reader. In 1962 he joined the University of Gorakhpur as Professor of Chemistry where continued until 1985. In 1985 he joined Banaras Hindu University as its Vice Chancellor, continued on there for full two terms and retired in April 1991. Currently he is a distinguished Emeritus Scientist of the Council of Scientific and Industrial Research and working at the Central Drug Research Institute Lucknow. Professor Rastogi's research interests include solution thermodynamics, thermodynamics of irreversible processes, combustion phenomenon, reactivity of solids, etc. His current involvement is the study of nonequilibrium processes in the far-from equilibrium region, oscillations and chaos, etc. He has authored more than 300 research papers, several books, and reviews and is the recipient of several national awards e.g. Khosla National Award, FICCI National Award, and Meghnad Saha National Award for excellence in research. He is a Fellow of The Indian National Science Academy.

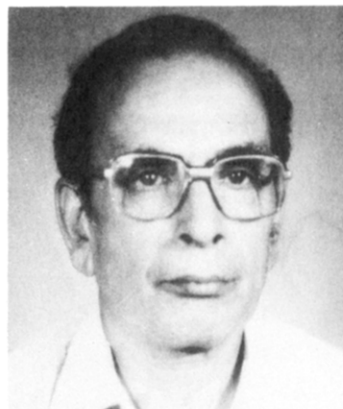
Electrokinetic phenomena are a good example of the study of the wider region of the nonequilibrium domain, due to the fact that they provide a variety of examples of nonequilibrium steady states which can be conveniently explored. Electrokinetic phenomena can be broadly classified under the following headings:

- (1) Electroosmotic phenomena: electroosmotic pressure and electroosmosis (electroosmotic efficiency).
- (2) Streaming phenomena: streaming current and streaming potential.
- (3) Electrophoretic phenomena: electrophoresis.
- (4) Sedimentation phenomena: sedimentation potential and sedimentation current.

Furthermore, in the case of such phenomena we are dealing with an open system (as far as the chambers separated by the membranes are concerned) such as a continuously stirred tank chemical reactor (CSTR). Just as in the case of chemical reactors, the system can be maintained at a definite distance from the equilibrium; in the same manner, electrokinetic systems can also be maintained at a definite distance from equilibrium by controlling the magnitude of the forces or fluxes. Thus, the stability of steady states in the near equilibrium and in the far equilibrium regions can be investigated. In fact dynamic instability in the form of bistability and oscillations is also observed in nonlinear situations.

Electrokinetic phenomena particularly electroosmotic phenomena provide a very wide spectrum of nonequilibrium regions which are easily accessible experimentally and hence one can expect that these may provide a good basis for deeper understanding of exotic phenomena in the far-from equilibrium region.

As the name implies, in the linear domain of nonequilibrium thermodynamics, linear equations of



R. C. Srivastava (born 1935) is one of Professor R. P. Rastogi's first students. For his doctoral studies he joined the group of Professor Rastogi in 1958 and received his Ph.D. degree in chemistry from Panjab University in 1962. From 1963 to 1965 he worked as Lecturer in the National Council of Educational Research and Training and from 1965 to 1969 as an Associate Professor of Physical Chemistry at the Panjab Agricultural University. In 1969 he joined the Harcourt Butler Technological Institute Kanpur as Professor of Chemistry and worked there until 1974. In 1974 he shifted to The Birla Institute of Technology and Science Pilani as Professor of Chemistry and continued there until 1989. In February 1989 he was invited by the Banaras Hindu University to join as Professor of Physical Chemistry in the Department of Chemistry where he is presently. Professor Srivastava's main area of research has been nonequilibrium thermodynamics and membrane transport. He has published more than 100 research papers, three reviews, and one monograph. His current interest is in the area of liquid membranes in the context of biological action. In 1986 he was awarded the prestigious Ranbaxy Research Award in Pharmaceutical Sciences for his outstanding contributions to the role of liquid membrane phenomenon in drug action. Professor Srivastava is a Fellow of The National Academy of Sciences India.



S. N. Singh (born 1945) received his M.Sc. degree in 1966 and worked in the group of Prof. R. P. Rastogi for his Ph.D. degree, which he received in 1969 from Gorakhpur University. He has worked on electroosmotic transport in anisotropic membranes which continues to be his current interest. He joined Udia Pratap College, Varanasi, in 1970 where he is presently occupying the position of Reader in Chemistry.

motion (phenomenological relations between fluxes and forces) are considered, and the Gibbs' entropy equation, which is utilized to make the proper choice of the conjugate pairs of fluxes and forces, and the Onsager's reciprocal relations are obeyed. Since the domain of validity for Gibbs' equation is larger than those for both linear phenomenological relations and Onsager's relations<sup>4,10</sup> attempts have been made to explore the nonlinear region by considering nonlinear relationships between fluxes and forces which of course are chosen using the Gibbs entropy equation. Thus, this nonlinear

region is certainly within the domain of validity for the Gibbs equation. Thus we have far-from-equilibrium regions where the linear thermodynamics of irreversible processes is no longer applicable. In this region, we observe exotic phenomena of dynamic instability.<sup>11-13</sup> It may be noted that this division is not a clearcut one. Some nonlinear systems may be very far from the equilibrium (for example when they have high dissipation) without being unstable, and some may have instabilities and/or multiple steady states as soon as the first nonlinearity appears.

The purpose of this article is to review the experimental and theoretical studies on electrokinetic phenomena in (1) the near-equilibrium linear range (2) the beyond linear range but within the domain of validity of the Gibbs equation, and (3) the nonlinear region beyond the validity of the Gibbs equation and (4) the far-from-equilibrium region. In the context of linear thermodynamics of irreversible processes, the emphasis would be on (a) the verification of linear phenomenological relations, (b) the verification of Onsager's reciprocal relation, (c) the test of steady-state relations, and (d) the approach to steady states. Experimental studies yielding nonlinear flux equations for 2 are also examined. Bistability and electrokinetic oscillations are discussed including (i) the nature of stability, (ii) the locus of steady states, (iii) the approach to equilibrium/steady states, as indicated in Figure 1.

A second objective of this review is to consolidate studies on electrokinetic phenomena in soil-water systems, plant-water systems, and systems of biological and physiological relevance.

## II. General Formalism

### A. Thermodynamic Formalism for Steady States in the Linear Region

As an example we shall consider electroosmotic and streaming phenomena as represented in Figure 2. Let us consider the isothermal case. The pressure, concentration, and potentials are different in the two chambers. Accordingly there is a volume flow of solvent,  $J_v$ , a flow of current,  $I$  and a flow of solute,  $J_s$ , which can be coupled. Just as in continuously stirred tank reactor (CSTR), one can keep the reaction system at a fixed level from equilibrium by controlling the flow rate; similarly an external electrical current can act as a bifurcating parameter for an electrokinetic system such as Teorell's oscillator.<sup>14,15</sup> An additional advantage in the case of the electrokinetic system is that we can easily move from the equilibrium state to the far-from-equilibrium state by systematically increasing the magnitude of the pressure difference, the potential difference or the concentration difference between the two chambers.

In the system described in Figure 2 the forces are the pressure difference,  $\Delta P$ , the potential difference,  $\Delta\phi$ , and the concentration difference  $\Delta C$ . By following the usual procedure described in the standard texts<sup>16</sup> on nonequilibrium thermodynamics, the linear phenomenological equations for the simultaneous flow of matter and current can be written as<sup>17</sup> in eqs 1-3. (For a detailed derivation see ref 17.)

$$J_v = L_{11}(\Delta P - \Delta\Pi) + L_{12}\Delta\phi + L_{13}(\Delta\Pi_s/\bar{C}_s) \quad (1)$$

$$I = L_{21}(\Delta P - \Delta\Pi) + L_{22}\Delta\phi + L_{23}(\Delta\Pi_s/\bar{C}_s) \quad (2)$$

$$J_s = L_{31}(\Delta P - \Delta\Pi) + L_{32}\Delta\phi + L_{33}(\Delta\Pi_s/\bar{C}_s) \quad (3)$$

since, the entropy production  $\sigma$  is given by

$$T\sigma = J_v(\Delta P - \Delta\Pi) + I\Delta\phi + J_s(\Delta\Pi_s/\bar{C}_s) \quad (4)$$

where  $\bar{C}_s = (C_2 - C_1)/\ln(C_2/C_1)$  and  $C_2 > C_1$ . Furthermore,

$$\Delta\Pi = \text{osmotic pressure difference} = RT\Delta C \quad (5)$$

In the linear range of the thermodynamics of irreversible processes, Onsager's reciprocity relation exists between the cross phenomenological coefficient  $L_{ik}$  so that

$$L_{12} = L_{21} \quad L_{31} = L_{13} \quad L_{23} = L_{32} \quad (6)$$

Equation 4 follows from the basic equation for the entropy production. When we consider the solutes of the electrolyte,

$$T\sigma = J_1\Delta\mu_1 + J_2\Delta\mu_2 + J_w\Delta\mu_w \quad (7)$$

where  $\mu_1$  and  $\mu_2$  are the electrochemical potentials of cation and anion denoted by subscripts 1 and 2, respectively,  $J_1$  and  $J_2$  are the corresponding flows,  $J_w$  is the flow of the solvent water denoted by the subscript  $w$  and  $\mu_w$  is the chemical potential of water. Equation 7 can be transformed into a more general form (eq 8) to include the case of nonelectrolytes as well, i.e.

$$T\sigma = J_s\Delta\mu_s + J_w\Delta\mu_w + I\Delta\phi \quad (8)$$

and finally to eq 4. In deriving eq 7, 8, and 4 the following relations have been used:

$$\Delta\Pi = \Delta\Pi_s + \Delta\Pi_i \quad (9)$$

$$\Delta\mu_w = \bar{V}_w(\Delta P - \Delta\Pi) \quad (10)$$

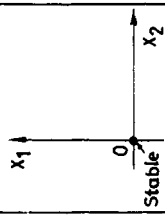
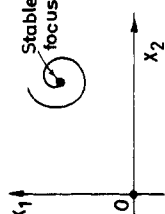
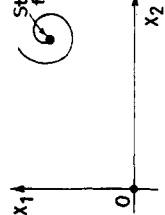
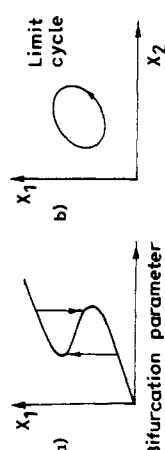
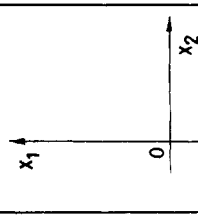
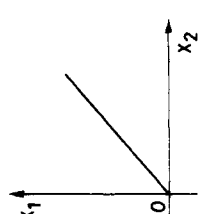
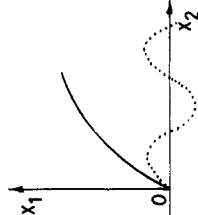
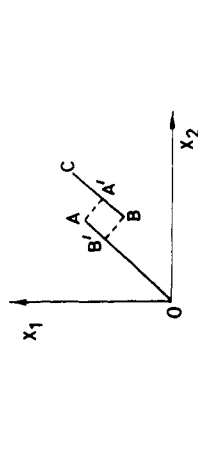
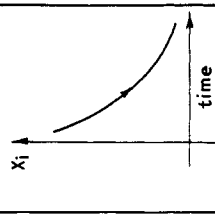
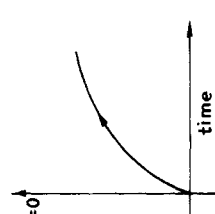
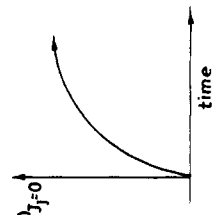
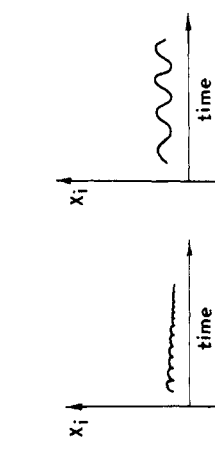
$$\Delta\mu_s = \bar{V}_s\Delta P + (\Delta\Pi_s/\bar{C}_s) \quad (11)$$

where  $\bar{V}_w$  and  $\bar{V}_s$  are the partial molar specific volumes of water and solute, respectively. Furthermore,  $\Delta\Pi_s$  is the osmotic pressure difference of the permeable solute and  $\Delta\Pi_i$  the osmotic pressure of the impermeable solute. In fact  $\Delta\Pi_s/\bar{C}_s$  is better represented by

$$(\Delta\Pi_s/\bar{C}_s) = RT\Delta(\ln a_s) \quad (12)$$

where  $a_s$  is the activity of the solute which, for simplicity, can be equated to the concentration.

A more rigorous derivation of entropy production has been attempted by a number of workers particularly from the point of view of (a) the frame of reference and (b) the local formulation of irreversible thermodynamics. The frame of reference for membranes can be (1) the local center of mass, (2) the local center of volume, (3) any of the individual components of the system, in particular the solvent, or (4) the membrane. It is obvious that for membrane transport, the most convenient frame of reference is the membrane itself. This is possible when the radii of the pores of the membrane are larger when compared to the mean free path of the permeating molecules. Whatever the nature of the reference frame, it is desirable that Onsager's symmetry in the local phenomenological coefficients be preserved. It has been shown that this is so when the gradients across the membranes are all linear.<sup>1</sup> However, Kirkwood et al.<sup>18</sup> claimed that in certain circumstances, transforming the reference frame to the walls of the

Non - Equilibrium				
State Characteristics	Equilibrium	Near Equilibrium	Non - Linear	Complex Non-Equilibrium
Magnitude of force $X_i$ and of flux $J_i$	$X_i = 0$ $J_i = 0$	$X_i \neq 0$ linear $X_j \neq 0$ relations (But magnitude small) $J_i = \sum L_{ik} x_k$ ; $L_{ik} = L_{ki}$	$X_i \neq 0$ Non-linear $X_j \neq 0$ relations (Magnitudes larger) $J_i = \sum L_{ik} x_k + \sum L_{ijk} x_k x_j$	$X_i \neq 0$ $L_{ik}$ , $J_{ik}$ $X_j \neq 0$ function of $X_k \neq 0$ flows and time
Nature of Stability	Equilibrium point is the stable focus 	Steady state away from equilibrium is the focus 	Steady states still further away from equilibrium 	Multiple steady states, undamped, hysteresis and damped oscillation 
Locus of Steady states				
Approach to equilibrium/steady states		$(X_i)_{J_i=0}$ 	$(X_i)_{J_i=0}$ 	

- (1) Stability in the Linear range ( $\Delta P$ ,  $\Delta \phi$ ,  $\Delta C \rightarrow 0$ )  $J_i = \sum L_{ik} x_k$   
 (2) Stability in the non-linear range also :  $J_i = \sum L_{ik} x_k + \sum L_{ijk} x_k x_j$   
 (3) Complex non-linear range ;  $L_{22}$ ,  $L_{11}$  straight coefficient also function of flows.  $\Delta P$ ,  $\Delta \phi$  and  $\Delta C$  (three forces):

a) Non-linear function of these forces.

b) Straight coefficient function of these forces.

Figure 1. Scenario of nonequilibrium region.

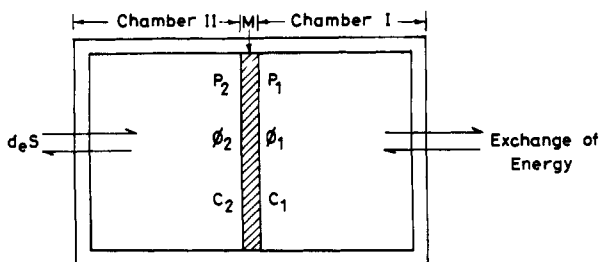


**Figure 2.** Schematic representation of the electrokinetic system. The figure is labeled as follows:  $\phi$  = potential;  $C$  = concentration, subscript 1 and 2 represent chambers I and II, respectively;  $M$  = membrane.

container does not result in symmetrical coefficients. On the other hand Schlögl<sup>19</sup> showed that the symmetry is preserved when (a) the fluid is homogeneous over the pore cross section and (b) the electrical space charge per unit volume of fluid is constant over the pore cross section. Again the treatment by Kobatake and Fujita<sup>20</sup> shows that the local phenomenological equations relating to a streamline within a pore are not symmetrical when referred to a membrane. However, Mikulecky and Caplan<sup>21</sup> removed this discrepancy by a correct averaging procedure involving the use of average flows over the plane of membrane which avoids the problem of velocity gradient.

When we disregard the possibility of chemical reaction, the local entropy production  $\sigma$  at any point within the membrane in the notation of de Groot and Mazur<sup>1</sup> is given by

$$T\sigma = -\sum_{k=1}^{n-1} \mathbf{J}_k \cdot [\{\text{grad}(\mu_k - \mu_n)\}_T - \mathbf{F}_k + \mathbf{F}_n] - \tilde{\Pi} : \text{grad } \mathbf{V} + 2\mathbf{P}^a \omega \quad (13)$$

where  $n$  represents the number of components present including the membrane. The  $\mathbf{J}_k$  are the flows relative to the local center of mass,  $\mathbf{v}$  is the barycentric velocity, and  $\mu_k$  and  $\mathbf{F}_k$  are, respectively, the chemical potential of the  $k$ th component and the external force acting on it. With the correct substitution eq 13 reduces to

$$T\sigma = -\sum_{k=1}^{n-1} \mathbf{J}_k^m \cdot (\text{grad } \tilde{\mu}_k)_T + \mathbf{v} \cdot \text{grad } p - \sum_{k=1}^n \rho_k \mathbf{F}_k \cdot \mathbf{v} - \tilde{\Pi} : \text{grad } \mathbf{v} + 2\mathbf{P}^a \omega \quad (14)$$

where

$$(\text{grad } \tilde{\mu}_k)_T = (\text{grad } \mu_k)_T - \mathbf{F}_k \quad (15)$$

$$\mathbf{J}_k^m = \mathbf{J}_k + \rho_k \mathbf{v} = \text{flows relative to membrane} \quad (16)$$

where  $\rho_k$  denotes the mass per unit volume of component  $k$  and

$$\sum_{k=1}^n \rho_k (\text{grad } \mu_k)_T = \text{grad } p \quad (17)$$

It has to be noted that the membrane does not move. Furthermore,  $\tilde{\Pi}$  stands for the transposed viscous pressure tensor.  $\mathbf{P}^a$ , the axial vector representing the antisymmetrical part of the total pressure tensor  $\mathbf{P}$ , and  $\omega$ , mean angular velocity of the constituent particles. If  $\phi = T\sigma$  which we may call the dissipation function, the average local dissipation function at a depth  $x$  within the membrane,  $\bar{\phi}_x$  is given by

$$\bar{\phi}_x = (1/V) \int_V \phi_{x,y,z} d\tau \quad (18)$$

where  $d\tau$  is the volume element in the slab:

$$d\tau = v_x \cdot dA \quad (19)$$

Noting that

$$\mathbf{J}_k^m = (1/A) \int_A \mathbf{J}_k^m dA \quad (20)$$

$A$  being the area of cross section of the membrane, so that

$$\bar{\phi}_x = -\sum_{k=1}^{n-1} \mathbf{J}_k^m \cdot (\text{grad } \tilde{\mu}_k)_T \quad (21)$$

and is equivalent to eq 7. In deriving eq 21 different tensorial orders of forces and flows have been ignored since these cannot couple among themselves. Hence, the tensorial character of the pressure as such will not complicate the thermodynamics of the flow processes in the electrokinetic experiments.

One may start with the following expression for  $\mathbf{J}_k$ , the diffusional flows of ions (relative to the local center of mass) along any streamline,

$$\mathbf{J}_k = -\sum_{i=1}^2 L_{ki} (\partial \tilde{\mu}_i / \partial x) = -\sum_{i=1}^i L_{ki} [e_i (\partial \psi / \partial x) + v_i (\partial p / \partial x) + \partial \mu_i^c / \partial x] \quad (22)$$

where  $k$  and  $i$  represent either the cation or anion (1 or 2 respectively),  $\partial \psi / \partial x$  is the potential gradient at any point,  $e_i$  is the specific charge of the species  $i$ ,  $\mu_i^c$  is the concentration-dependent part of the electrochemical potential  $\tilde{\mu}_i$ —the partial specific Gibbs free energy of the species  $i$ , and  $v_i$  is the partial specific volume of species  $i$ . After suitable transformation and noting that

$$\mathbf{I} = e_1 \mathbf{J}_1 + e_2 \mathbf{J}_2 \quad (23)$$

one can write the corresponding expression for  $\mathbf{I}$  also.

Caplan and Mikulecky<sup>21</sup> show that these equations can be easily transformed into the following form after some work:

$$\mathbf{J}_s^m = -[\bar{\alpha}_{11} + a^2 \rho_s^2 / 8\eta] (\partial \mu_s^c / \partial x) - [\bar{\alpha}_{12} + (\epsilon \zeta \rho_s / 2\pi a^2)] (\partial \psi / \partial x) - [a^2 \rho_s / 8\eta] [\partial (p - \nu R T \rho_s / M_s) / \partial x] \quad (24)$$

$$\bar{\mathbf{I}}_m = -[\bar{\alpha}_{21} + (\epsilon \zeta \rho_s / 2\pi a^2)] (\partial \mu_s^c / \partial x) - [\bar{\alpha}_{22} - (\epsilon / 2\pi a^2)] (x/2) (\partial \psi / \partial x) - [\epsilon \zeta / 2\pi a^2] [\partial (p - \nu R T \rho_s / M_s) / \partial x] \quad (25)$$

$$\bar{\nabla} = -[a^2 \rho_s / 8\eta] (\partial \mu_s^c / \partial x) - [\epsilon \zeta / 2\pi a^2] (\partial \psi / \partial x) - [a^2 / 8\eta] [\partial (p - \nu R T \rho_s / M_s) / \partial x] \quad (26)$$

so that the Onsager's reciprocity relation is satisfied, where

$$\epsilon \zeta / 2\pi a^2 = \frac{B}{\rho_s^{1/2}} \text{ and } B = -(\sigma e / \eta) (\epsilon k t / 4\pi |e_1| |e_2|)^{1/2}$$

and  $\rho_s$  is the salt concentration. In eq 26  $\bar{\nabla}$  is the average barycentric velocity. It follows that the cross coefficients depend on the salt concentration and these can superimpose nonlinearity in a complex manner since the integrals cannot be correctly evaluated. The above relations are based on a solution obtained through simplified assumptions.

In addition to Caplan and Mikulecky's critical account<sup>21</sup> of linear thermodynamics of transport processes, readers are encouraged to also consult the recent review by Boronowski.<sup>22</sup> Juo et al.<sup>23</sup> and Castillo et al.<sup>24</sup> have also attempted to extend nonequilibrium thermodynamics to membrane transport.

In order to have a formal understanding of steady states in electrokinetic phenomena, let us consider the case where there are no concentration differences i.e.  $\Delta C = 0$ . Following the usual procedure the linear phenomenological equations for the simultaneous flow of matter and electricity are written as<sup>1-4,16</sup>

$$\mathbf{J}_v = L_{11}\Delta P + L_{12}\Delta\phi \quad (27)$$

$$\mathbf{I} = L_{21}\Delta P + L_{22}\Delta\phi \quad (28)$$

where  $\mathbf{I}$  and  $\mathbf{J}_v$  are the flow of electricity and matter (volume flow) respectively,  $\Delta\phi$  and  $\Delta P$  are the electrical potential and pressure differences, respectively, and  $L_{ik}$  are the phenomenological coefficients. Since the electroosmotic systems are isothermal in nature, the coefficients  $L_{ik}$ , which are independent of the magnitude of the thermodynamic forces,  $\Delta\phi$  and  $\Delta P$ , in the linear region, are expected to be temperature sensitive. The equality (eq 29) i.e.

$$L_{12} = L_{21} \quad (29)$$

takes into account of Onsager's theorem and the inequality  $L_{11}L_{22} > L_{12}L_{21}$  holds on account of the definite positive character of entropy production. Steady states would be obtained, when any of the variables  $\mathbf{J}_v$ ,  $\mathbf{I}$ ,  $\Delta P$ , or  $\Delta\phi$  attain zero value.

According to Prigogine's theorem<sup>1-4</sup> in which the linear region stationary states are the states of minimum entropy production, the equation for entropy production  $\sigma$ , in the linear region, is given by the equation

$$\sigma = \mathbf{I}\Delta\phi + \mathbf{J}_v\Delta P = L_{11}(\Delta P)^2 + (L_{12} + L_{21})\Delta P\Delta\phi + L_{22}(\Delta\phi)^2 \quad (30)$$

If we represent  $\Delta P$ ,  $\Delta\phi$ , and  $\sigma$  on the rectangular coordinate axes as  $x$ ,  $y$ , and  $z$ , respectively, eq 30 would represent an elliptic paraboloid with vertex at  $\sigma = 0$ . The major and minor axes would be inclined to the axes of  $x$  and  $y$  by an angle  $\theta$  given by the equation,

$$\theta = (3\pi/2) + 1/2 \tan^{-1}(2L_{12}/L_{11} - L_{22}) \quad (31)$$

One can easily get a geometrical picture when the constraint  $\Delta P = \text{constant}$  is imposed on the system. The plane corresponding to  $\Delta P = \text{constant}$  would then intersect the paraboloid, and the section would be a parabola given by the equation

$$\sigma = L_{22}(\Delta\phi)^2 + B(\Delta\phi) + C \quad (32)$$

where  $B = 2L_{12}\Delta P$  and  $C = L_{11}(\Delta P)^2$ . The vertex of the parabola, which represents a new minimum in  $\sigma$  corresponds to the stationary state. It should be noted that a minimum in the value of  $\sigma$ , when no constraint is imposed, is nothing but the equilibrium state corresponding to  $\sigma = 0$ . The equilibrium state is known as the stationary state of zero order, whereas the state of  $(\sigma)_{\min}$  when one constraint is imposed on the system is called the stationary state of first order.

The coordinates of the vertex of the parabola represented by eq 32 are given by

$$\sigma_{\text{stat}} = [(\Delta P)^2(L_{11}L_{22} - L_{12}L_{21})]/L_{22} \quad (33)$$

and

$$\Delta\phi_{\text{stat}} = -(L_{21}/L_{22})\Delta P \quad (34)$$

which represent the values of these parameters in the stationary state. The latus rectum of the parabola would then be equal to  $1/L_{22}$ . Thus, there are two stationary states possible, consistent with the constraints  $\Delta P = \text{constant}$  and  $\Delta\phi = \text{constant}$ . When the variables are changed and similar constraints are imposed even then only two stationary states would be obtained.

Since, from a mathematical standpoint, it is entirely irrelevant which of the variables are called flows and which are called forces in the case of the  $\alpha$ -variables (unaffected by time reversal), it follows that any mathematical theorem deduced from eqs 27 and 28 will remain valid when the variables are interchanged. In simple terms, a similar exercise can be done by writing the phenomenological eqs 27 and 28 in the inverted matrix form. The values of different variables in the stationary states can be obtained by calculating the coordinates of the vertex of the parabola.<sup>25,26,29</sup>

On account of Onsager's reciprocal relations the following equations automatically follow from eqs 27 and 28:

$$(\Delta P/\Delta\phi)_{\mathbf{J}_v=0} = -(\mathbf{I}/\mathbf{J}_v)_{\Delta\phi=0} \quad (35)$$

$$(\Delta\phi/\Delta P)_{\mathbf{I}=0} = -(\mathbf{J}_v/\mathbf{I})_{\Delta P=0} \quad (36)$$

$$(\mathbf{J}/\Delta\phi)_{\Delta P=0} = (\mathbf{I}/\Delta P)_{\Delta\phi=0} \quad (37)$$

Equation 35 is the well-known Saxen's relation.<sup>27</sup> Although the Saxen's relation attracted the attention of thermodynamicists in 1951, Mazur and Overbeek<sup>28</sup> had already proved that they can be deduced in a general way from the phenomenological relations (eqs 27 and 28). The geometrical interpretation of the equation for the entropy production in the stationary state was suggested by Rastogi and Srivastava.<sup>29</sup> Another notable contribution to the early development of nonequilibrium thermodynamics of electrokinetic phenomena was that of Staverman and associates.<sup>30,31</sup>

A schematic arrangement for the measurements of parameters in the various stationary states is depicted in Figure 3, parts a-d.

A similar exercise can be carried out for the stationary states in electrophoretic phenomena.

## B. The Composite Membrane System

The linear phenomenological equations (eqs 27 and 28) are for a single membrane, and the coefficients  $L_{ik}$  are the various permeability coefficients for the system. It would be worthwhile to develop a similar formalism for complex membranes such as biological membranes. Biological membranes are composite structures and are built in an infinite number of ways from their constituent elements. Two tissues made from the same proportion of collagen, elastin, and ground substance may behave quite differently depending on how these basic elements are put together.<sup>32</sup> The urinary bladder is an example of transitional epithelial tissue which has elastic muscular walls and membranous folds.<sup>33</sup> It has been suggested that cells in urinary bladder

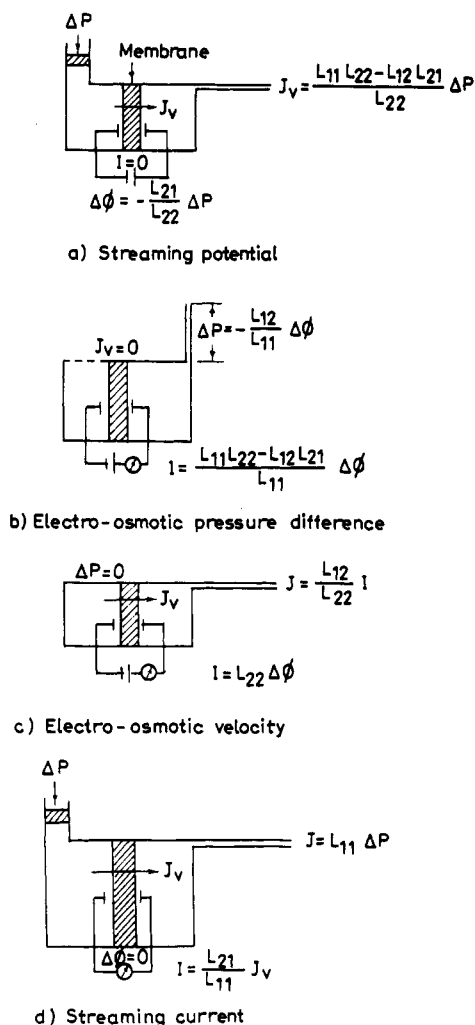


**Figure 3.** Schematic arrangements for the measurement of various steady-state effects.

membrane are essentially coupled in series<sup>34</sup> and the relation between cell length and bladder radius deviates from linearity at a very small bladder volume. A series membrane may be composed of a number of solid or liquid layers, some of these layers may be intermediate solutions.

Thus, composite membranes are complex systems in which the constituent membrane elements can be arranged in an infinite number of ways with regard to the nature of the constituent membrane elements, the fraction of the area covered by each element, and the geometrical array. However, these complex arrangements may be analyzed in terms of two fundamental cases viz. (a) the parallel membrane and (b) the series membrane. The theory of the permeability of the parallel composite membrane and the series composite membrane has been developed by Kedem and Katchalsky.<sup>17,35,36</sup>

Analysis of the permeability of parallel composite membranes<sup>35</sup> consisting of, say, two homogeneous constituent membrane elements is based on the following assumptions: (1) Linear phenomenological relations between fluxes and forces hold good for the parallel composite membrane as well as for the constituent membrane elements. (2) The flows are assumed to be parallel to the  $x$  coordinate, i.e. perpendicular to the membrane surface. (3) The driving forces are considered to be potential differences acting across the

membrane. (4) Since the same compartment maintains contact with both constituent membrane elements on each side of the membrane, the same forces that operate on the composite membrane are also operative on both the constituent membrane elements. This means that the forces are perpendicular to the membrane surface and that no lateral forces and hence no lateral flows creating internal circulation need to be taken into account. Thus, the total flow through the composite membrane is built up additively from their elementary contributions.

Similarly, analysis<sup>36</sup> of the permeability of a series composite membrane assumes that (1) the same flow passes by all the elements and the partial elementary flow equals the observable external flow, (2) all flows passing through the membrane are perpendicular to the membrane surface, (3) flows through the series composite membrane and also through the constituent membrane elements are adequately described by the linear phenomenological relations between fluxes and forces, and (4) the potentials of the thermodynamic driving forces are continuous across all boundaries in the system. This condition of continuity, first formulated by Kirkwood,<sup>37</sup> means that approaching any point  $x$  in the system from the right or the left leads to the same potential. The compelling reason for invoking this assumption is that if the transition layer between the two neighboring phases (e.g. the two constituent membrane elements) is infinitely thin its resistance to flow will be zero. If the potential difference across the transition layer does not vanish, infinite local flow will develop. What is implied, therefore, is that there cannot be a potential drop across the transition boundary within the series composite membrane. As a consequence of this assumption, the thermodynamic forces  $X^s$  acting across the series membrane are equal to the sum of the forces acting across the constituent membrane elements, i.e.

$$X^s = \sum X^i \quad (38)$$

In practice, however, it is likely that there will be a jump in potential at each membrane-solution and membrane-membrane interface because of the differences in the standard free energy and single ion activity coefficients of the individual ions in each phase and because of the fixed charges (Donnan potentials). Therefore, the last assumption leading to eq 38 would not necessarily be valid.

Since the assumptions made in the analysis of parallel and series membrane, have a striking similarity to the postulates of the network theory, the methods of network thermodynamics<sup>38,39</sup> have been utilized to construct equivalent electrical networks of the parallel and the series composite membranes.<sup>40</sup> The parallel and the series composite membranes, their schematic and network representation, and combination rules etc. are summarized in Figure 4. By using the combinations rules (Figure 4) it is possible to write the expressions for electroosmotic and streaming effects for the composite membrane in terms of the expressions for the constituent membrane elements.

### C. Double-Layer Considerations

Since the nonequilibrium thermodynamic derivation of electrokinetic effects does not make use of any model,



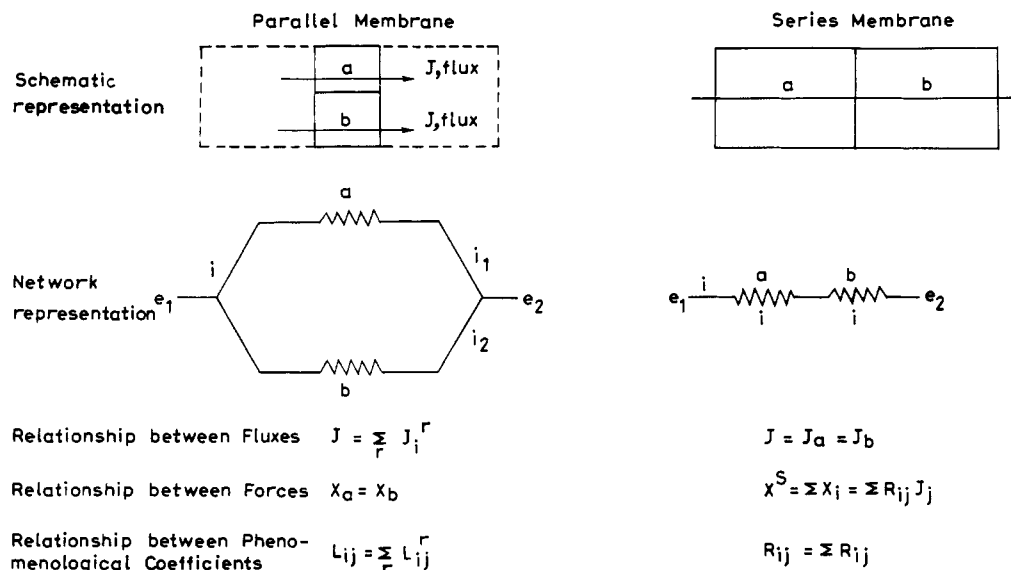


**Figure 4.** Schematic representation, network analogues, combination rules for phenomenological coefficients of parallel, and series composite membranes.

it is generally applicable. This generality however can be a serious limitation unless the phenomenological coefficients are translated in to mechanistic parameter terms. If this is not done the phenomenological coefficients remain mere coefficients or constants which will yield no information except in describing or predicting trends in the electrokinetic data. The traditional treatment of electrokinetic phenomena is based on a double-layer model first proposed by Helmholtz<sup>41</sup> and later modified by Gouy,<sup>42</sup> Chapman,<sup>43</sup> and Stern.<sup>44</sup> Comparing the expressions for various electroosmotic effects obtained from the double-layer theory, particularly the Helmholtz theory, with the corresponding expressions obtained from the nonequilibrium thermodynamic treatment, one can write<sup>25,45</sup>

$$L_{11} = n\pi r^4 / 8\eta l \quad (39)$$

$$L_{22} = n\pi r^2 k / l \quad (40)$$

$$L_{21} = n\epsilon r^2 \zeta / 4\eta l = L_{12} \quad (41)$$

In eqs 39–41,  $r$  is the radius and  $l$  the length of the capillary,  $\eta$  is the viscosity coefficient and  $\epsilon$  the dielectric constant of the liquid,  $k$  is the specific conductance of the liquid,  $n$  is the number of capillaries, and  $\zeta$  is the zeta potential. These equations can be similarly modified by considering modified versions of the double-layer theory. In fact it is the determination of the cross coefficients  $L_{12}$  and or  $L_{21}$  which is quite important in colloid chemistry because it leads to the determination of the zeta potential. Since the mechanism of electrokinetic phenomena involves a double layer it would be expected, *prima facie*, that nonconstancy of the phenomenological coefficients leading to nonlinear electrokinetic effects would be related to modifications in the structure of the double layer under the conditions responsible for the breakdown of linearity. Efforts made in that direction will be discussed later in this article when we come to the nonlinear region.

Sørensen and Koefoed<sup>46</sup> have theoretically dealt with electrokinetic effects in charged capillary tubes. They have developed reasonably general relationships for the electrokinetic phenomenological coefficients of volume

and charge transport through narrow tubes with steady laminar flow. The tubes were considered to be filled with uniform Newtonian electrolyte solutions and to carry a fixed charge per unit of inside surface area stemming from fixed ionizable groups. The electrokinetic phenomenological coefficients for such electrolyte-filled narrow tubes were calculated by solving the linearized Poisson–Boltzmann equation just as in the classical electrolyte theory of Debye and Hückel.<sup>47</sup> The expressions for the phenomenological coefficients found in this manner have been shown to fulfill Onsager's reciprocity relations in the whole range of values of the dimensionless radius of the tube, i.e. tube radius divided by the Debye–Hückel length. It has been shown that these coefficient expressions, in the limit of large pores, reduce to those in the classical formulae due to Helmholtz. In fact the fulfillment of the reciprocity relations is not the characteristic of any special charge distribution. Rather it originates from the general feature of the hydrodynamic and electrostatic differential equations and the boundary conditions. It has been shown that the treatment can be generalized to any arbitrary cross section with an arbitrary charge distribution. Sørensen and Koefoed's<sup>46</sup> treatment is more general and straightforward than the earlier treatments where either the radius of the tube is much larger than the thickness of the double layer<sup>48</sup> or the double-layer description is completely eliminated by use of the argument that the pore's radius is so small that the charge density in the electrolyte can be considered to be uniform in the whole pore.<sup>49–51</sup>

Rastogi et al.<sup>25,52</sup> have outlined a method for estimating the average pore's radius  $r$  of a membrane, using eqs 39 and 41:

$$r = \left( \frac{2\epsilon\zeta L_{11}}{\pi L_{12}} \right)^{1/2} \quad (42)$$

In classical physiology work described in the literature,<sup>53,54</sup> the pore's radius expressed in simple terms without corrections for steric hindrance and molecular sieving is given by



$$r = [8\eta L_{11}(1/A)_w]^{1/2} \quad (43)$$

where  $A$  is the pore area for the passage of water,  $w$ . Lakshminarayaniah<sup>55</sup> has commented on the use of eq 42 vis a vis eq 43 for estimating the value of the average pore's radius of a membrane. He considers eq 43 more convenient in comparison to eq 42 because the former requires three measurements, viz.  $L_{11}$ ,  $L_{12}$ , and  $\zeta$ , whereas eq 43 requires only two measurements, viz.  $L_{11}$  and  $(1/A)_w$ . In both cases the values of  $\epsilon$  and  $\eta$  for the pore liquid may be assumed to be equivalent for the bulk liquid although this may not be strictly true. In our opinion, this advantage is only marginal. Moreover, by implication, the term  $(1/A)_w$  in eq 43 contains  $r$  and hence the uncertainties associated with it. For a precise determination of  $r$  it would have been much better if the right-hand side of eq 43 did not contain a term in which  $r$  is implied. Thus, eq 42 in which  $n$  has been eliminated, using eqs 39 and 41, has this advantage.

As pointed out, Lakshminarayaniah has suggested that the zeta-potential values derived from electrophoretic measurements,<sup>56</sup> need not be substituted in eq 42. In fact the zeta-potential values to be used in eq 42 should be obtained from electroosmotic experiments (i.e. from  $L_{12}$ ). In classical work, however, it is considered that the electrophoretic velocity is equal to the velocity of electroosmosis both obeying the equation of Helmholtz-Smoluchowski.<sup>57</sup> Lakshminarayaniah has suggested<sup>55</sup> that hydrodynamic and electroosmotic permeability measurements alone are sufficient to derive a value of  $r$ . Using these considerations, he deduced a relationship equivalent to eq 43 for computing the value of  $r$ . The value of  $r$ , thus computed using eq 43 for the Pyrex sinter membrane, works out to be  $1.7 \times 10^{-5}$  cm which may be compared with the value of  $3 \times 10^{-4}$  cm obtained by Rastogi et al.<sup>58</sup> Since the zeta-potential values in colloid chemistry are only estimates and not the exact values, the qualitative agreement with regard to the order can be considered reasonable. Thus, eq 42 can be considered at least as reliable as Lakshminarayaniah's<sup>55</sup> for the estimation of average pore size of membranes.

## D. The Frictional Formalism

Comparing the expressions for electrokinetic effects obtained from the nonequilibrium thermodynamic treatment with the corresponding expressions from the consideration of the double-layer model is one way of assigning physical meaning to various phenomenological coefficients. The other notable attempt to interpret the phenomenological coefficients in terms of a physical model has been made by Hans Vink<sup>58,59</sup> who developed a theory of electrokinetic phenomena based on the frictional formalism of nonequilibrium thermodynamics utilizing the earlier work by Lamm,<sup>60,61</sup> Spiegler,<sup>62</sup> and Kedem and Katchalsky.<sup>63</sup> He succeeded in writing the phenomenological coefficients in the flow equations of the nonequilibrium thermodynamics in terms of molar frictional coefficients and showed that the relationship between cross-phenomenological coefficients is consistent with Onsager's reciprocal relations. The frictional formalism provides a theoretical basis for the study of mechanistic aspects of transport processes in

porous media which otherwise is not possible when using formal thermodynamics of irreversible processes. The essential features of the model based on frictional formalism are as follows.

Consider a gel system consisting of  $n$  ionic species ( $i$ ), water ( $w$ ), and a stationary gel matrix ( $o$ ). Let us assume that the temperature and all concentrations are uniform throughout the system. When an electric field or a pressure gradient is applied to the system, flow of the ions and water ensues. After a very short time a steady state develops, in which the external forces are balanced by the internal frictional forces between the components in the system. In the total balance of force, an external electric force on the boundary of the gel matrix is also involved.

In a coordinate system fixed in the gel matrix (with its  $x$  axis parallel to the applied forces), the equations for balance of force for a component at unit concentration are as follows:

for the  $i$ th species

$$f_{iw}(\mathbf{v}_i - \mathbf{v}_w)C_w + f_{io}\mathbf{v}_iC_o + \sum f_{ij}(\mathbf{v}_i - \mathbf{v}_j)C_j = Z_iFE - \bar{v}_i \text{grad } p \quad (44)$$

and for water

$$\sum f_{wi}(\mathbf{v}_w - \mathbf{v}_i)C_i + f_{wo}\mathbf{v}_wC_o = \bar{v}_w \text{grad } p \quad (45)$$

where  $f_{iw}$ ,  $f_{ij}$  etc. are the molar friction coefficients between the components specified by the subscripts (in  $\text{N m}^2 \text{S mol}^{-2}$ ),  $\mathbf{v}_i$  and  $\mathbf{v}_w$  are the average velocity ( $\text{m s}^{-1}$ ),  $C_i$  and  $C_w$  are the concentrations ( $\text{mol m}^{-3}$ ), and  $\bar{v}_i$  and  $\bar{v}_w$  are the partial molar volumes ( $\text{m}^3 \text{mol}^{-1}$ ) of the respective components.  $E$  is the electric field strength,  $p$  is the pressure,  $Z_i$  is the charge number of the  $i$ th species, and  $F$  is the Faraday constant. Although the molecular weight of the gel matrix may not be defined, it is always possible to express  $C_o$  in terms of the molecular weight of a hypothetical repeating unit of the gel matrix corresponding to its average composition. From eqs 44 and 45 it follows that the frictional force between the components  $k$  and  $l$  having concentrations  $C_k$  and  $C_l$  is given by

$$f_{kl}r(\mathbf{v}_k - \mathbf{v}_l)C_kC_l$$

Because of Newton's third law, the force from  $k$  to  $l$  is equal but opposite to the force from  $l$  to  $k$ . Hence the frictional coefficients are subject to symmetry relations

$$f_{lk} = f_{kl} \quad \text{for } k, l = 1, \dots, n, w, o \quad (46)$$

Equations 44 and 45 are also subject to constraints imposed by the condition of electroneutrality i.e.

$$\sum_{i=1}^n Z_i C_i = 0 \quad (47)$$

Introducing into eqs 44 and 45, the fluxes of the mobile components, i.e.

$$\mathbf{J}_i = C_i \mathbf{v}_i \quad i = 1, \dots, n \quad (48)$$

$$\mathbf{J}_w = C_w \mathbf{v}_w \quad (49)$$

we arrive at the following phenomenological equations of nonequilibrium thermodynamics:

$$\sum_{j=1}^n R'_{ij} \mathbf{J}_j + R'_{iw} \mathbf{J}_w = Z_i FE - \bar{v}_i \text{grad } p \quad (50)$$

$$\sum_{i=1}^n R'_{wi} \mathbf{J}_i + R'_{ww} \mathbf{J}_w = -\bar{v}_w \text{grad } p \quad (51)$$

where

$$R'_{ii} = (1/C_i)(f_{i0}C_0 + f_{iw}C_w + \sum_{j \neq i} f_{ij}C_j) \quad (52)$$

$$R'_{ij} = -f_{ij} \quad (53)$$

$$R'_{iw} = R'_{wi} = -f_{iw} \quad (54)$$

$$R'_{ww} = (1/C_w)(f_{w0}C_0 + \sum_i f_{iw}C_i) \quad (55)$$

Obviously the Onsager's reciprocity relations are satisfied as a consequence of Newton's third law.

Strong agreement of frictional formalism has been provided by Hans Vink's<sup>64</sup> experiments on the flow of polyelectrolyte solutions in narrow capillaries. The experiments were carried out with polystyrene sulfonate and carboxymethyl cellulose polyelectrolyte solution in glass capillaries with diameters in the range of 0.3 to 1.5 mm. The electrokinetic effects were very large compared to similar effects in simple salt solutions and could not be explained in classical theory terms of electrokinetic phenomena. The computed value of the zeta potential for HPSS (hydrogenated form of polystyrene sulfonate) was of the order of 25 V which is many orders of magnitude higher than the value normally considered in electrokinetics (<100 mV). The theory developed on the basis of frictional formalism<sup>68,69</sup> was, however, found to be adequate. Frictional formalism shows that the main cause of the large electrokinetic effects is the high-wall friction coefficient of the polyion, which is a manifestation of large frictional interactions in the polyion matrix.

## E. Relaxation Times

In view of the importance of the relaxation time in the study of buildup and decay of electrokinetic steady states such as electroosmotic pressure and streaming potential; we now introduce a discussion of the subject. Later we shall see that the relaxation phenomenon is useful in understanding temporal oscillations where a time delay has to be introduced at some stage. Haase<sup>65</sup> has deduced the following relationship for the time course of the approach to the steady-state value of electroosmotic pressure:

$$\ln[h_\infty - h_0/h_\infty - h] = t/\tau \quad \text{or} \quad \ln[(\Delta P)_\infty/(\Delta P)_\infty - (\Delta P)_t] = t/\tau \quad (56)$$

where  $h_\infty$  is the height level corresponding to the steady state of electroosmotic pressure,  $h$  is the height at any time  $t$ , and  $h_0$  is the value of  $h$  at  $t = 0$ . The relaxation time  $\tau$  is related to, the density of the fluid, the cross-sectional area, the thickness and permeability of the diaphragm, and the cross-sectional area of the tube in which the liquid rises during electroosmotic flow. Blokhra et al<sup>66,67</sup> have studied the electroosmotic relaxation time for the binary mixtures of acetonitrile with dimethyl formamide and nitromethane.

Kumar and Singh<sup>68</sup> have used nonequilibrium thermodynamic considerations to predict relaxation times of electroosmotic pressure and streaming potential. The validity of the derived equations which were consistent with those Haase's has been demonstrated by the data obtained on the buildup and decay of electroosmotic pressure and also of the streaming potentials for ion-exchange membrane-methanol systems. The ion-exchange membranes were made from Amberlite IRC (50), and Zeokarb 225 resins. Kumar and Singh's<sup>68</sup> theoretical treatment may be summarized as follows:

In order to consider the buildup and decay of electroosmotic pressure let us focus attention on eq 27. On the right-hand side of the equality sign, the second term represents the electroosmotic flow, i.e.  $(\mathbf{J}_v)_{\Delta P=0}$ , and the first term represents the flow induced by the pressure differences, i.e.  $(\mathbf{J}_v)_{\Delta \phi=0}$ . If it is remembered that the directions of the pressure difference induced flow and of the electroosmotic flow are opposite to each other, the eq 27 for net flow at any time  $t$  can be read as

$$(\mathbf{J}_v)_{\text{net}}(t) = (\mathbf{J}_v)_{\Delta P=0} - (\mathbf{J}_v)_{\Delta \phi=0}(t) \quad (57)$$

At the steady state (at  $t = \infty$ ) the net flow vanishes, therefore,

$$(\mathbf{J}_v)_{\Delta P=0} = (\mathbf{J}_v)_{\Delta \phi=0}(\infty) \quad (58)$$

In view of eq 58, eq 57 can be rewritten as:

$$(\mathbf{J}_v)_{\text{net}}(t) = (\mathbf{J}_v)_{\Delta \phi=0}(\infty) - (\mathbf{J}_v)_{\Delta \phi=0}(t) \quad (59)$$

If the radius of the electroosmotic pressure measuring the tube/capillary is  $r$ , using eq 27, eq 59 can be transformed to give

$$\pi r^2 \frac{d(\Delta P)(t)}{dt} = L_{11}(\Delta P)(\infty) - L_{11}(\Delta P)(t) \quad (60)$$

or

$$\frac{d(\Delta P)(t)}{(\Delta P)(\infty) - (\Delta P)(t)} = \frac{L_{11}}{\pi r^2} dt \quad (61)$$

Integrating eq 61 and using the initial condition that at  $t = 0$   $(\Delta P)(t) = 0$ , one can then write

$$(\Delta P)(t) = (\Delta P)(\infty)[1 - \exp(-t/\tau_e)] \quad (62)$$

where  $\tau_e = \pi r^2/L_{11}$ .  $\tau_e$  is the relaxation time, i.e. the time required for the electroosmotic pressure to rise  $(1 - 1/e)$  of its steady value. During the decay of the electroosmotic pressure i.e. when  $\Delta \phi$  is switched off,  $(\mathbf{J}_v)_{\Delta P=0} = 0$  and therefore it follows from eq 57 that

$$(\mathbf{J}_v)_{\text{net}}(t) = -(\mathbf{J}_v)_{\Delta \phi=0}(t) \quad (63)$$

or

$$\frac{d(\Delta P)(t)}{(\Delta P)(t)} = -\frac{L_{11}}{\pi r^2} dt$$

Integration of eq 63 using the condition that at  $t = 0$   $(\Delta P)(t) = (\Delta P)(\infty)$  leads to

$$(\Delta P)(t) = (\Delta P)(\infty) \exp\left(-\frac{t}{\tau_e}\right) \quad (64)$$

Equations 63 and 64 show the time-dependent buildup and decay of electroosmotic pressure, respectively.

For the streaming potential one has to focus attention on eq 28. By using similar arguments to the case of

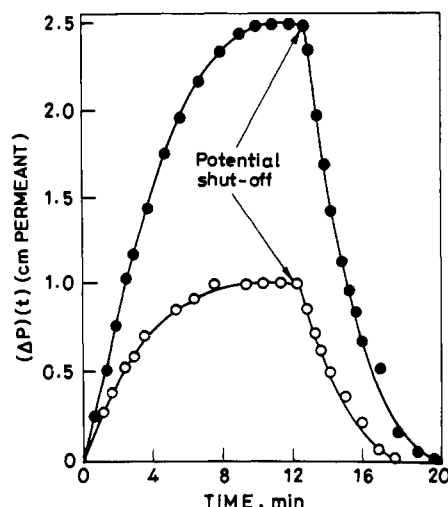


**Figure 5.** Buildup and decay of electroosmotic pressure with time for Amberlite IRC (50) membrane/methanol system:<sup>68</sup> (O)  $\Delta\phi = 100$  V; (•)  $\Delta\phi = 200$  V.

electroosmotic pressure, eq 28 can be viewed as

$$(I)_{\text{net}}(t) = (I)_{\Delta\phi=0} - (I)_{\Delta P=0}(t) \quad (65)$$

At the steady state,  $(I)_{\text{net}}$  vanishes and a stationary electrical potential called the streaming potential  $(\Delta\phi)_{I=0}$  is established. Hence

$$(I)_{\Delta\phi=0} = (I)_{\Delta P=0}(\infty) = [(\Delta\phi)(\infty)]/2 \quad (66)$$

If  $\mathcal{R}$  is the electrical resistance of the membrane/permeant system, substituting eq 65 into eq 66 one can write

$$\text{And since } (I)_{\text{net}}(t) = \frac{(\Delta\phi)(\infty)}{\mathcal{R}} - \frac{(\Delta\phi)(t)}{\mathcal{R}} \quad (67)$$

$$(I)_{\text{net}}(t) = \left[ \tilde{C} \frac{d}{dt} (\Delta\phi)(t) \right] \quad (68)$$

where  $\tilde{C}$  is the capacitance of the membrane, it follows from eq 67 that

$$\frac{d(\Delta\phi)(t)}{(\Delta\phi)(\infty) - (\Delta\phi)(t)} = \frac{dt}{\mathcal{R}\tilde{C}} \quad (69)$$

Integration of eq 69 using the initial condition that at  $t = 0$   $(\Delta\phi)(t) = 0$  one gets

$$(\Delta\phi)(t) = (\Delta\phi)(\infty)[1 - \exp(-t/\tau_s)] \quad (70)$$

where the relaxation time

$$\tau_s = 1/\mathcal{R}\tilde{C} \quad (71)$$

Equation 71 has the familiar form of a  $\mathcal{R}\tilde{C}$  time constant from the network theory.<sup>38</sup> Equation 71 shows an exponential buildup of streaming potential with time.

The authors<sup>68</sup> experimentally examined the implications of the derived eqs 62, 64, and 70 for Amberlite IRC(50) membrane/methanol and Zeokarb 225/methanol systems and have estimated the values of the relaxation times  $\tau_s$  and  $\tau_e$ . A typical buildup and decay curve is shown in Figure 5. The values of  $\tau_e$ , estimated using eq 62, were shown to be in agreement with those calculated from the hydraulic conductivity data. Further as expected, the values of  $\tau_e$  estimated from the data on buildup and decay of electroosmotic pressure were found to be in agreement and independent of the applied potential difference across the membrane. A

**Table I.** Relaxation Times Estimated from Buildup and Decay of Electroosmotic Pressure Data for Amberlite IRC (50) Membrane(II)/Methanol System<sup>a</sup>

$\Delta\phi$ (V)	$\tau_e$ (min)	
	buildup	decay
100	2.60	2.55
200	2.66	2.89

<sup>a</sup> Taken from ref 68.

**Table II.** Relaxation Time Estimated from Buildup of Streaming Potential for Zeokarb 225/Methanol System

$\Delta P$ (cm) permeant	$\tau_s$ (min)		
	Na <sup>+</sup> form	Ba <sup>2+</sup> form	Al <sup>3+</sup> form
10	0.95	0.80	0.79
30	0.95	0.81	0.81
50	0.92	0.80	0.76
70	0.93	0.82	0.77
90	0.94	0.83	0.77

<sup>a</sup> Taken from ref 68.

similar trend is observed in the case of  $\tau_s$ . These trends are apparent from Tables I and II (data taken from Kumar and Singh's paper).<sup>68</sup> The data obtained earlier by Singh and Srivastava<sup>69</sup> also support these results.

The question of the relaxation time in electroosmotic effects, particularly streaming potential has been investigated recently by Tasaka et al.<sup>70-72</sup> for the case of polymer chains dissolved in the liquid phase of the membrane. These authors have shown that the time dependence of the streaming potential is caused by the relaxation phenomena of polymer chains dissolved in the liquid phase of the membranes rather than by either the concentration polarization<sup>50,73</sup> or the relaxation due to the establishment of a double layer.<sup>68</sup> Tasaka et al.<sup>71</sup> concluded that the relaxation time reflects the properties of the polymer chains of which the membrane is made. In many cases the relaxation time was found to be made up of the corresponding relaxation times for the different types of polymer chains constituting the membrane matrix. A detailed analysis of the relaxation phenomena has been conducted by Sekiguchi et al.<sup>72</sup> who discovered the correlations between the relaxation behavior and the membrane composition. The effects of cross linking, concentration of the outer solution, and the temperature on the relaxation behavior of each component were also explored. These studies<sup>72a</sup> were conducted on collodion membranes, oxidized collodion membranes, and interpolymer membranes of collodion and poly(acrylic acid). Subsequent studies<sup>72b</sup> confirmed these observations and further suggested that the time dependence of electroosmosis and the streaming potential could be correlated quantitatively. A recent study on the streaming potential of HCl, NaCl, and KCl solutions with ion-exchange membranes shows that concentration polarization does play a significant role during the buildup of the streaming potential.<sup>74</sup>

Quite recently Ibanez et al.<sup>75</sup> have presented a model for the streaming potential relaxation in charged membranes. They have compared the model with the experimental results obtained for Nucleopore membranes of 0.8- $\mu\text{m}$  nominal pore diameter and a dilute aqueous solution of sodium chloride at 24.6 °C. The structure of the model implies the validity of Onsager's reciprocal relation. The following significant conclu-

sions were drawn: (i) The complete relaxation process can be divided into two different parts or partial relaxations. (ii) The first relaxation is the fastest and is exponential in nature and corresponds to the suppression of mechanical action (pressure difference). The other relaxation may be due to the redistribution of electrical charges which tend to regain the state they were in, prior to the establishment of pressure gradient. (iii) Relaxation studies can be utilized to determine the phenomenological coefficients.

The relaxation time for electroosmosis has also been investigated by many workers from the point of view of elucidating relaxation mechanisms. This has been ascribed to various factors, viz. (1) the bending of membranes due to the applied electric field,<sup>76,77</sup> (2) the concentration polarization,<sup>73,78</sup> and (3) the relaxation time for the buildup of the electrical double layer<sup>68,78</sup> which is, of course, too short and hence cannot account for the observed facts. The electroosmotic volume flow through oxidized collodion membranes and interpolymer membranes of collodion and poly(acrylic acid) partially cross linked with  $\text{Fe}^{3+}$  was measured. In all cases the volume flux-time plots were nonlinear. The magnitude of curvature varied from one plot to another. The time dependence of electroosmosis was explained with the same relaxation of polymer chains dissolved in the liquid phase of the membranes that specifies the time dependence of the streaming potential. The dependence of the streaming potential on time was measured by applying a pressure difference across collodion poly(acrylic acid) membranes and poly(styrenesulfonic acid) type cation exchange membranes. It has become apparent that the time dependence of the streaming potential reflects the relaxation phenomena of the polymer chains dissolved in the liquid phase of the membranes.<sup>71</sup> The number of relaxation components depends on the number of chemical components of which the membrane is made. The relaxation components are assignable to each chemical component. The relaxation time becomes longer, the longer and more flexible the polymer chains in the liquid phase.

It may be pointed out that relaxation studies have a value in the context of electrokinetic oscillations where time delay in the buildup of electroosmotic pressure plays an important role. This aspect will be discussed later in this article.

## F. Electrokinetic Energy Conversion

On a priori grounds, electrokinetic effects can be viewed as energy conversion devices. For example in an electroosmotic flow or pressure, electrical energy is converted into mechanical energy (work) and in a streaming potential or current, mechanical energy (work) is converted into electrical energy. The pumping of fluid may be called the pumping mode while the generation of electrical power may be called the generation mode. An analysis of electrokinetic energy conversion to explore its feasibility as an operating device was first attempted by Osterle.<sup>79,80</sup> In Osterle's formalism, the membranes in the schematic representations, shown in Figure 3, were called the capillary tube bank, which simply means a set of  $n$  paralleled identical capillary tubes. The double-layer phenomena, giving rise to electrokinetic effects, were invoked. The

charge density within the tubes in the tube bank, established due to the selective ion adsorption mechanism, will be a function of the radial position within the individual tubes. The charge density can be positive or negative depending upon whether the tube walls adsorb more negative ions than positive and vice versa.

Using the electrical double-layer model of a membrane having parallel identical capillary tubes, Osterle deduced the operating equations for an electrokinetic energy converter in the pumping mode as well as in the generation mode. Due to the linear dependence of flow on the pressure, the maximum pumping power occurs when the pressure is one-half the zero-flow pressure. The maximum pumping efficiency is obtained by dividing the value of the maximum pumping power by the product of voltage and current. It is found that the maximum pumping efficiency is equal to the maximum generating efficiency which is a consequence of Onsager's reciprocal relations.

The characteristics of a steady-state electrokinetic energy converter in both the fluid pumping and electrical generation modes of operation in the case of a glass/water system were computed.<sup>79,80</sup> For pure water, the maximum conversion efficiency in either direction was found to be 0.392%. A tube bank of 100-cm<sup>2</sup> open cross-sectional area and 1-cm length subject to an applied voltage of 1000 V was shown to be capable of pumping 0.07 L per second at about 0.05 atm pressure at this efficiency. The same unit subjected to an applied pressure of about 1 atm was shown to be capable of generating 0.49 W at 70 V at the same efficiency.

Osterle's analysis<sup>79,80</sup> has been extended by Morrison and Osterle<sup>81</sup> who studied energy conversion analytically utilizing the electrokinetic effect associated with the flow of an electrolyte through ultrafine capillary tubes constituting the tube bank. In Osterle's earlier analysis, a Stern-type double layer was assumed and the radii of the tubes considered were large enough in comparison to the thickness of the mobile part of the double layer. Furthermore, the contribution of the surface conductivity was entirely neglected. These restrictions were dispensed with in Morrison and Osterle's treatment.<sup>81</sup> Since Osterle's earlier analysis indicated that the efficiency of the energy conversion is favored by small tube radii, an extension of his theory to smaller tubes was obviously desirable. In a numerical analysis of the Poisson-Boltzmann equation governing the radial potential distribution in the tubes for the case of pure water in glass capillaries, results were obtained for the surface conductivity and the maximum conversion efficiency as a function of the capillary radius.

It was found that the conversion efficiency attains a maximum of about 0.90% for a tube radius of about  $1.2 \times 10^{-7}$  m and tails off rapidly for both smaller and larger tubes. Using their analytical expression, Morrison and Osterle<sup>81</sup> evaluated the values of surface conductivity over the range of tube radii. For tube radii from  $10^{-5}$  to  $10^{-8}$  m, the surface conductivity was shown to decrease from about  $6 \times 10^{-9}$  mhos to  $2 \times 10^{-9}$  mhos. Thus it would appear that surface conductivity has a significant effect in tubes of radii of less than about  $10^{-4}$  m.

A unified theory of the steady-state energy conversion, using nonequilibrium thermodynamic methods was presented by Osterle<sup>82</sup> and Kedem and Caplan.<sup>83</sup> Kedem and Caplan<sup>83</sup> and Paterson<sup>84</sup> have discussed

the phenomena of energy conversion in the context of the phenomenon of active transport in biology. This however lies outside the scope of this review and will not be considered here. However, the skeleton features of the nonequilibrium thermodynamic theory of energy conversion in the context of electrokinetic phenomena, are summarized below.

The efficiency of energy conversion  $\beta$  can be written as:

$$\beta = \frac{J_o X_o}{J_i X_i} \quad (72)$$

where the subscript  $i$  and  $o$ , respectively, represent the quantities as "input" and "output". Since in electroosmosis the input force is the applied potential difference  $\Delta\phi$  and the output force is the consequent pressure difference  $\Delta P$ , for electroosmosis eq 72 would be

$$\beta_e = \frac{J_v \Delta P}{I \Delta \phi} = \frac{J_v \Delta P}{(\Delta \phi)^2 / \mathcal{R}} \quad (73)$$

where the subscript  $e$  represents the phenomenon of electroosmosis,  $J_v$  represents the volume flux,  $I$  represents the current flow, and  $\mathcal{R}$  is the electrical resistance of the system. Similarly for the streaming potential where the input force is the applied pressure difference  $\Delta P$  and the output force is the consequent  $\Delta\phi$ , eq 72 would be

$$\beta_s = \frac{I \Delta \phi}{J_v \Delta P} = \frac{(\Delta \phi)^2 / \mathcal{R}}{J_v \Delta P} \quad (74)$$

The subscript  $s$  in eq 74 represents the phenomenon of the streaming potential.

In an electroosmosis experiment the applied potential difference  $\Delta\phi$  across the membrane is used to drive the liquid uphill. This liquid if allowed to accumulate would exert a hydraulic pressure difference across the membrane causing a back-flow of the liquid. When  $\Delta P$  equals the electroosmotic pressure the net water flux  $J_v$  becomes zero. Thus, from eq 73 it is obvious that  $\beta_e$  would be zero when either  $\Delta P = 0$  or when it equals the electroosmotic pressure which corresponds to the condition  $J_v = 0$ . It, therefore, appears that the plot of  $\beta_e$  against  $\Delta P$  for a fixed value of  $\Delta\phi$  would pass through a maximum when  $\Delta P$  is varied from zero to electroosmotic pressure. Naturally the optimum value of  $\beta_e$  would occur when  $\Delta P$  is less than the electroosmotic pressure. A similar situation would apply to  $\beta_s$  represented by eq 74. The condition at which the maximum value of  $\beta_e$  or  $\beta_s$  would occur can be obtained from very simplistic considerations.<sup>85,86</sup> Let us consider electroosmosis as an example.

Equation 73 in view of the phenomenological eq 27 can be written as

$$\beta_e = \frac{(L_{12}\Delta\phi + L_{11}\Delta P)\Delta P}{I\Delta\phi} \quad (75)$$

Treating the input power  $I\Delta\phi$  as constant and applying the condition

$$\partial\beta_e/\partial\Delta P = 0 \quad (76)$$

from eq 75 for the maximum we get

$$(2L_{11}\Delta P/I) + (L_{12}/I) = 0 \quad (77)$$

since

$$(\Delta P/\Delta\phi)_{J_v=0} = -L_{12}/L_{11}$$

eq 77 yields

$$(\Delta P)_{\max} = \frac{1}{2}(\Delta P)_{J_v=0} \quad (78)$$

Equation 78 implies that  $\beta_e$  would be at a maximum when  $\Delta P$ , at a fixed value of  $\Delta\phi$ , equals half of the value of the electroosmotic pressure. A similar conclusion can be drawn for  $\beta_s$ . The condition given by eq 78 is in agreement with Osterle's conclusion.<sup>80</sup>

In their study Gross and Osterle<sup>87</sup> considered a three flux-three force system, the forces being  $\Delta P$ ,  $\Delta\phi$ , and the osmotic pressure difference  $\Delta\pi$ , whereas in earlier studies<sup>79-81</sup> only  $\Delta P$  and  $\Delta\phi$  were considered. Thus the equations developed by Gross and Osterle<sup>87</sup> could also include the phenomenon of osmosis in addition to electroosmosis and the streaming potential. Previous attempts<sup>16,88,89</sup> at relating the fluxes to forces for the capillary model (tube bank) have either made use of restrictive model simplifications or considered the osmotic force inactive. These simplifications result from the assumption that (i) the Debye length is very small in comparison to the tube radius so that the fluid is electrically neutral over virtually the entire cross section of the tube and (ii) the charge on the wall is so small that the zeta potential given by the Chapman-Gouy equation<sup>42,43</sup> is small enough to permit use of the Debye-Hückel linearization of the Poisson-Boltzmann equation. Making only the first assumption, Osterle<sup>90</sup> solved the capillary model for only very small values of  $\Delta\pi$  across the membrane. Using both assumptions i and ii, Kobatake and Fujita<sup>20</sup> obtained a solution for the capillary model neglecting the role of the pressure-induced electrical current. Assumptions i and ii, however, are untenable for many membranes for which the capillary model is appropriate. For example, in physiological membranes the pore sizes are too small for assumption i to be valid and in certain membranes, e.g. glass, the charge in the wall is too large for assumption ii to be valid. Both Morrison and Osterle<sup>81</sup> and Dresner<sup>91</sup> have solved the capillary model for electroosmosis by assuming  $\Delta\pi = 0$  and without making use of either assumption i or ii. Gross and Osterle<sup>87</sup> obtained expressions for nine coupling coefficients (for the three flux-three force system) in terms of properties of the capillary and the permeating fluid which characterize near equilibrium membrane transport as predicted by the capillary model. These authors<sup>87</sup> did not assume a small Debye length to radius (of capillary) ratio nor did they resort to the Debye-Hückel linearization of the Poisson-Boltzmann equation. They combined the coefficients appropriately to form dimensionless groups which characterize the energy conversion efficiency of the capillary membrane in its various modes of operation.

Considering the cases of dilute sodium chloride and potassium chloride solutions, the computations of Gross and Osterle<sup>87</sup> show the following: (1) In osmosis the capillary membrane has a value of maximum  $b$  ( $b$  being the figure of merit defined<sup>81,87</sup> as

$$L_{io}^2/(L_{ii}L_{oo} - L_{io}^2)$$

for the  $i, o$  conversion mode) of about 0.067 corresponding to an efficiency of about 2% at a radius to Debye length ratio of 1.5 for both cases. (2) In

electroosmosis  $(b)_{\max} = 0.16$  corresponding to an energy conversion efficiency of 4% at a radius to Debye length ratio = 3 for both cases. (3) In electrodialysis,  $b$  decreases monotonically as the radius to Debye length ratio increases from a maximum value of 103 for NaCl<sup>67</sup> and for KCl, corresponding to efficiencies of energy conversion equal to about 82% and 78%, respectively. (4) Onsager's reciprocal relations were obeyed for all values of radius to Debye length ratio.

Thus, the capillary membrane is found to be more efficient in electrodialysis than in either osmosis or electroosmosis.

Martinez et al.<sup>92</sup> have recently conducted a detailed study of some electrokinetic phenomena in charged microcapillary porous membranes, i.e. a solid membrane consisting of parallel cylindrical pores of equal radius perpendicular to the membrane surface and carrying an electrical charge which is uniformly distributed over the pore walls. These authors have improved upon the earlier attempts of Dresner<sup>91</sup> and Osterle and associates<sup>81,87,93</sup> who made use of the Poisson-Boltzmann and Nernst-Planck equations under restrictive conditions valid for specific experimental conditions.<sup>94</sup> Martinez et al.<sup>92</sup> developed a numerical solution method specifically designed for the problem. Predictions for the concentration potential and solute permeability made by the theory were experimentally verified for some microporous polycarbonate membranes of regular porous structure/electrolyte (LiCl or MgCl<sub>2</sub>) systems. Narebska and Koter<sup>95</sup> have studied the efficiency of energy conversion in separation processes with Nafion 120 membrane from phenomenological transport coefficients. The equations for energy conversion in transport of ions and water across a cation exchange membrane were derived by treating the system as a three-flow process and employing nonequilibrium thermodynamic phenomenological transport equations.

Literature data, demonstrating the validity of nonequilibrium thermodynamic theory of electrokinetic energy conversion, will be discussed later in this article. Srivastava and Rastogi<sup>96</sup> have obtained equations showing the dependence of  $\beta_e$  and  $\beta_s$  on the properties of membrane/permeant i.e. on the zeta potential, viscosity, dielectric constant, conductance, etc.

There are not many attempts in the literature designed toward building a device based on the principle of electrokinetic energy conversion. One from the Carnegie Institute of Technology<sup>81</sup> and another by Phillips and Mastrangelo<sup>97</sup> report that a cascade electroosmotic cell utilizing *n*-propanol in combination with a Pyrex glass sinter produced a pressure proportional to the number of stages and to the applied voltage. Flow rates were directly proportional to the applied voltage and were independent of the number of stages.

An important feature common to energy conversion devices is the direct coupling between the spontaneous process which serves as the energy source and the output. Intuitively, a tight coupling between the natural and unnatural process taking place simultaneously is necessary for effective energy conversion. Calculations based on this definition show that the maximum efficiency achieved with a given machine is uniquely determined by the degree of coupling. Similar considerations apply to biological energy conversion—the maximum efficiency is determined by the degree

of coupling between the chemical reaction and the transport.

### III. Studies in the Linear Region

#### A. Electroosmotic Studies

Several aspects from the view point of the linear formalism of the nonequilibrium thermodynamics of electrokinetic phenomena are important. These are as follows: (i) the testing of phenomenological flux relations; (ii) the testing of steady-state thermodynamic relations including stability; (iii) the testing of Onsager's reciprocity relations; and (iv) the studying of the approach to the steady state and its stability.

The validity of Onsager's relations also furnishes as evidence for the internal consistency of the data. Early attempts at demonstrating the validity of Onsager's relations through Saxena's relations<sup>27</sup> have been compiled by Miller<sup>98</sup> and Hanley.<sup>99</sup> The earliest evidence in favor of Onsager's relations comes from the data obtained which demonstrates the validity of Saxen's relation in clay plugs/aqueous electrolytic solution (ZnSO<sub>4</sub>, CuSO<sub>4</sub>, or CdSO<sub>4</sub>) systems. Dubois and Roberts<sup>100</sup> proved the validity of eq 36 in glass slit/aqueous electrolytic solution (KCl, BaCl<sub>2</sub>, or AlCl<sub>3</sub>) systems. However, Dubois and Roberts' results are believed to include significant experimental errors.<sup>101</sup> Much of the data verifying eq 37 are from data showing that the values of the zeta potentials from electroosmotic velocity experiments are equal to the values obtained from the streaming potential<sup>98,102,103</sup> experiments.

The data obtained by Rutgers and deSmet<sup>104</sup> on electroosmotic velocity and streaming current for isoamyl ammonium picrate in organic solvents were also used for the verification of Onsager's relations. These authors found that the electroosmotic velocity  $(J_v/\Delta\phi)_{\Delta P=0}$  is dependent on the value of  $\Delta\phi$  when the values of the latter are high. Thus by implication, they have drawn attention to the inadequacy of the linear phenomenological equation in their system.

It is necessary to test the validity and domain of validity of both Onsager's relations and linear phenomenological relations to have a complete test of the validity of the linear formalism. In fact, it is ideal that both these tests (Onsager's relations and linear laws) are carried out on the same system. None of the earlier studies on electrokinetic phenomena summarized in Miller's review<sup>98</sup> (with the exception of the studies conducted by Rutgers and deSmet<sup>104</sup> where comments on the validity of linear laws have been made by implication) attempt to test the validity of the linear laws in a direct manner. In fact, generally the validity of linear phenomenological relations has been assumed.

A recent straightforward attempt at testing the validity of linear phenomenological relations, in the phenomenon of electroosmosis, was made by Rastogi and Jha.<sup>105</sup> The experimental setup used is depicted in Figure 6 and is self-explanatory. The strategy adopted in these experiments was based on the fact that the phenomenological eq 27 can be viewed as

$$J_v = (J_v)_{\Delta P=0} + (J_v)_{\Delta\phi=0} \quad (79)$$

which means that the resultant flow  $J_v$  is made up of two terms, the electroosmotic flow  $(J_v)_{\Delta P=0}$  and the hydraulic flow  $(J_v)_{\Delta\phi=0}$ . Since all three terms in eq 79



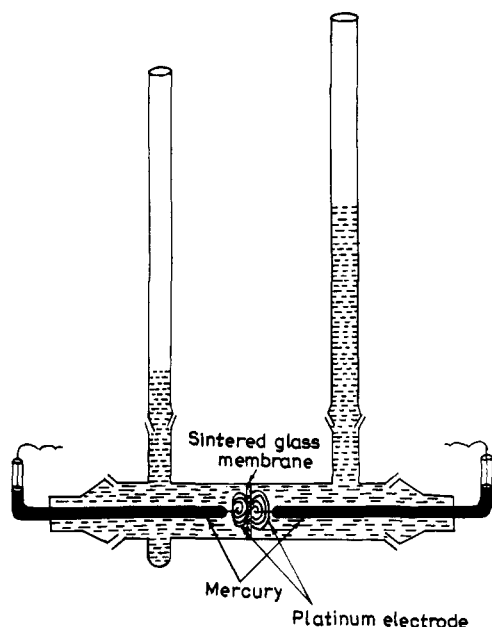


Figure 6. Apparatus for the measurement of electroosmotic pressure and electroosmotic permeability.

are directly and even successively measurable the linear phenomenological eq 27 can be conveniently tested. The test was performed on the Pyrex sinter membrane/water system. These are quite careful experiments wherein the validity and the domain of validity of

$$(\mathbf{J}_v)_{\Delta P=0} L_{12} \Delta \phi \quad (80)$$

and

$$(\mathbf{J}_v)_{\Delta \phi=0} = L_{11} \Delta P \quad (81)$$

have been tested along with the validity of eq 79. The values of the phenomenological coefficients  $L_{11}$  and  $L_{12}$  were also estimated. Although meticulously conducted, those experiments do not provide a complete test of the linear formalism because, in these studies, validity of Onsager's relations has not been demonstrated.

While discussing the temperature dependence of the cross coefficients, these authors<sup>105</sup> invoked the relationship (eq 41) based on the classical double-layer model. They reported that the product ( $L_{12} \cdot \eta/\epsilon$ ) was more or less independent of temperature. This finding indicates that the temperature variations related to viscosity and dielectric constant compensate each other and also the fact that the zeta potential in their system was invariant with temperature in the temperature range studied.

Blokhra et al.,<sup>106-108</sup> on the basis of their studies on liquid mixtures of varying dielectric constant and viscosity, concluded that the domain of the validity of the phenomenological equations increases with an increase in the viscosity of the mixture and decreases with an increase in the dielectric constant of the mixture. They also attempted to correlate the phenomenological coefficients with the physical properties of the liquids, e.g. viscosity and dielectric constant, and also to the structure-making and structure-breaking properties of the solutes dissolved in them.<sup>109-111</sup>

Blokhra et al.,<sup>108,112-118</sup> have explicitly demonstrated the validity of Onsager's reciprocal relations within the domain of the validity of linear phenomenological relations in electroosmotic phenomena. In these stud-

Table III. Values of Cross-Phenomenological Coefficients  $L_{12}$  and  $L_{21}$  for Different Systems

system	$L_{12} \times 10^4$ (cm <sup>3</sup> A J <sup>-1</sup> )	$L_{21} \times 10^4$ (cm <sup>3</sup> A J <sup>-1</sup> )
25% methanol <sup>a</sup>	7.05	6.90
75% methanol <sup>a</sup>	8.88	8.94
10 <sup>-6</sup> M KCl in DMF <sup>a</sup>	4.41	4.50
10 <sup>-6</sup> M KCl in H <sub>2</sub> O <sup>a</sup>	8.40	8.38
acetonitrile <sup>b</sup>	0.26	0.27
25% MeOH-MeCN <sup>b</sup>	0.69	0.71
75% MeOH-MeCN <sup>b</sup>	0.36	0.35
70% ethylene glycol acetonitrile- dimethylformamide mixture (percentage w/w of EG)		
5 <sup>c</sup>	2.90	2.83
7.5 <sup>c</sup>	5.35	5.28
10.0 <sup>c</sup>	3.25	3.08
ammonium chloride-ammonium nitrate solutions <sup>d</sup>		
1 × 10 <sup>-2</sup> M NH <sub>4</sub> Cl	0.26	0.27
1 × 10 <sup>-2</sup> M NH <sub>4</sub> Cl + 1 × 10 <sup>-2</sup> M NH <sub>4</sub> NO <sub>3</sub>	0.84	0.84
1 × 10 <sup>-2</sup> M NH <sub>4</sub> Cl + 1 × 10 <sup>-3</sup> M NH <sub>4</sub> NO <sub>3</sub>	0.47	0.47
1 × 10 <sup>-2</sup> M NH <sub>4</sub> Cl + 1 × 10 <sup>-4</sup> M NH <sub>4</sub> NO <sub>3</sub>	0.20	0.20
1 × 10 <sup>-3</sup> M NH <sub>4</sub> Cl	0.11	0.11
1 × 10 <sup>-3</sup> M NH <sub>4</sub> Cl + 1 × 10 <sup>-2</sup> M NH <sub>4</sub> NO <sub>3</sub>	0.41	0.41
1 × 10 <sup>-3</sup> M NH <sub>4</sub> Cl + 1 × 10 <sup>-3</sup> M NH <sub>4</sub> NO <sub>3</sub>	0.14	0.14
1 × 10 <sup>-3</sup> M NH <sub>4</sub> Cl + 1 × 10 <sup>-4</sup> M NH <sub>4</sub> NO <sub>3</sub>	0.12	0.12
1 × 10 <sup>-4</sup> M NH <sub>4</sub> Cl	0.07	0.07
1 × 10 <sup>-4</sup> M NH <sub>4</sub> Cl + 1 × 10 <sup>-2</sup> M NH <sub>4</sub> NO <sub>3</sub>	0.35	0.34
1 × 10 <sup>-4</sup> M NH <sub>4</sub> Cl + 1 × 10 <sup>-3</sup> M NH <sub>4</sub> NO <sub>3</sub>	0.14	0.14
1 × 10 <sup>-4</sup> M NH <sub>4</sub> Cl + 1 × 10 <sup>-4</sup> M NH <sub>4</sub> NO <sub>3</sub>	0.12	0.12
NH <sub>4</sub> Cl-NH <sub>4</sub> Br solutions <sup>e</sup>		
1 × 10 <sup>-2</sup> M NH <sub>4</sub> Cl	0.26	0.27
1 × 10 <sup>-2</sup> M NH <sub>4</sub> Cl + 1 × 10 <sup>-2</sup> M NH <sub>4</sub> Br	0.68	0.67
1 × 10 <sup>-2</sup> M NH <sub>4</sub> Cl + 1 × 10 <sup>-4</sup> M NH <sub>4</sub> Br	0.54	0.52
1 × 10 <sup>-3</sup> M NH <sub>4</sub> Cl	0.10	0.11
1 × 10 <sup>-3</sup> M NH <sub>4</sub> Cl + 1 × 10 <sup>-2</sup> M NH <sub>4</sub> Br	0.60	0.62
1 × 10 <sup>-3</sup> M NH <sub>4</sub> Cl + 1 × 10 <sup>-3</sup> M NH <sub>4</sub> Br	0.31	0.32
1 × 10 <sup>-3</sup> M NH <sub>4</sub> Cl + 1 × 10 <sup>-4</sup> M NH <sub>4</sub> Br	0.20	0.19
1 × 10 <sup>-4</sup> M NH <sub>4</sub> Cl	0.08	0.07
1 × 10 <sup>-4</sup> M NH <sub>4</sub> Cl + 1 × 10 <sup>-2</sup> M NH <sub>4</sub> Br	0.28	0.28
1 × 10 <sup>-4</sup> M NH <sub>4</sub> Cl + 1 × 10 <sup>-3</sup> M NH <sub>4</sub> Br	0.13	0.13
1 × 10 <sup>-4</sup> M NH <sub>4</sub> Cl + 1 × 10 <sup>-4</sup> M NH <sub>4</sub> Br	0.11	0.11

<sup>a</sup> Taken from ref 112. <sup>b</sup> Taken from ref 113. <sup>c</sup> Taken from ref 114. <sup>d</sup> Taken from ref 118. <sup>e</sup> Taken from ref 116.

ies, the transport through a sintered glass membrane of different porosities and also through sintered glass disks impregnated with cellulose acetate was studied. The liquids chosen for the electroosmotic transport studies were either pure organic (polar) liquids or mixtures of two organic liquids or solutions of electrolytes and mixtures of electrolytic solutions. The data obtained by Blokhra et al. on some of the systems demonstrating the validity of Onsager's relations in the linear region is reproduced in Table III. In their studies, Blokhra et al. have also produced data to substantiate the conclusions from the nonequilibrium thermodynamic theory of electrokinetic energy conversion. Blokhra's et al.,<sup>119</sup> most recent effort in this direction involves electrolyte-dextrose solutions/inorganic ion exchange membrane systems and acetonitrile-nitromethane mixtures/sintered glass membrane systems.<sup>120</sup> They<sup>120</sup> have also generated data to verify Glanssorf and Prigogine's<sup>121</sup> generalization related to the rate of entropy production, which states that for both the linear and nonlinear region and function

$$m = -\mathbf{J}_i \cdot \mathbf{X}_i > 0 \quad (82)$$

This equality holds for the stationary states.<sup>121</sup> Haase deals with the question of the entropy production rate in electroosmotic systems approaching steady states.<sup>65,122</sup> For electroosmotic experiments the relationship (eq 82) reads as



**Table IV. Dependence of Phenomenological Coefficients on Direction of Flow (Cellulose Acetate Membrane/Water System)<sup>a</sup>**

	flow direction	
	→	←
$L_{11}$ (cm <sup>5</sup> dyn <sup>-1</sup> s <sup>-1</sup> )	$2.95 \times 10^{-10}$	$1.69 \times 10^{-10}$
$L_{12}$ (cm <sup>3</sup> A J <sup>-1</sup> )	$1.30 \times 10^{-6}$	$2.02 \times 10^{-6}$
$L_{21}$ (cm <sup>3</sup> A J <sup>-1</sup> )	$1.33 \times 10^{-6}$	$2.14 \times 10^{-6}$
$L_{22}$ (ohm <sup>-1</sup> )	$1.724 \times 10^{-5}$	$1.724 \times 10^{-5}$

<sup>a</sup> Taken from ref 85.

$$m = -(J\Delta\dot{P} + I\Delta\dot{\phi}) > 0 \quad (83)$$

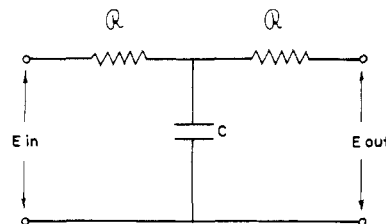
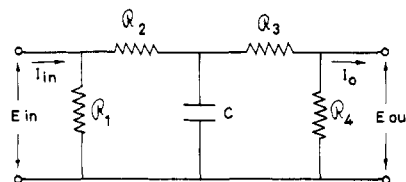
Blokhras et al.<sup>114,120</sup> have plotted  $J\Delta\dot{P}$  at a fixed value of  $\Delta\phi$  (i.e.  $\Delta\phi = 0$ ) against time in the case of their experiments with (i) an ethylene glycol in 70% dimethylformamide (DMF)–30% acetonitrile (ACN) mixture/sintered glass membrane system and (ii) with an ACN–nitromethane mixture of varying composition/sintered glass membrane<sup>120</sup> system and shown that the curve asymptotically approaches the time axis in each case. This is as it should be according to eq 83.

Srivastava and Jain<sup>85</sup> studied the electroosmosis of water through a cellulose acetate membrane and have produced data with a view to testing the linear formalism. The cellulose acetate membrane was prepared by a casting technique following the procedure of Manjikian.<sup>123</sup> All four phenomenological coefficients ( $L_{ik}$ ) were determined within the domain of validity linear phenomenological relations. Onsager's relations were found to be valid. One novel finding of these studies was that all phenomenological coefficients excepts  $L_{22}$  were found to be direction dependent revealing the anisotropic nature of the cellulose acetate membrane. The values of the various phenomenological coefficients in both directions of the flow are reproduced in Table IV and demonstrate the directional dependence of the coefficients and also the validity of Onsager's reciprocal relations in the data for each direction.

The anisotropy of the membrane has earlier been explained on the basis of the fact that by following the evaporation technique (casting technique) one is likely to get a membrane of graded porosity,<sup>124</sup> i.e. the membrane can be seen as consisting of layers of a large number of membranes of increasing porosity arranged in series. It has been suggested in recent years<sup>125,126</sup> that asymmetric cellulose acetate (CA) membranes owe their asymmetry to an incomplete evaporation of the casting solvent (acetone) mixture with water in the top layer. Thus it enters into a two-phase region in the CA–water–acetone diagram phase inversion and forms the small water droplets smallest at the top layer, because of the high degree of supersaturation found there, resulting in the formation of a dense skin layer.

Srivastava and Mehta<sup>127</sup> have utilized network thermodynamics<sup>38,39</sup> to illustrate the anisotropic character of such cellulose acetate membranes.

Oster, Perelson, and Katchalsky<sup>38</sup> have done network modeling of an isotropic membrane by considering a single permeant diffusing through the homogeneous membrane. In doing this, capacitances were assigned to the membrane as well as to the two reservoirs which the membrane separates to allow for the reversible charging and discharging of the permeant. Since

**Figure 7.** Network representation of a homogeneous membrane system.  $R$  and  $C$  are the resistance and the capacitance, respectively.<sup>127</sup>**Figure 8.** Network representation of an anisotropic membrane system.  $R_1$ ,  $R_2$ ,  $R_3$ , and  $R_4$  are resistances, and  $C$  is the capacitance.<sup>127</sup>

dissipation follows each flow process, a resistive element of equal value was assigned at both the entrance and the exit. By using these considerations the isotropic membrane system was represented as shown in Figure 7. The bounding compartments were assumed to be so large that they may be effectively time independent, that is, an infinite capacitance is equivalent to a constant effort source denote by  $E$ ,  $E_{in}$ , and  $E_{out}$  in Figure 7. In the case of an anisotropic membrane, the following considerations should apply: (1) Resistance to flow as viewed from one side of the membrane should be different as viewed from the other side. Hence resistive elements of unequal value (say  $R_2$  and  $R_3$ ) should be assigned at the entrance and at the exit. (2) Some energy is always wasted during the flow—in the case of an anisotropic membrane it is unequal as viewed from the two sides of the membrane. To account for the dissipation of energy due to this wastage, resistive elements of unequal magnitude (say  $R_1$  and  $R_4$ ) should be assigned at the entrance and at the exit. In view of these considerations the equivalent electrical network for an anisotropic membrane is represented<sup>127</sup> in Figure 8. It should be pointed out that in the case of flow through a series membrane Kedem and Katchalsky<sup>36</sup> hinted at anisotropic behavior.

Srivastava and Jain,<sup>85</sup> have also determined the values of the efficiency of energy conversion for both modes of conversion ( $\beta_e$  and  $\beta_s$ ) for the two directions of flow. The data has been used to verify the nonequilibrium thermodynamic theory of energy conversion for both directions of flow.

Recently, Benavente and Fernandez-Pineda have conducted<sup>128</sup> a thorough study of electroosmosis and the streaming potential of different concentrations of sodium chloride solutions through commercial porous membranes obtained from Millipore Iberica and Pall corporation with a pore size of 0.1  $\mu\text{m}$ . These authors determined all four phenomenological coefficients occurring in eqs 27 and 28 and demonstrated the validity of Onsager's reciprocal relation. Proceeding on the lines of Haase and Horff,<sup>129</sup> they verified the inequality ( $L_{12}L_{21} < L_{11}L_{22}$ ) which is a consequence of the positive definite character of the dissipation function. The concentration dependence of phenomenological coef-

**Table V. Concentration Dependence of Phenomenological Coefficients for Different Liquid Mixtures<sup>a</sup>**

mass fraction of methanol ( $\bar{x}_m$ )	$L_{22} \times 10^6$ (ohm <sup>-1</sup> )	$L_{11} \times 10^6$ (cm <sup>5</sup> dyn <sup>-1</sup> s <sup>-1</sup> )	$L_{21} \times 10^4$ (cm <sup>3</sup> A J <sup>-1</sup> )	$L_{12} \times 10^4$ (cm <sup>3</sup> A J <sup>-1</sup> )
Acetone–Methanol Mixture				
0.0	9.33	7.14	3.13	3.30
0.1	9.18	8.72	3.57	3.40
0.2	8.72	10.31	3.84	3.66
0.3	7.92	12.74	4.16	3.92
0.4	7.47	15.73	4.54	4.32
0.5	7.16	19.38	4.75	5.00
0.7	6.30	25.09	5.55	5.23
0.9	5.50	36.50	5.87	5.75
1.0	5.08	52.40	6.45	6.25
Methanol–Water Mixture				
0.0	1.41	5.50	10.52	11.03
0.1	1.83	5.40	9.75	9.80
0.3	2.55	5.26	9.09	8.81
0.5	3.30	4.54	8.33	8.19
0.7	4.05	4.00	7.66	7.78
0.9	4.73	3.12	7.02	7.39
1.0	5.08	2.50	6.34	6.29
Acetone–Water Mixture ( $\bar{x}_w$ )				
0.0	9.33	7.14	3.30	3.28
0.1	8.50	7.75	3.96	3.98
0.2	7.70	8.54	4.67	4.77
0.3	6.92	9.52	5.20	5.28
0.4	6.15	10.94	6.02	6.16
0.6	5.35	12.48	6.79	6.69
0.8	2.95	21.87	8.77	8.92
0.9	2.30	31.46	9.43	9.56
1.0	1.41	50.00	10.18	10.35

<sup>a</sup> Taken from refs 132–134.

ficients has been studied and the viscous pore model<sup>130</sup> was utilized to estimate the average pore radius of the membrane. The concentration dependence of the zeta potential estimated from the values of the cross coefficients was studied. The apparent transport number of the cation was estimated from the diffusion potential expression and the true cation transport number and the water transport number were obtained using the electrometric method for different solution concentrations. The true transport number of the cation estimated by taking into account water transport across the membrane showed good agreement with the value of the true transport number of the cation estimated electrometrically. These authors also estimated the value of the fixed charge density in the membrane using Aizawa et al.'s<sup>131</sup> method.

Srivastava et al.<sup>132–134</sup> have studied the electroosmotic effect in a mixture organic polar liquids/sintered glass membrane system. In addition to verifying the linear formalism, i.e. the linear phenomenological relations and Onsager's relations, they also studied the concentration dependence of the phenomenological coefficients and should that the trends in the concentration-dependence data are consistent with Spiegler's frictional model.<sup>62</sup> The data obtained on the concentration dependence of phenomenological coefficients in the case of the acetone–methanol, acetone–water and methanol–water systems and reproduced in Table V. The validity of Onsager's relation is obvious from Table V.

It was shown that in the case of acetone–methanol mixtures, the data on the concentration dependence of the coefficients  $L_{11}$  and  $L_{12}$  can be quantitatively

expressed as

$$L_{11} = \bar{x}_A(L_{11})_A + \bar{x}_M(L_{11})_M \quad (84)$$

and

$$L_{12} = \bar{x}_A(L_{12})_A + \bar{x}_M(L_{12})_M \quad (85)$$

where  $\bar{x}$  stands for the mass fraction and the subscripts A and M, respectively, indicate that the quantities are for acetone and methanol. A similar dependence was found to hold for other mixtures as well.<sup>132–134</sup>

The efficiencies of energy conversion for both electroosmosis and the streaming potential were also determined for various compositions of acetone–methanol mixtures. The data were shown to be consistent with the nonequilibrium thermodynamic theory of electrokinetic energy conversion. The concentration dependence of the maximum value of the efficiency of energy conversion for both modes of conversion, i.e.  $(\beta_e)_{\max}$  or  $(\beta_s)_{\max}$ , was found to be given by the equation

$$(\beta)_{\max} = \bar{x}_A(\beta_{\max})_A + \bar{x}_M(\beta_{\max})_M \quad (86)$$

These studies were extended to acetone–water and methanol–water systems by Srivastava and Abraham,<sup>133,134</sup> and similar results were obtained. An attempt was also made to rationalize the concentration dependence of the phenomenological coefficients in terms of structural modifications that occur in the mixture.<sup>133</sup> For example, in the case of acetone–water mixtures it was observed that the values of the coefficients  $L_{11}$  and of  $1/L_{22}$  decrease as the composition changes from 100% acetone to 100% water while the values of the cross coefficients increase. For this discussion eqs 39–41 based on a double-layer model were invoked. Equations 39–41 are written for a membrane consisting of a parallel array of  $n$  capillaries. The increased molecular interaction in hydrogen-bonded systems decreases the freedom of molecular motion and therefore tends to increase viscosity.<sup>135</sup> This means that the viscosity should increase as one goes from 100% acetone, which is a non-hydrogen-bonded system, to 100% water which is a strongly-hydrogen-bonded system. This explains the decreasing trend in the values of  $L_{11}$  with an increase in the concentration of water in the mixture because  $L_{11}$  varies inversely with viscosity—eq 39. A similarly increasing trend in electrical conductivity as one goes from 100% acetone to 100% water is obviously due to an increase in concentration of hydrogen ions.

From eq 41 it is apparent that the coefficient  $L_{12}$  varies directly with  $\epsilon$  and  $\zeta$  and inversely with  $\eta$ . Although both  $\epsilon$  and  $\eta$  increase<sup>135,136</sup> as  $\bar{x}_w$  increases, the increase in viscosity is not expected to be as pronounced as the increase in dielectric constant, because during the process of flow through the restricted barrier, e.g. sintered glass membrane, the frictional forces are likely to break weak physical interactions and hydrogen bonds. This results in a net increase in the value of  $L_{12}$  as we go from  $\bar{x}_w = 0$  to  $\bar{x}_w = 1$ . Moreover from double-layer considerations<sup>45</sup> it can be seen that the value of the quantity  $(\epsilon\zeta)$  is likely to increase because of a possible increase in the thickness of the double layer.

Several other groups, e.g. Blokhra et al.,<sup>108</sup> Singh et al.,<sup>137</sup> and Jain et al.,<sup>138</sup> have studied the concentration dependence of electrokinetic phenomenological coefficients in the case of various liquid mixtures and

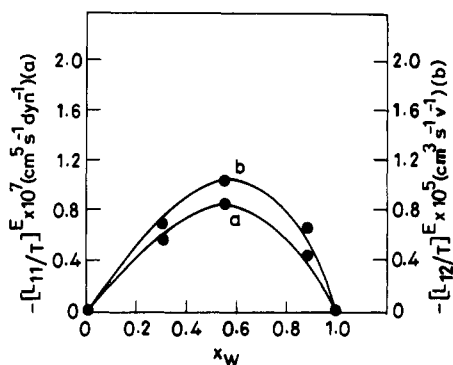


**Figure 9.** Dependence of  $(L_{11}/T)^E$  (curve a) and  $(L_{12}/T)^E$  (curve b) on mole fraction of water ( $x_w$ ).<sup>139</sup>

attempted to explain any departures from eqs 84 and 85 in terms of the structural modifications that are likely to occur in the mixtures. Since the eqs 84, 85, etc. resemble the well-known mixture law in the thermodynamics of solutions, where departures from ideality are quantified in terms of excess thermodynamics function, one is likely to be tempted to make similar attempts in respect of eqs 84, 85, etc. Singh et al.,<sup>139</sup> have in fact, made such an attempt. They defined the excess phenomenological coefficients as the difference between the experimentally determined value of the phenomenological coefficient and the one computed using eqs 84, 85, etc. These authors experimented with methanol–water mixture/sintered glass membrane systems to evaluate the values of the excess phenomenological coefficient and interpret them in terms of the structural modifications that occur in methanol–water mixtures. The excess phenomenological coefficients in the case of methanol–water mixtures were written as

$$L_{11}^E = L_{11} - [(L_{11})_M x_M + (L_{11})_w x_w] \quad (87)$$

$$L_{12}^E = L_{12} - [(L_{12})_M x_M + (L_{12})_w] x_w \quad (88)$$

etc. where  $L_{11}$  and  $L_{12}$  are the experimentally determined values of the phenomenological coefficients and the superscript E denotes the excess coefficient. The values of  $L_{11}^E$  and  $L_{12}^E$  were found to be negative, which indicates that hydrodynamic and electroosmotic permeation of the mixtures has lowered values because of interactions between the components of the mixture. Variation of both  $L_{11}^E$  and  $L_{12}^E$  with the composition of the mixture is depicted in Figure 9.

The correspondence between the excess phenomenological coefficient and the excess volume  $V^E$  as discovered by these authors is shown in Figure 10. From the linear dependence (Figure 10), it was inferred that an excess phenomenological coefficient predominantly arises on account of the interaction between the components of the mixture during transport. The membrane–permeant interactions are not significantly affected during permeation. Spectral studies show that surface–permeant interactions are significant only when narrow pores of molecular dimensions are involved.<sup>140</sup>

The idea of excess phenomenological coefficients, *prima facie*, is an attractive idea and in our opinion merits further investigation and development. However, so far, it has not been further pursued.

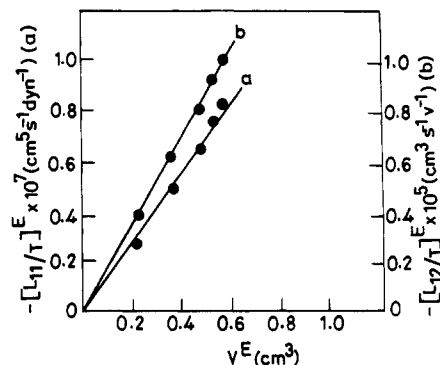


**Figure 10.** Plots of (a)  $(L_{11}/T)^E$  versus  $V^E$  and (b)  $(L_{12}/T)^E$  versus  $V^E$ .<sup>139</sup>

## B. Electroosmotic Effects in the Context of Water Desalination

In characterizing hyperfiltration, particularly by polyelectrolyte membranes, the common practice has been to rely on two coefficients determined under pressure: the salt rejection  $S_r$  defined by the equation

$$S_r = 1 - (C''/C') \quad (89)$$

where  $C'$  and  $C''$  are the salt concentration in the feed compartment and the product compartment, respectively, and the hydraulic permeability.<sup>141,142</sup> The determination of other membrane characteristics, e.g. ion selectivity and electroosmotic coefficients, has usually been determined under conditions quite remote from those of a hyperfiltration experiment. However, pioneers<sup>143</sup> in the use of charged membranes for salt filtration recognized the importance of the hyperfiltration streaming potential which is related to the latter two coefficients.<sup>144</sup> Tanny and Kedem<sup>145</sup> have demonstrated how the streaming potential can provide useful information on membrane structure under pressure. These authors have furnished experimental verification of the frictional model developed earlier.<sup>146</sup>

In a hyperfiltration setup, a membrane separates two aqueous solutions of the same electrolyte, e.g. NaCl, whose concentrations, pressures and electrical potentials are different. Consequent to an applied pressure difference  $\Delta P$ , the flow of water ( $J_w$ ) and of the salt commences from the feed compartment to the product compartment. During the stationary hyperfiltration the product concentration is given by

$$C''_s = J_s/J_v \quad (90)$$

with

$$J_v = J_s \bar{V}_s + J_w \bar{V}_w \approx J_w \bar{V}_w \quad (91)$$

where  $\bar{V}_s$  and  $\bar{V}_w$  represent the partial molar volumes of salt and water, respectively. It has been consistently found<sup>141,142,147</sup> in hyperfiltration systems that, with increasing volume flow  $J_v$ , the salt rejection increases and approaches a maximum value, characteristic of the membrane. Kedem and associates<sup>148,149</sup> have shown that integration of the usual phenomenological equations also leads to the same expectation.

By considering the hyperfiltration system as a three flux–three force system, the three fluxes being  $J_v$ ,  $J_s$ , and  $I$  with the corresponding conjugate forces being  $(\Delta P - \Delta \Pi_s)$ , the electroosmotic force and the difference in chemical potential of the salt, Tanny and Kedem<sup>145</sup>

**Table VI. Numerical Values of the Phenomenological Coefficients in Eqs 27 and 28 for Kaolinite, Crysofile, Parallel Composite, and Series Composite Clay Systems<sup>a</sup>**

phenomenological coefficients	kaolinite	crysofile	parallel composite membrane	series composite membrane
$L_{11} \times 10^{11} (\text{m}^5 \text{s}^{-1} \text{N}^{-1})$	$0.2193 \pm 0.0034$	$0.2482 \pm 0.0065$	$0.46 \pm 0.0158$	$0.1183 \pm 0.001$
$L_{12} \times 10^{10} (\text{m}^3 \text{A J}^{-1})$	$0.2995 \pm 0.0221$	$1.216 \pm 0.0414$	$1.537 \pm 0.07$	$0.3754 \pm 0.021$
$L_{21} \times 10^{10} (\text{m}^3 \text{A J}^{-1})$	$0.292 \pm 0.0124$	$1.178 \pm 0.074$	$1.506 \pm 0.056$	$0.3706 \pm 0.0178$
$L_{22} \times 10^4 (\text{ohm}^{-1})$	$0.555 \pm 0.005$	$0.77 \pm 0.005$	$1.25 \pm 0.05$	$0.305 \pm 0.005$

<sup>a</sup> Taken from ref 170.

deduced a phenomenological expression for the hyperfiltration streaming potential. They experimented with polyelectrolyte [collodion poly(vinylamine)] membranes and obtained data on the hyperfiltration streaming potential, water flow, and electroosmotic and osmotic transport. The criteria for membrane homogeneity were defined using the equivalent pore radius calculated from the electroosmotic coefficient and the hydraulic permeability. The hyperfiltration streaming potential and water flow data for the polyelectrolyte membranes were compared to the electroosmotic and osmotic results for the same membrane. The homogeneity criteria were used to show that at 1 atm, the membranes contain parallel paths for water and ion flow, while at elevated pressures only a single path exists for both species. The electroosmotic coefficient which measures the coupling between the counterion and water in the membrane was used as a probe to detect changes in water structure. Measurement of the electroosmotic coefficient, as a function of temperature,<sup>150</sup> revealed a precipitous decline beginning in the vicinity of 35–36 °C. This decline was attributed to a change in water structure as suggested by Drost-Hansen.<sup>151</sup>

### C. Studies on Soil Systems

The suggestion that nonequilibrium thermodynamics could be a powerful tool in the analysis of the kinetics encountered in soil water systems was made by Wintekorn<sup>152</sup> and Taylor and Cary.<sup>153</sup> Russel<sup>154</sup> made a similar suggestion for plant systems. Philip,<sup>155</sup> however, had reservations and felt that this approach may be of little value for the nonlinear soil-moisture problem. A few good reviews on the subject are available in the literature.<sup>156–161</sup> However, not many studies are available on the nonequilibrium thermodynamics of electrokinetic phenomena. In this subsection we will take up such studies on electroosmosis which significantly demonstrate the workability of nonequilibrium thermodynamics as a tool in the study of soil systems. Studies on electrophoretic effects will be included in another section.

Although several interesting studies on electroosmotic effects—electroosmosis/streaming potential, conducted with a view to understanding permeability characteristics and related phenomena are documented in the literature,<sup>162–168</sup> none of these shed light on the nonequilibrium thermodynamic aspects.

The first experiments on electroosmotic effects from the viewpoint of nonequilibrium thermodynamics were those of Taylor and Cary.<sup>153</sup> In these experiments saturated soil samples of Millville silt loam were packed into leucite cylinders to bulk densities of approximately 1.5 g/cm<sup>3</sup>. Thermal, electrical, or salt concentration

gradients were then applied individually across the soil, and the flows were measured.

The studies conducted by Olsen<sup>169</sup> are among the few studies that are comprehensive in nature and were intended to test the postulates of nonequilibrium thermodynamics for the electroosmotic transport in soil systems. The experiments were conducted on a liquid saturated sample of sodium kaolinite consolidated under 408 kg/cm<sup>2</sup>. The data obtained show that the simultaneous fluxes of liquid and charge under hydraulic, electrical, and electrolyte concentration gradients, although they obey linear relationships, do not conform to the usual linear phenomenological equations of the form  $J_i = \sum L_{ij} X_j$ . The plots of experimental flux against the driving force show definite hydraulic and electrical potential intercepts. It was proposed that the intercepts arise from an electrolyte concentration gradient within the clay sample generated by differential salt filtering at the sample surfaces during the consolidation process. This mechanism was suggested in view of the nonsymmetrical details in the mechanical system used to consolidate the clay sample and was used to explain the intercepts which are disallowed in the linear phenomenological equations. Because of this artifact, Olsen's experiments did not serve the intended purpose.

The later detailed studies planned to throw light on nonequilibrium thermodynamics of electroosmotic effects in soil systems, in the linear region are by Srivastava and Abraham.<sup>170</sup> These authors studied the electroosmotic effects in composite clay membranes/water systems. The composite clay membranes consisted of kaolinite and crysofile clay membrane elements in both a parallel array and in a series array. In these experiments,<sup>170</sup> the area of cross section and thickness of the two constituent membrane elements was more or less the same.

The linear phenomenological relations (eqs 27 and 28) were shown to be valid for the parallel composite membrane, for the series composite membrane as well as for the constituent membrane elements crysofile clay and kaolinite clay membranes. Experimentally determined values of the various phenomenological coefficients for the constituent membrane elements and also for the composite membrane systems are presented in Table VI.

The combination rules, deduced from Kedem and Katchalsky's theory<sup>35,36</sup> for the permeability coefficients of composite membrane systems are summarized in Figure 4. Rewriting these for the kaolinite-crysofile system we have for a parallel composite membrane

$$(L_{ij})_{\text{composite membrane}} = (L_{ij})_{\text{kaolinite}} + (L_{ij})_{\text{crysofile}} \quad (92)$$

and for a series composite membrane

Table VII. Resistance Coefficients for Kaolinite, Crysolite, and Series Composite Clay Systems<sup>a</sup>

phenomenological coefficients	kaolinite	crysolite	series composite membrane
$R_{11} \times 10^{-11} \text{ (m}^{-5} \text{ s N)}$	$4.559 \pm 0.075$	$4.029 \pm 0.105$	$8.45 \pm 0.072$
$R_{12} \times 10^{-6} \text{ (m}^{-3} \text{ A}^{-1} \text{ J)}$	$-0.246 \pm 0.002$	$-0.636 \pm 0.038$	$-1.047 \pm 0.150$
$R_{21} \times 10^{-6} \text{ (m}^{-3} \text{ A}^{-1} \text{ J)}$	$-0.239 \pm 0.014$	$-0.617 \pm 0.055$	$-1.033 \pm 0.170$
$R_{22} \times 10^{-6} \text{ (ohm)}$	$0.170 \pm 0.005$	$0.130 \pm 0.005$	$0.325 \pm 0.005$

<sup>a</sup> Taken from ref 170.

$$(R_{ij})_{\text{composite membrane}} = (R_{ij})_{\text{kaolinite}} + (R_{ij})_{\text{crysolite}} \quad (93)$$

where

$$R_{ij} = \frac{|L|_{ij}}{|L|} \quad (94)$$

in which  $|L|$  is the determinant of the matrix of the coefficients  $L_{ij}$ , and  $|L|_{ij}$  is the minor of the determinant corresponding to the term  $L_{ij}$ . The validity of the combination rules (eqs 92 and 93) is obvious from the data in Tables VI and VII. The validity of Onsager's reciprocal relations is also obvious from the data (Tables VI and VII). The data were also shown<sup>170</sup> to corroborate the nonequilibrium thermodynamic theory of electrokinetic energy conversion.

Studies in the nonlinear region on soil systems will be considered later when we come to the discussion of the nonlinear region. Until then we will discuss electrokinetic studies in the linear region for biologically relevant systems.

## D. Studies on Biologically Relevant Systems

### 1. Model Membrane and Related System

Black liquid membranes (BLM) are the most widely used model systems for biomembranes. Detailed account of BLM systems can be found in the excellent monographs by Tien<sup>171</sup> and Jain.<sup>172</sup> Although electrokinetic phenomena are of relevance to biology no concerted study except for a few on chloroplast BLMs, of electrokinetic phenomena on BLM system is available. In fact, in conjunction with bifacial tension measurements and light-induced water flow in chloroplast BLMs, the observations were explained in terms of electroosmosis and streaming potentials.<sup>171,172</sup> The phenomena of electroosmosis and streaming potential were observed in chloroplast BLMs.<sup>171,173</sup> Linear plots between the net volume flow and the applied potential difference and between the induced potential difference and the applied pressure difference were observed. These could, at best, be regarded as a qualitative and partial demonstration of the linear phenomenological equations. No effort was made to make a quantitative comparison of the data with either the double-layer theory or with the nonequilibrium thermodynamic theory.

In recent years, Srivastava and associates have attempted to develop an alternative system.<sup>174,175</sup> This is known as the liquid membrane bilayer system, and it has shown promise of being a mimetic system of biomembranes. In fact quite a few illustrative membrane mimetic studies have been conducted on the liquid membrane bilayer system.<sup>176-186</sup> Straightforward electroosmotic studies, particularly from the point of view of nonequilibrium thermodynamics, have been conducted in one particular case only, that of the liquid

membrane bilayers generated by cholesterol.<sup>174</sup> Other studies on photoosmosis can in fact be considered as photoelectroosmosis studies.<sup>176,177,180,182-186</sup> Both of these will be discussed in this section. But before embarking on this discussion a brief introduction to liquid membrane bilayer systems is necessary.

Liquid membrane bilayer systems are generated using Kesting's liquid membrane hypothesis<sup>187-189</sup> which was originally propounded to account for the enhanced salt rejection in reverse osmosis. This is due to the addition of very small amounts, of the order of a few parts per million, of surfactants such as poly(vinyl methyl ether) to the saline feed. The hypothesis states that, when a surfactant is added to an aqueous phase, the surfactant layer which forms spontaneously at the interface acts like a liquid membrane and modifies mass transfer across the phase boundary. It further states that as the concentration of the surfactant is increased, the interface gets progressively covered with the surfactant layer liquid membrane and at the critical micelle concentration (CMC) of the surfactant it is completely covered. The idea of "progressive coverage" implies that if the concentration of the surfactant is half its CMC, the area of the interface covered with the liquid membrane is half the total area of the interface and if the concentration of the surfactant is three-fourths its CMC, three-fourths of the total area of the interface is covered with surfactant layer liquid membrane and so on. The liquid membrane hypothesis was further substantiated by Srivastava and Yadav<sup>190</sup> using electroosmotic transport through a hydrophobic supporting membrane in the presence of aqueous solutions of the surfactants such as poly(vinyl methyl ether) of varying concentrations. The logic underlying these experiments was the following:

If the idea of "progressive coverage" contained in Kesting's hypothesis is correct, the values of the various conductivity coefficients occurring in the phenomenological eqs 27 and 28 should show a progressive decrease with increasing concentration of the surfactant. The decreasing trend should continue up to the CMC of the surfactant beyond which it should become more or less constant. Analysis in the light of the mosaic model<sup>148,191,192</sup> shows that if concentration of the surfactant is  $n$  times its CMC,  $n$  being less than or equal to 1, the value of the conductivity coefficients e.g. any of the coefficients  $L_{ik}$  occurring in eqs 27 and 28 should be given by the relationship

$$L_{ik} = [(1-n)L_{ik}^c + nL_{ik}^s] \quad (95)$$

where the superscripts  $c$  and  $s$  represent the bare supporting membrane and the supporting membrane covered completely with the surfactant layer liquid membrane, respectively. Functionally the values of  $L_{ik}^c$  and  $L_{ik}^s$  are the values of  $L_{ik}$  when concentration of the surfactant is equal to zero and its CMC.

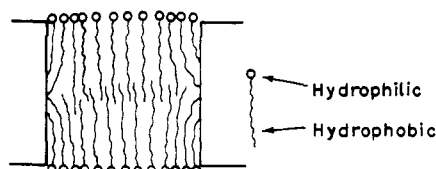


**Figure 11.** Gross picture of the liquid membrane bilayer within the pores of the supporting membrane.

Srivastava and Yadav<sup>190</sup> investigated the domain of validity of various electroosmotic effects predicted by the linear phenomenological relations (eqs 27 and 28) in the case of a liquid membrane generated by poly-(vinyl methyl ether), in series with the supporting membrane. Except in the case of hydraulic conductivity where a nonlinear exponential type of relationship between  $J_v$  and  $\Delta P$  was found to be obeyed, the linear formalism (eqs 27–29) was found to be obeyed throughout the region studied. The variation of the conductivity coefficients  $L_{ik}$  with the concentration of the surfactant showed a decreasing trend upto the CMC beyond which it became more or less constant. The values of the coefficients  $L_{ik}$  computed using eq 95 were shown to be in agreement with the experimentally determined values at concentrations below the critical micelle concentration of the surfactant.

Since at the CMC the interface is completely covered with the surfactant layer liquid membrane it follows that, if two cell compartments separated by a hydrophobic supporting membrane are each filled with the solution of surfactant of concentration equal to its CMC, a bilayer of the surfactant layer liquid membrane would be generated, i.e. one layer on either side of the supporting membrane. It is also apparent that the hydrophobic tails of the surfactant molecules in the liquid membrane would be preferentially oriented toward the hydrophobic supporting membrane and the hydrophilic moieties would be drawn outward away from it. The following additional assumptions also hold: (i) the pores have just the right length for a bilayer, (ii) the hydrophobic tails are more oriented toward themselves than toward the supporting membrane, and (iii) surfactants adhere to the pore wall and also in the pore. Such liquid membrane bilayers would be generated within the pores of the supporting membrane. The gross picture resembles the one shown in Figure 11. It is on liquid membrane bilayers generated by the constituents of biomembranes, e.g. lecithin-cholesterol mixtures, chloroplast extract, etc., such as these that membrane mimetic experiments have been performed in recent years.<sup>174–186</sup> Their workability as an alternative model/mimetic system of biomembranes is gradually being established. A discussion of the relative merits/demerits of this new system vis à vis BLM lies outside the scope of the article.

Where electroosmotic studies are concerned, these have been performed only on liquid membranes generated by cholesterol<sup>174,193,194</sup> in series with a supporting membrane. Cholesterol, though very slightly soluble in water, has been shown to considerably lower the surface tension of water.<sup>195,196</sup> Cholesterol has a maximum solubility<sup>197,198</sup> of 4.7  $\mu\text{M}$  in aqueous solution and the measured surface tension of a saturated solution in water is 33 dyn/cm. Its CMC is in the range of 25–40 nM.<sup>197,198</sup> All these data indicate that cholesterol is a very effective surfactant and hence capable of gener-

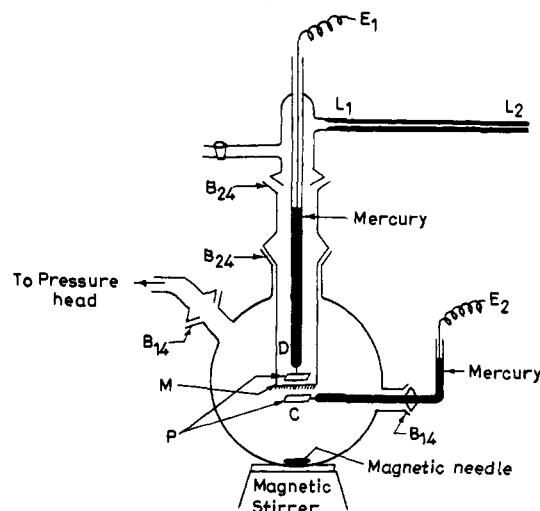


**Figure 12.** Transport cell: M, supporting membrane (cellulose acetate microfiltration membrane (Sartorius catalog no. 11107); P, platinum electrode;  $L_1, L_2$ , capillary tube;  $E_1$  and  $E_2$ , electrode terminals.<sup>174</sup>

ating liquid membranes at the interface.

The all-glass cell designed<sup>174</sup> for electroosmotic transport studies is depicted in Figure 12.

Two sets of experiments were performed. In the first, aqueous solutions of varying concentrations of cholesterol were put in compartment C and distilled water was put in compartment D and the second in which both compartments C and D were filled with cholesterol solutions of a concentration equal to its CMC. In all cases straight plots for various electroosmotic effects were obtained. The values of the various conductivity coefficients  $L_{ik}$  obtained at different concentrations of cholesterol are reproduced in Table VIII. The data in Table VIII demonstrate the validity of the linear formalism, linear laws and Onsager's reciprocal relations.

The variation of conductivity coefficients  $L_{ik}$  with the concentration of cholesterol (Table VIII) was found to be in accordance with Kesting's hypothesis, i.e. the values of  $L_{ik}$  decrease with increasing concentration of cholesterol up to the CMC, at which the complete liquid membrane is formed in series with the supporting membrane. Beyond the CMC the values of  $L_{ik}$  become more or less constant. A typical plot in the case of the hydraulic conductivity coefficient  $L_{11}$  is reproduced in Figure 13. Agreement between the computed values of the coefficient  $L_{ik}$  using eq 95 and the experimental values further indicated that the data (Table VIII) are consistent with the phenomenon of liquid membrane formation in accordance with Kesting's hypothesis. In the case where both compartments C and D of the transport cell (Figure 12) were filled with a cholesterol solution of concentration equal to its CMC it was possible to use the data to demonstrate the formation of liquid membrane bilayers on the supporting membrane. By using Kedem and Katchalsky's theory of the permeability of the series composite membrane<sup>36,199</sup> it was possible to deduce the following relationship:<sup>174</sup>

$$R_{ik}^* = 2R_{ik}^s - R_{ik}^c \quad (96)$$

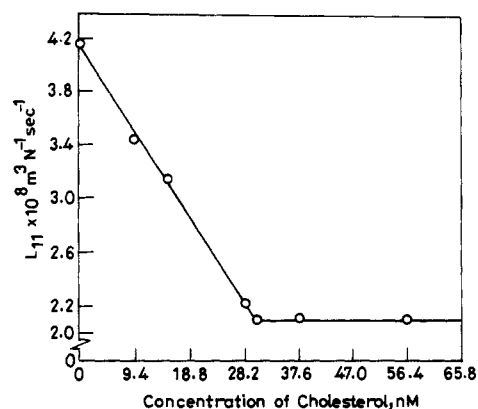
where  $R_{ik}^*$  stands for the resistance coefficient of the series composite membrane consisting of the supporting membrane plus the two layers of the liquid membrane,



Table VIII. Values of Phenomenological Coefficients at Different Concentrations of Cholesterol<sup>a</sup>

concentration (nM)	$L_{11} \times 10^8 \text{ (m}^3 \text{ N}^{-1} \text{ s}^{-1}\text{)}$	$L_{12} \times 10^6 \text{ (m A J}^{-1}\text{)}$	$L_{21} \times 10^6 \text{ (m A J}^{-1}\text{)}$	$L_{22} \times 10^8 \text{ (ohm}^{-1}\text{)}$
0.0	$4.17 \pm .008$	$5.36 \pm .03$	$5.36 \pm .12$	$2.62 \pm .17$
9.4	$3.43 \pm .03$	$4.65 \pm .05$	$4.67 \pm .03$	$2.31 \pm .14$
15.04	$3.14 \pm .02$	$3.99 \pm .03$	$3.99 \pm .06$	$2.07 \pm .11$
28.02	$2.22 \pm .03$	$2.83 \pm .02$	$2.85 \pm .04$	$1.78 \pm .08$
30.08 (CMC)	$2.11 \pm .04$	$2.62 \pm .04$	$2.60 \pm .04$	$1.63 \pm .07$
37.6	$2.13 \pm .03$	$2.63 \pm .04$	$2.62 \pm .04$	$1.57 \pm .06$
56.4	$2.14 \pm .01$	$2.61 \pm .02$	$2.59 \pm .01$	$1.51 \pm .06$
b	$1.34 \pm .04$	$1.70 \pm .03$	$1.67 \pm .04$	$1.26 \pm .04$

<sup>a</sup> Taken from ref 17. <sup>b</sup> Values for the system when both compartments C and D were filled with cholesterol solution of concentration equal to its CMC.

Figure 13. Variation of  $L_{11}$  with the concentration of cholesterol.<sup>174</sup>Table IX. Values of Various Resistance Coefficients  $R_{ik}$ 

resistance coefficients	computed values using eq 96	exptl values
$R_{11}^* \times 10^{-7} \text{ (m}^{-3} \text{ N s)}$	$7.10 \pm .16$	$7.47 \pm .23$
$-R_{12}^* \times 10^{-2} \text{ (m}^{-1} \text{ A}^{-1} \text{ J)}$	$10.33 \pm .31$	$9.79 \pm .42$
$-R_{21}^* \times 10^{-2} \text{ (m}^{-1} \text{ A}^{-1} \text{ J)}$	$10.23 \pm .40$	$9.62 \pm .36$
$R_{22}^* \text{ (ohm)}$	$8.41 \pm .26$	$7.92 \pm .25$

<sup>a</sup> Taken from ref 174.

one on either side of it. Values of the various resistance coefficients  $R_{ik}^*$  computed using eq 96 were shown to be in agreement with the experimental values (Table IX). This agreement is consistent with the formation of the liquid membrane bilayers generated by cholesterol.

Jain and colleagues<sup>193,194</sup> have also substantiated the linear formalism of electroosmosis through liquid membranes generated by cholesterol via their studies on electrokinetic energy conversion. The conclusions reached using the nonequilibrium thermodynamic theory of electrokinetic energy conversion were verified. In one of their papers<sup>193</sup> they used Srivastava and Jakhar's data,<sup>174</sup> whereas in the other study they generated their own data.

The electrochemical characterization of cholesterol liquid membranes in series with a cellulose acetate supporting membrane has been attempted by Singh and Tiwari.<sup>200,201</sup> Singh and Tiwari<sup>202</sup> have also conducted hydrodynamic and electroosmotic transport studies on cholesterol liquid membranes (supported on cellulose acetate membranes) with varying concentrations of sodium chloride and pH. Rizvi and Zaidi studied electrokinetic effects using sintered glass membrane impregnated with single lipid or lipid mixtures<sup>203-206</sup> and verified the linear formalism of non-

equilibrium thermodynamics. However, although the lipid filled pores of the sintered glass membranes they used do constitute a liquid membrane system, they are quite different from the liquid membrane systems, discussed above, generated using Kesting's hypothesis. Thus, the biological relevance of the liquid membrane systems studied by Rizvi and Zaidi remains only tangential. Nonetheless, these experiments constitute another example where the nonequilibrium thermodynamic formalism of electroosmotic effects has been vindicated in the linear region.

The next important category of electroosmotic studies using liquid membranes is on the phenomenon of photoosmosis which, as we will, see is defacto photoelectroosmosis.

## 2. Photoelectroosmosis

The first report of light-induced water permeation was made by Tien and coworkers.<sup>171,173</sup> These authors experimented with chloroplast BLMs. More elaborate studies on this phenomenon have been carried out by other groups.<sup>176,177,180,182,184,186,207</sup> Srivastava and associates have experimented with liquid membrane bilayers generated by photoactive biological materials.<sup>176,177,180,182,184,186</sup> Rastogi and associates<sup>207</sup> made an in-depth study of chlorophyll pigments incorporated in cellulose acetate membranes, prepared using evaporation techniques. The former group set out to demonstrate the workability of the liquid membrane bilayer system as biomembrane mimetic system. Since light-induced volume flow is mimicked on chloroplast BLMs, Srivastava and associates tried to demonstrate that the same can be achieved on liquid membrane bilayer systems generated by chloroplast extract and similar materials.

Chloroplast extract is known to be surface active in nature<sup>208</sup> and hence is capable of generating liquid membranes in accordance with Kesting's hypothesis. The liquid membrane bilayers generated by chloroplast extract did show photoosmosis,<sup>176,177,184,186</sup> i.e. light-induced volume flow. The liquid membrane bilayers generated from hemoglobin which is structurally similar to chlorophyll—the main light absorbing material in chloroplast extract—is known to be surface active<sup>209</sup> and photoconducting.<sup>210,211</sup> This observation coupled with the data on variation of photoosmotic velocity with the wave length of exciting light led to the suggestion that light absorption by porphyrins, which are present in both chloroplast extract and hemoglobin, may be responsible for the observed phenomenon of photoosmosis. This being so, protoporphyrin, alone, should not only exhibit photoosmosis but should also reproduce



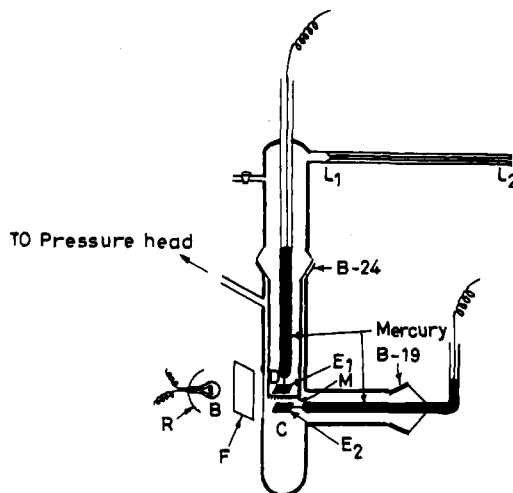


**Figure 14.** The photoosmosis transport cell. The thick lines indicate the blackened portions, R, reflector; B, 100-W bulb; F, optical filters; E<sub>1</sub> and E<sub>2</sub>, platinum electrodes; M, the cellulose acetate microfiltration supporting membrane (Sertorius catalog no. 11107).<sup>177</sup>

the trends in photoosmotic velocity observed in the case of liquid membrane bilayers generated from chloroplast extract and from hemoglobin which in turn should match with the trends reported in the case of chloroplast BLMs. The liquid membrane bilayers generated from protoporphyrin<sup>177</sup> and also from cytochrome C<sup>180</sup> showed positive results. Cyanobalamin whose central structure—the “Corrin” ring system—is very similar to that of porphyrin also exhibited photoosmosis with trends similar to those observed in case of chloroplast extract, hemoglobin and protoporphyrin.<sup>177</sup>

The experimental setup used to study the phenomenon of photoosmosis is depicted in Figure 14. The distance between the light source and the cell was kept fixed. To alter the intensity of the exciting light different voltages were fed to the light source. Wavelengths were varied by interposing suitable optical filters between the light source and the cell. To measure the photoosmotic velocity, compartments C and D of the transport cell (Figure 14) were filled with an aqueous solution of the photoactive material, e.g. chloroplast extract at a concentration slightly higher than its CMCs, along with the desired concentrations of electron donors in compartment D and electron acceptors in compartment C. Formation of liquid membrane bilayers on the supporting membrane was demonstrated using hydraulic permeability data.<sup>174,175,177</sup> The light was switched on after ensuring that  $\Delta P = 0$ , and the movement of the liquid meniscus in the capillary  $L_1L_2$  with time was noted. To demonstrate that the observed moment of the liquid meniscus in the capillary  $L_1L_2$  (Figure 14) was due only to the light-induced electrical potential difference across the membrane and not due to the thermal gradients produced across the membrane due to light absorption, it was shown that during photoosmotic movement if electrodes E<sub>1</sub> and E<sub>2</sub> were short circuited the photoosmotic movement of the meniscus in the capillary  $L_1L_2$  (Figure 14) stopped instantaneously and on reopening the short circuit it recommenced. The fact that the observed movement cannot be due to thermal effects is also obvious from another observation. As soon as the light was switched

on, instantaneous movement of the liquid in the capillary  $L_1L_2$  was noticed and as soon as the light was switched off the flow stopped immediately. Since establishment and abolition of thermal gradients cannot be an instantaneous process, the observed light-induced flow cannot be due to a thermal effect.

A general observation in these experiments was that the direction of the photoosmotic flow was always from the illuminated compartment to the dark compartment which is in agreement with Tien's observation for chloroplast BLMs. He explained his results in terms of semiconductor physics and classical electrokinetics,<sup>171,212,213</sup> invoking the production of electrons and holes on asymmetric illumination of the BLM leading eventually to a potential difference across the membrane. The light-induced voltage across the BLM was considered to be the primary driving force in photoosmosis.

A similar explanation was put forward in the case of liquid membrane bilayers to account for the origin of the effect and the direction of the flow.<sup>177</sup> For example, the chloroplast liquid membrane bilayer on light excitation ejects electrons which are captured by electron acceptors, e.g. Fe<sup>3+</sup> ions present in the illuminated compartment. In these experiments the illuminated compartment always contained an electron acceptor and the dark compartment an electron donor. On reduction of the Fe<sup>3+</sup> ions by photoelectrons or hydrated electrons, an electrical double layer is generated which consists of a layer of anions in the solution—the mobile phase of the double layer and a layer of positively charged oxidized chloroplast in the membrane phase. Since the illuminated compartment where the electrons are generated due to the action of light is negative with respect to the dark compartment, the negatively charged mobile phase of the double layer moves from the illuminated compartment to the dark compartment.

The magnitude of the electrical potential difference developed across the pigmented BLMs when it is illuminated from one side is known<sup>212</sup> to be enhanced in asymmetrical systems, e.g. when different redox chemicals are present in the two bathing solutions separated by the pigmented BLM. Since the light-induced electrical potential difference across the membrane is the primary driving force for the observed photoosmotic flux, the magnitude of the photoosmotic velocity should vary with the choice and concentration of the redox chemicals in the two compartments of the transport cell. It was observed<sup>177</sup> that: (i) The stronger the electron acceptor is in the illuminated compartment, the greater the value of the photoosmotic velocity. (ii) The higher the concentration of the electron acceptor is in the illuminated compartment, the greater the magnitude of the photoosmotic velocity. (iii) When an external electric field was applied across the membrane, making the illuminated compartment positive with respect to the dark compartment, the magnitude of the photoosmotic velocity increased with the increase in the value of the externally applied voltage.

All these observations are in agreement with those reported on BLM and do not contradict Tien's mechanism on the basis of semiconductor physics and classical electrokinetics, although one may have some reservations about the semiconductor mechanism.

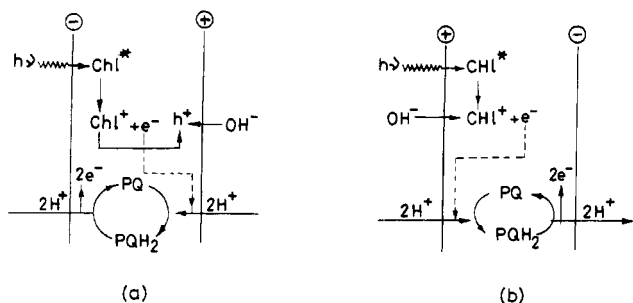


**Figure 15.** Model of chlorophyll membranes (a) at high pH and (b) at low pH; Chl\* is excited chlorophyll, Chl<sup>+</sup> is positively charged chlorophyll, PQ is plastoquinone, and PQH<sub>2</sub> is plastoquinone.<sup>207</sup>

In the case of chloroplast BLMs, the open-circuit photovoltages ( $E_{op}$ ) are known to vary with the intensity ( $I$ ) of exciting light in the following manner:<sup>212</sup>

$$E_{op} = \ell \log[1 + (I/L)] \quad (97)$$

where  $\ell$  and  $L$  are constants for a given chloroplast BLM at a given temperature. Under conditions of low intensities,  $E_{op}$ , becomes directly proportional to  $I$  as has indeed been found to be the case for liquid membrane bilayers.<sup>179</sup> One implication of this is that the photoosmotic velocity should vary both linearly and proportionally with the intensity of the exciting light in regions of low intensities. This indeed was found to be the case.<sup>177</sup>

The variation with the wavelength of the exciting light revealed that the magnitude of the photoosmotic velocity was at a maximum at 400 nm which is the well-known Soret band for porphyrins.<sup>214,215</sup> This observation suggests that all substances having a porphyrin ring in their structure should exhibit the phenomenon of photoosmosis which indeed was found to be the case.

Rastogi and associates<sup>207</sup> have also studied the phenomenon of photoelectroosmosis through cellulose acetate membranes impregnated with chlorophyll pigments and other relevant materials, e.g.  $\beta$ -carotene, xanthophyll, anthraquinone, benzoquinone, etc., as well as measured photoinduced potential differences and currents. The overall trends were consistent with the trends reported in earlier studies.<sup>171,173,176,177,179</sup> In these studies<sup>207</sup> it was also observed that the direction of flow was always from the illuminated compartment to the dark compartment. The major point of difference in Rastogi et al.'s<sup>207</sup> report was with respect to the explanation offered for the origin of the effect and direction of the flow. An alternative mechanism to explain their observation<sup>207</sup> involved the pH dependence of the photoinduced potentials and currents. Unlike the earlier model,<sup>171,173,177</sup> Rastogi et al.<sup>207</sup> did not consider the simultaneous generation of an electron and a hole (pair) necessary. Since they found photopotentials and photocurrents to be pH dependent they envisaged the participation of both electrons and hydrogen ions in the phenomenon. Their model for charge separation is schematically depicted in Figure 15. Figure 15a represents the situation when the membrane is in contact with an alkaline medium while Figure 15b represents the state of affairs when the bathing medium is acidic. Plastoquinone shown in the scheme (Figure 15) is always present in the system as an impurity.

Photoosmotic studies have also been conducted on liquid membrane bilayers generated by bacteriorhodopsin.<sup>182</sup> The trends observed were quite similar to those observed on the chloroplast extract liquid membrane bilayers.<sup>177</sup> The explanation offered for the origin of the effect in the case of bacteriorhodopsin was quite similar to that offered for chloroplast extract liquid membrane bilayers. One difference was that, when the bacteriorhodopsin membranes were asymmetrically illuminated, protons were pumped into the illuminated compartment, whereas the chloroplast extract/chlorophyll membranes pumped electrons into the illuminated compartment.

The phenomenon of photoosmosis is therefore a light-induced electroosmosis (photoelectroosmosis). The relevant nonequilibrium thermodynamics are not clear. Since photopotential differences across the membranes are proportional to the intensity of the exciting light and the photoosmotic velocity is proportional to the intensity of the exciting light one can only say that the linear law for the photoelectroosmotic velocity is possibly obeyed. Hence formulating linear phenomenological relations for photoelectroosmotic phenomena, investigating their domain of validity, and demonstrating the validity of Onsager's reciprocal relations are gaps which need to be filled.

### 3. Electroosmosis in Plant Physiology

The circulation of fluids in plants is a well-known thoroughly studied phenomenon. Fensom<sup>216</sup> was the first to suggest that the circulation may be electroosmotically driven. The electrical potential differences required for the purpose are caused by the diffusion of hydrogen ions which is metabolically regulated. Subsequent studies<sup>217</sup> on sunflowers showed that correlations do exist between transport patterns and biopotential patterns and that the measured changes in liquid flow may be interpreted in terms of prior electrical changes. Fensom<sup>218</sup> argued that the production of continuous potentials across membranes in plant tissues is due to the circulation of hydrogen ions. Of the three types of membranes which occur generally in plant cells, lipid, protein, and cellulose, a protein-coated grid of cellulose can be envisaged as surrounding the cells. Such membranes were suggested as having the right pore size and properties to allow almost unfettered hydrogen ion diffusion at the same time as permitting intercell biopotentials to be built up. Spanner put forward a theory<sup>219</sup> to account for the translocation of sugars in sieve tubes in terms of electrokinetic forces developed in the cytoplasm of the sieve plates. It was suggested that potassium plays a major role responsible for both the solution movement and for being the necessary potential across the sieve plates. A more elaborate account of the theory based on potassium ions is found in Spanner's review.<sup>220</sup>

Measurements<sup>221</sup> on *Nitella translucens* showed that there could be an electroosmotic transport of the order of 100 mol of water per Faraday in the direction of positive ion flow. This implies that the existence of water filled charged pores through the plasmalemma and tonoplast of the *Nitella* cell. However it was finally concluded that the pores available for ion movement are far too few to account for the high water permeability of the cell membrane, and the possible extra turgor

pressures which might be produced by electroosmotic flow could not be more than  $10^{-4}$  atm. Dainty, Croghan, and Fensom<sup>222</sup> used nonequilibrium thermodynamic expressions of electrokinetic phenomena and concluded that: (i) the pressure contribution of electroosmosis to the turgor of *Nitella* or *Chara* cells is found to be negligible, (ii) the power used by an electroosmotic pump can never be less than that used by a pressure mechanism, (iii) electroosmosis may account for the discrepancies between the calculation of membrane conductance using tracer ion fluxes and those using applied potential differences, and (iv) the streaming potential developed by pressure across biological membranes would be too small to detect but in large pores such as xylem or phloem vessels or in cell walls, small pressures would result in easily measured potentials.

Fensom et al. have collected evidence to substantiate their viewpoint on the role of electroosmosis in the transport of water in plants/turgidity of the cell. An attempt was made to induce water transport in sections of roots of lens through the application of electrical potential differences<sup>223</sup> using currents of between 3 and 50  $\mu$ amp. The efficiency of water transport was found to be of the order of 20 to 80 water moles per Faraday in living roots and 4–6 times more in dead roots, the highest efficiency coinciding with the best conductivity in the zone of elongation. The electroosmotic transport coefficient was shown to possess tensorial character which, in part, appeared to be linked with the asymmetry of the plant material. From the low magnitudes of the electrical currents used in the electroosmosis experiments ( $<10$   $\mu$ amp) it was concluded that the phenomenon might persist down to the physiological level where currents of the order of  $10^{-7}$  amp  $\text{cm}^{-2}$  may be expected according to bioelectrical measurements on roots. For example, the results of Pilet and Meylan<sup>224</sup> for lens, of Scott et al.<sup>225</sup> for *Vicia faba*. Thus, although Fensom et al.<sup>223</sup> could not produce evidence to support the view that a specialized tissue may be responsible for conducting appreciable quantities of water electroosmotically, their studies<sup>223</sup> did indicate the possibility of small quantities of water and some organic substances moving around the cells in the living root under the drive of natural biopotential gradients which are already known to exist there.

Fensom and Wanless<sup>226</sup> have estimated the pore density in samples of *Nitella* (both transleucens and flexiles) using electroosmotic transport data for water and cations, sodium and potassium. In each species the electroosmotic efficiency was found to be greater with  $\text{Na}^+$  ions than with  $\text{K}^+$  ions. The effect of indol-3-ylacetic acid (IAA) on the electroosmotic efficiency was also investigated. IAA in the concentration range  $10^{-4}$ – $10^{-5}$  M tended to decrease the electroosmotic efficiencies while IAA after a 30-min treatment produced a significant increase in water flow into the treated end of the living cell. Calculations suggested that about  $10^8$ – $10^9$  pore sites per  $\text{cm}^2$  exist on the surface membranes for  $\text{Na}^+$  or  $\text{K}^+$  ion transport.

Investigations of the electroosmotic mechanism of phloem transport using the formalism of nonequilibrium thermodynamics have been made by Fensom et al.<sup>227,228</sup> and Spanner.<sup>229</sup> Two theories of electroosmotic translocation in phloem have been proposed. These theories differ primarily in the pathway envisaged for

the electric current. Fensom<sup>216,218</sup> proposed a continuous circulation of "sap carrying" ions down the entire length of the phloem tissue or at least down the length of several sieve tubes. Spanner,<sup>219</sup> on the other hand, envisaged a microcirculation of "sap carrying" ions in which the ions followed a more or less a circular pathway between the sieve plates and companion cells which supply the driving force. The flow dynamics of both theories has been treated quantitatively using nonequilibrium thermodynamics.<sup>228,229</sup> The plausibility of the electroosmotic theory by Fensom<sup>216,218</sup> rests upon the magnitude of the cross coefficient measuring of electroosmotic velocity.

From the nonequilibrium thermodynamic analysis<sup>228</sup> it appears that a high value of electroosmotic efficiency could favor the electroosmotic theory because it could correspond to a high value of the cross coefficient representing electroosmotic velocity. However, this may not always be true because, as has been shown by Tyree and Spanner<sup>230</sup> in *Nitella* cell walls,  $(J_v/I)$  increases as the saline concentration decreases in spite of the fact that the cross coefficient representing electroosmotic velocity decreases because the straight coefficient representing electrical conductivity decreases much faster. If the electroosmotic mechanism of the type proposed by Fensom<sup>216,218</sup> is dominant and if the distance measured downstream is taken as positive, then the potential gradient measured in phloem in situ must be positive. If, however, the pressure flow mechanism is dominant, then the potential gradient in situ should be negative. These facts, of course, should be ascertained by independent observation. It should be emphasized that in Fensom's electroosmotic mechanism one has to consider current flux,  $I$ , down the entire length of the phloem while in Spanner's<sup>219,229</sup> electroosmotic mechanism it is postulated that a finite microcirculation of current can exist while the potential gradient is negative.

Tyree and Fensom<sup>228</sup> measured the phenomenological coefficients on cut and uncut phloem and cut xylem strands of *Heracleum mantegazzianum* and analyzed the data using the nonequilibrium thermodynamic formalism to check if these coefficients are indeed constant over reasonable ranges of the thermodynamic forces and also to check the validity of the Onsager's relations. They also attempted to measure the potential gradient on conducting (but laterally detached) phloem bundles in order to gain insight into the possible translocation mechanism by following the reasoning based on nonequilibrium thermodynamics. The authors,<sup>228</sup> themselves, point out that their measurements and data are tentative since the blockage of the sieve plates is an interfering factor. However, if these are valid, the conclusion would be that neither a pressure flow nor an electroosmotic flow mechanism encompassing a long distance current pathway can substantially contribute to the transport in mature phloem. Measurement of biopotentials along conducting, laterally detached phloem bundles of *Heracleum* suggest, nevertheless, that there may be a small electroosmotic component of at least  $0.1$  mV  $\text{cm}^{-1}$  endogenous in the phloem.

Spanner<sup>229</sup> critically discusses Tyree and Fensom's experiments<sup>228</sup> in the context of the electroosmotic theory of phloem transport. He used the phenome-

nological equations written in the inverted matrix form, making use of Kedem and Katchalsky's theory for the permeability of composite membranes<sup>36</sup> and Spiegler's frictional model.<sup>62</sup> He claims<sup>220,229</sup> that his theory "remains almost the only theory offering a plausible suggestion for the presence of several peculiar features of the sieve tube, in particular the slime fibrils and the high concentration of potassium".

Spanner has also criticized<sup>231,232</sup> the pressure flow hypothesis on the grounds that there is little foundation for the belief that the sieve plate pores in functioning phloem are open and quite free from obstruction.

On the other hand, Fensom et al. present evidence<sup>227,233-236</sup> which does not corroborate the electroosmotic theory. They propose a new theory<sup>233</sup> in which sucrose transport occurs in two chief modes—the first is based on the microperistaltic movement of contractile lipoprotein which is thought to extend axially through the sieve tube, the second is a mass flow of the solution around the contractile microfibrillar material but chiefly activated by it in addition to a third small surface layer component of translocation.

Although, the electroosmotic theory of phloem transport remains to be fully clarified it is clear that as pointed out by Tyree and Fensom,<sup>228</sup> non-equilibrium thermodynamics provides a powerful tool for transport studies in plant system.

#### 4. Electroosmosis in Animal Physiology

Electroosmosis in the axons of freshly killed squids has been studied.<sup>237</sup> Nerve axons were tested within 40 min of their removal from the living animal and the results closely approach measurements in the living state. Electroosmotic efficiency for water molecules was measured and the general conclusions/observations were as follows: (i) the direction of water flow was always toward the negative electrode, (ii) the flows were reversible, (iii) a mean of 28 molecules of water per positive charge is transported at 21–22 °C (a value which seems to be appreciably greater than the water of hydration), (iv) the results indicate that the zeta potential in the nerve membrane was negative, and (v) pores do exist in nerve membranes. Experiments indicate that the electroosmotic efficiency is constant and the linear formalism of nonequilibrium thermodynamics is applicable.

Measurements of electroosmotic flow through biological membranes have been made. Electroosmosis has been considered as being small in biological membranes. On the other hand, the osmotic pressure difference has been estimated as playing an important role in water transport. The streaming potential and other apparent electrokinetic phenomena were investigated by Wedner and Diamond,<sup>238</sup> who attributed it to unstirred layer effects. However, Hill<sup>239</sup> has emphasized the theoretical role of electroosmosis in fluid transport in this epithelial model. There is no experimental support of the model since electroosmotic measurements are difficult. Miyamoto et al.<sup>240-242</sup> have measured electroosmotic flow using the oscillation method. In a recent experiment by Miyamoto et al.,<sup>243</sup> electroosmotic flow was evoked by an externally applied oscillating field. It was measured directly using a photodiode or indirectly using a pressure transducer. Flow increased in proportion to the amplitude of the

applied rectangular electric potential in the ratios 5.2 nL s<sup>-1</sup> cm<sup>-2</sup> V<sup>-1</sup> in skin and 11.5 nL s<sup>-1</sup> cm<sup>2</sup> V<sup>-1</sup> in gastric mucosa. In a pH 7.4 Ringer solution, skin behaved as a cation exchange membrane but gastric mucosa behaved as an anion exchange membrane. The effect of drugs such as cimetidine and histamine on the electroosmosis in gastric mucosa was also investigated. In order to compare the electroosmotic driving force with the osmotic driving force, the electroosmotic flow was measured against the finite osmotic flow. The balanced potentials were -241 mV/200 mosM sucrose gradient in frog skin and 156 mV/100 mosM sucrose gradient in gastric mucosa. The most surprising observation was that the osmotic driving force of milliosmolar order could be compared with the electric driving forces of millivolt order. Thus there is no valid reason for ignoring electroosmotic effects. The electroosmotic coupling is so large that it cannot be ignored in discussing the water transport mechanism in epithelia.<sup>243</sup> Mechanosensitive currents in single neurons have been reported recently.<sup>244</sup> However, it is not clear whether or not it is in fact a case of the streaming (electrokinetic) effect.

#### 5. Iontophoresis

We have decided to include this section in view of the considerable interest in transdermal drug delivery and the possible relationship with electroosmosis.<sup>245-247</sup> The electrical driving of charged molecules into tissues is related with iontophoresis which has applications in dentistry, ophthalmology, surgery, and general medicine. There is considerable enhancement of transport via iontophoresis over that observed in conventional transdermal or "passive transport" of the same compound.<sup>248,249</sup> The iontophoretic transport of a negatively charged bone resorption agent etidronate disodium [1-hydroxyethylidenebis(phosphonic acid), EHDP] has been investigated<sup>250</sup> by Kasting et al. An enhancement factor of 50–70 over passive diffusion was obtained using a constant current density of 140  $\mu$ A cm<sup>-2</sup> and a factor of approximately 100 was obtained using a constant voltage of -0.5 V. Normally it is believed that enhanced transport is the direct result of the increased driving force resulting from the action of the electric field on the ionic solute. However, Gangarosa et al.<sup>251</sup> observed increased transport of normally neutral species on application of an electric field. Furthermore, Burnette et al.<sup>252,253</sup> demonstrated enhanced transport of a neutral thyrotropin releasing hormone and mannitol when delivered from the anode compartment of the apparatus. Electroosmotic flow was suggested as a possible mechanism responsible for the transport of neutral species.

As far as nonequilibrium thermodynamics is concerned there is no inconsistency in the above suggestion. Macroscopic thermodynamics does not place any restriction on the model. However, the hypothesis based on electrical double-layer theory may require clarification about the nature of the double layer. On the other hand the frictional model, discussed earlier in this article, could account for the observation. Further confirmation is obviously necessary.

#### E. Electrophoretic Effects<sup>254-256</sup>

Before we close this section on the studies in the linear region we will describe representative studies on the

nonequilibrium thermodynamics of electrophoresis and sedimentation potential. The first and most representative studies by Rastogi et al.<sup>254-256</sup> are described below.

Consider a system having a neutral fluid between two electrodes 1 cm apart. Insoluble solid particles of a definite size are allowed to fall under gravity in the medium in a tube of radius  $r$ . The potential energy is converted into electrical energy, and a sedimentation current flows. Alternatively, when an electric field is applied, particles move giving rise to the phenomenon of electrophoresis.

For a two-component system, e.g. a neutral fluid and glass particles, the change in concentration  $C_k$  of component  $k$  is given by

$$\rho(dC_k/dt) = -\text{div } \mathbf{J}_k \quad (k = 1, 2) \quad (98)$$

where  $\rho$  is the density and  $\mathbf{J}_k$  is the mass flow per unit area. It is convenient to define it with respect to velocity of the center of mass  $\bar{\mathbf{V}}$  i.e.

$$\mathbf{J}_k = \rho_k (\mathbf{V}_k - \bar{\mathbf{V}}) \quad (99)$$

where  $\rho_k$  is the density of the component  $k$ .

According to deGroot, Overbeek, and Mazur<sup>257</sup> entropy production  $\sigma$  is given by the equation

$$T\sigma = \sum_{k=1}^n \mathbf{J}_k \cdot \mathbf{X}_k \quad (100)$$

where the forces  $\mathbf{X}_k$  are given by

$$\mathbf{X}_k = e_k \mathbf{E} + g - (v_k \text{ grad } \mu_k) \quad (101)$$

where  $e_k$  is the charge per unit mass of species  $k$ ,  $\mathbf{E}$  is the electric field,  $g$  is the gravitational field per unit mass and  $\mu_k$  is the chemical potential of the species  $k$ . In eq 100  $\mathbf{J}_k \cdot$  are fluxes to a mean volume reference velocity.<sup>1</sup> At a constant temperature eq 101 reduces to

$$\mathbf{X}_k = e_k \mathbf{E} + g - (v_k \text{ grad } P) \quad (102)$$

where  $v_k$  is the partial specific volume of component  $k$ . Since the total volume flow through a section vanishes

$$\sum_{k=1}^n v_k \mathbf{J}_k \cdot = 0 \quad (103)$$

Hence for a two-component system

$$T\sigma = \mathbf{J}_1 \cdot \{e_1 \mathbf{E} [1 - (v_1/v_2)(e_1/e_2)] + [1 - (v_1/v_2)]g\} \quad (104)$$

The subscript 1 refers to pyrex glass particles and subscript 2 to the medium. It follows from eq 104 that for the two fluxes, i.e. electric current density  $\mathbf{I}$  and mass flow  $\mathbf{J}$ , given by the equations

$$\mathbf{I} = e_1 \mathbf{J}_1 \cdot [1 - (v_1/v_2)(e_2/e_1)] \quad (105)$$

$$\mathbf{J} = \mathbf{J}_1 \cdot [1 - (v_1/v_2)] \quad (106)$$

the corresponding conjugate forces are  $\mathbf{E}$  and  $g$ , respectively. Therefore, the linear phenomenological equations can be written as

$$\mathbf{J} = L_{11}g + L_{12}\mathbf{E} \quad (107)$$

$$\mathbf{I} = L_{21}g + L_{22}\mathbf{E} \quad (108)$$

with  $L_{12} = L_{21}$  because of Onsager's relations. From eqs 107 and 108 it follows that

$$L_{21} = -(E/g)_{I=0} L_{22} \quad (109)$$

and

$$L_{12} = (J/E)_{g=0} \quad (110)$$

In eqs 107-110,  $E = (\Delta\phi/l)$  where  $\Delta\phi$  is the electrical potential difference and  $l$  is the distance between the two electrodes. The coefficient  $L_{22}$  is related to the conduction and hence  $L_{21}$  can be estimated from the measured values of sedimentation potential. To estimate  $L_{12}$  one can measure  $\mathbf{J}$  using the following equation

$$\mathbf{J} = m[1 - (\rho_2/\rho_1)]\mathbf{V}_e \quad (111)$$

where  $m$  is the mass per unit volume of the particles suspended between the two electrodes and  $\mathbf{V}_e$  is the electrophoretic velocity ( $\text{cm s}^{-1}$ ). If  $r$  is the radius of the particles,  $n$  the number of particles suspended between the two electrodes, and  $v$  the volume,  $m$  would be equal to  $^{4/3}n\pi r^3/(1/V)$  provided the particles are assumed to be spheres. Since  $m$  and  $\mathbf{V}_e$  can be known experimentally  $L_{12}$  can be estimated.

Expressions for electrophoretic velocity  $\mathbf{V}_e$  and for the sedimentation potential  $E$ , as obtained from the classical theory based on the electrical double layer<sup>258</sup> are written as

$$\mathbf{V}_e = (\epsilon\zeta\mathbf{E})/(4\pi\eta) \quad (112)$$

and

$$E = [(\epsilon\zeta)/(4\pi\eta\lambda)](n/V) (^{4/3})\pi r^3(\rho_1 - \rho_2)g \quad (113)$$

where  $\eta$  is the viscosity of the medium,  $\epsilon$  is its dielectric constant,  $\zeta$  is the zeta potential of the interface, and  $\lambda$  is the specific conductivity. From eqs 109-113, it follows that<sup>254</sup>

$$L_{12} = L_{21} = [(\epsilon\zeta)/(4\pi\eta)](n/V)(^{4/3})\pi r^3\rho_1[1 - (\rho_2/\rho_1)] \quad (114)$$

showing that the classical theory is consistent with the nonequilibrium thermodynamic theory.

Rastogi et al.<sup>254,255</sup> have provided an experimental proof of Onsager's relations by measuring the sedimentation potential and electrophoretic velocity. They experimented<sup>254,255</sup> with Pyrex-water, Pyrex-acetone, and quartz-water systems. Since the experimental assembly and the procedures were ingeniously designed, they merit description.

The experiments, as the theory requires, must be carried out on particles of same shape and size. Particles of different size were obtained by grinding Pyrex/quartz and passing through sieves of different mesh. These particles were then allowed to fall through a water column and those sedimenting at different time intervals were collected. The sedimentation column, the optical assembly, and the amplification unit used in the measurements are shown in Figures 16-18. In order to measure the sedimentation potential, the particles were allowed to fall freely in the medium, the total time  $t_1$  taken by the weighed amount  $w$  of the particles to flow from a particular point was noted using a stopwatch. Since glass/quartz particles were not visually observable, their movement was noted by using an optical assembly. A beam of light was allowed to fall horizontally on the vertical sedimentation column and also on the photocell which recorded the intensity of light (Figure 17). A deflection in the galvanometer

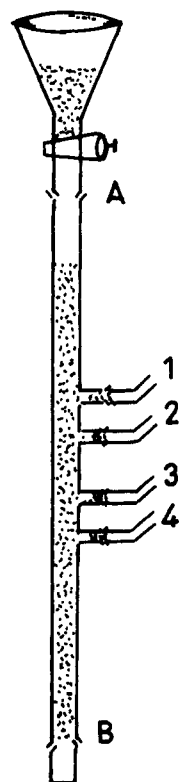


Figure 16. Sedimentation column. A, B, 1, 2, 3, and 4 are ground-glass standard joints.<sup>254</sup>

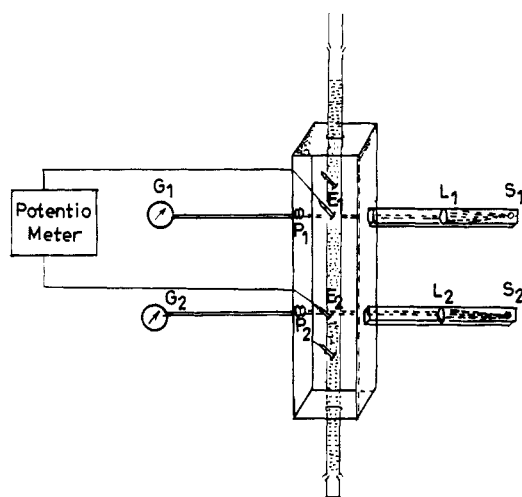


Figure 17. Assembly for the measurement of sedimentation potential and sedimentation rate.  $S_1$  and  $S_2$  are light sources;  $L_1$  and  $L_2$ , double convex lenses;  $P_1$  and  $P_2$ , photocells; and  $G_1$  and  $G_2$ , scalamp galvanometers.<sup>254</sup>

was observed when the particles passed through the region. In this manner time  $t_1$  was measured. The quantity  $w/t_1$  gave the rate of flow of the particles in grams per second. If  $t_2$  is the time taken by the particles to traverse the distance between two electrodes the amount of particles suspended between them would be ( $wt_2/t_1$ ).

The two electrodes, lower and upper, were connected to the potentiometer circuit. The particles were allowed to fall in the medium. The sedimentation potential developed immediately as the particles reached the lower electrodes, which was measured using the potentiometer with amplification units (Figure 18). The asymmetry potentials of the electrodes were taken into account while measuring the sedimentation potential.

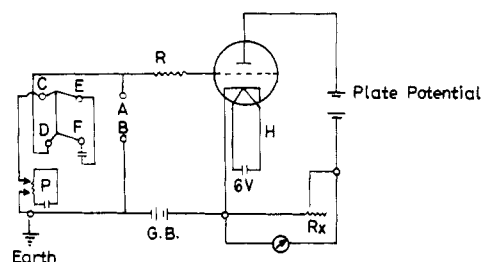


Figure 18. Circuit diagram for amplification of sedimentation current. G B is the grid battery; G, galvanometer; R, input resistance,  $R_x$ , variable impedance; P, potentiometer; and A-F are terminals of key.<sup>254</sup>

Table X. Test of Onsager's Relations (Temperature 35 °C)

run number	$L_{21} \times 10^{13}$ (A g cm <sup>-1</sup> erg <sup>-1</sup> )	$L_{12} \times 10^{13}$ (A g cm <sup>-1</sup> erg <sup>-1</sup> )
1	2.9	2.66
2	2.9	2.62
3	3.1	2.80
4	3.1	2.58
5	2.9	2.82
6	2.7	2.56
7	2.7	2.70

<sup>a</sup> Taken from ref 254 (from the data on electrophoretic velocity and sedimentation potential on Pyrex-water system).

Table XI. Validity of Onsager's Reciprocal Relation<sup>a</sup>

system	tempera- ture (°C)	$L_{21} \times 10^{13}$ (A g cm <sup>-1</sup> erg <sup>-1</sup> )	$L_{12} \times 10^{13}$ (A g cm <sup>-1</sup> erg <sup>-1</sup> )
Pyrex-acetone	30	$1.16 \pm 0.03$	$0.981 \pm 0.02$
	35	$1.32 \pm 0.03$	$1.15 \pm 0.02$
quartz-water	35	$2.26 \pm 0.02$	$1.96 \pm 0.05$

<sup>a</sup> Taken from ref 255 (from the data on electrophoretic velocity and sedimentation potential on quartz-water system).

To measure the electrophoretic velocity a fine suspension of particles (Pyrex/quartz) of known weight was prepared. The apparatus was half filled with this suspension. The medium was slowly added until its level was above the upper electrode. Great care was taken to avoid disturbances in the liquid column during addition of the medium to ensure the formation of a sharp boundary. The two electrodes were connected to an electronically operated stabilized dc power supply and movement of the boundary in the vertical sedimentation column was noted with time.

The coefficient  $L_{22}$  was estimated from the specific conductance values of the medium. The coefficient  $L_{21}$  was estimated using eq 109. In the estimation of  $L_{21}$  the value of  $g$  was calculated using the formula

$$g = 980.616 - 2.5928 \cos 2\varphi + 0.0069 \cos^2 2\varphi - 0.7086h \quad (115)$$

where  $\varphi$  is the latitude in degree and  $h$  is the altitude in kilometers. The coefficients  $L_{12}$  and  $L_{11}$  were estimated from the straight line plot of  $J$  against  $E$  the slope gave the value of  $L_{12}$  and the intercept gave the value of  $L_{11}g$  in accordance with eq 107.

Values of the cross coefficients as estimated from their experiments and recorded in Tables X and XI show that Onsager's relations are more or less obeyed. Equation 107 transformed using eq 111, i.e.



$$V_e = \frac{L_{12}}{m(1 - \rho_2/\rho_1)} \frac{\Delta\varphi}{1} + \frac{L_{11}}{m(1 - \rho_2/\rho_1)} g \quad (116)$$

was tested by plotting  $V_e$  against  $\Delta\varphi$ . For all three systems studied, Pyrex-water, Pyrex-acetone, and quartz-water, straight lines were obtained<sup>255,256</sup> showing the validity of the linear phenomenological equation. They also attempted to explore the domain of validity of linear laws in their systems. For example, in the case of the Pyrex-water system it was shown that  $L_{12}$  remains constant at least up to  $\Delta\varphi = 150$  V. The temperature dependence of the cross coefficients was also studied. It was found that an equation of the type

$$L_{21} = a + bT + cT^2 + \dots \quad (117)$$

where  $a, b, c$ , etc. are constants, represents the data on temperature variation. The reliability of their data<sup>255,256</sup> was tested by comparing the values of zeta potentials estimated using their data with those reported by other workers.

We close this section on the linear region with these studies on electrophoresis, which are probably the only ones from the nonequilibrium thermodynamic point of view, and pass on to the nonlinear region. Electrophoretic studies in the nonlinear region will also be included in this section.

#### IV. Nonlinear Region Studies

##### A. Nonlinear Flux Equations

The domain of validity of the Gibbs's equation is larger than those of the linear laws and Onsager's relations. Hence, within the extended domain, the fluxes would be a function of appropriate forces as chosen for linear laws. In view of this it is possible to extend the domain of validity of nonequilibrium thermodynamics by considering nonlinear phenomenological relations between fluxes and forces. From this point of view the major points of investigation, therefore, have been to discover (i) what exactly is the form of the phenomenological relations between fluxes and forces, (ii) what symmetry relations are obeyed by the phenomenological coefficients, and (iii) what is the origin of nonlinearity.

Nonlinearity in the near-equilibrium region may be of three types: (i) The linear laws may not be valid just beyond equilibrium. The typical examples are the soil-water system (bentonite water system) where even Darcy's law does not hold. (ii) Local nonlinearity, e.g. in the case of the Wien effect observed in the case of nonelectrolytes, where the Ohm's law is not obeyed or the case of chemical reactions where the linear law holds only asymptotically. (iii) Global nonlinearity may arise from the local phenomenological coefficients through the medium. In this section we are concerned mainly with global nonlinearity.

The first attempt to suggest the form of nonlinear phenomenological relations in the case of electroosmotic effects was made by Rastogi and Srivastava.<sup>29</sup> It was suggested that the nonlinearity may arise in the first instance due to nonconstancy of the cross coefficients. It was, intuitively suggested that nonlinear phenomenological equations for electroosmotic effects should be written as

$$\mathbf{J} = L_{11}\Delta P + L_{12}\Delta\varphi + \alpha(\Delta\varphi)^2 + \dots \quad (118)$$

$$\mathbf{I} = L_{21}\Delta P + L_{22}\Delta\varphi + \beta(\Delta P)^2 + \dots \quad (119)$$

where  $\alpha, \beta$ , etc. are constants.

$L_{ij}$ ,<sup>259</sup> using Taylor's expansion of flows around equilibrium, suggested that any flow  $\mathbf{J}_i$  can be expressed as a function of the forces  $X_1, X_2, \dots$  etc., in the following manner:

$$\mathbf{J}_i = L_{ij}X_j + \frac{1}{2} \sum_{j,k} L_{ijk} X_j X_k + \dots \quad (120)$$

where  $L_{ij}$  and  $L_{ijk}$  are the derivatives of various orders of  $\mathbf{J}_i$  given by

$$L_{ij} = \left( \frac{\partial \mathbf{J}_i}{\partial X_j} \right)_o, \quad L_{ijk} = \left( \frac{\partial^2 \mathbf{J}_i}{\partial X_j \partial X_k} \right)_o \quad (121)$$

where the subscript  $o$  represents the value of the derivative at equilibrium. It was shown that both Onsager's and the following symmetry relations

$$L_{ij} = L_{ji} \quad L_{ijk} = L_{jik} = L_{jki} \\ L_{ijkl} = L_{ijlk} = L_{ikjl} = L_{jilk} \quad (122)$$

should follow as a mathematical consequence.

The equalities eq 122 would only be valid provided the flux equations can be expressed as a Taylor series and the coefficients are the limiting derivatives for equilibrium. In fact the phenomenological flux equations have to be experimentally ascertained. Even if the flux equation is represented by a truncated power series in forces the equalities of eq 122 may not be true if the coefficients are not the corresponding derivatives at equilibrium. If  $\sum \mathbf{J}_i dX_i$  is a total differential, then the above equalities (eq 122) can be deduced. No physical justification can easily be given except for Onsager's symmetry. Broadly speaking we can express local flows  $\mathbf{J}_i$  as a function of local forces  $X_1, X_2, \dots$ , intensive parameters,  $T, P, C$ , and the structure factor  $G$  as follows

$$\mathbf{J}_i = f(X_1, X_2, \dots, T, P, C, G) \quad (123)$$

In the case of electrokinetic phenomena,  $G$  will be a function of the length and diameter of the capillaries constituting the membrane. For the flow of an electric current through a solution of electrolyte,  $G$  depends on the frequency of the alternating potential. The conductance does not depend on the frequency as long as the frequency is less than  $1/\theta$ , where  $\theta$  is the relaxation time. For the sedimentation rate and electrophoretic velocity,  $G$  depends on the size of the particles. It should be noted that, when intensive parameters are maintained constant, the structure factor is kept fixed, and  $\mathbf{J}_i$  are expanded<sup>259</sup> in the form of a Taylor's series with the equilibrium as reference point denoted by the subscript  $o$ , we get eq 120.

It was suggested that phenomenological equations for an electroosmotic situation would be

$$\mathbf{J}_v = L_{11}(\Delta P/T) + L_{12}(\Delta\varphi/T) + \frac{1}{2} L_{111}(\Delta P/T)^2 + \\ L_{112}(\Delta P \Delta\varphi/T^2) + \frac{1}{2} L_{122}(\Delta\varphi/T)^2 + \dots \quad (124)$$

$$\mathbf{I} = L_{21}(\Delta P/T) + L_{22}(\Delta\varphi/T) + \frac{1}{2} L_{211}(\Delta P/T)^2 + \\ L_{212}(\Delta P \Delta\varphi/T^2) + \frac{1}{2} L_{222}(\Delta\varphi/T)^2 + \dots \quad (125)$$

The nonlinear phenomenological eqs 124 and 125 have been subjected to extensive experimental examination by Rastogi and his group. The first study, was conducted by Rastogi and Jha<sup>261</sup> on the electroosmosis



**Table XII. The Values of Phenomenological Coefficients<sup>a,c</sup>**

mem-branes	$(L_{11}/T) \times 10^6$ (cm <sup>5</sup> dyn <sup>-1</sup> s <sup>-1</sup> )	$(L_{12}/T) \times 10^4$ (cm <sup>3</sup> s <sup>-1</sup> V <sup>-1</sup> )	$(L_{21}/T) \times 10^4$ <sup>b</sup> (cm <sup>3</sup> s <sup>-1</sup> V <sup>-1</sup> )	$(L_{122}/T^2) \times 10^8$ (cm <sup>3</sup> s <sup>-1</sup> V <sup>2</sup> )	$(L_{112}/T^2) \times 10^{10}$ (cm <sup>5</sup> s <sup>-1</sup> dyn <sup>-1</sup> V <sup>-1</sup> )	$(L_{1112}/T^3) \times 10^4$ (cm <sup>7</sup> s <sup>-1</sup> dyn <sup>-2</sup> V <sup>-1</sup> )	$(L_{1122}/T^3) \times 10^{12}$ (cm <sup>5</sup> s <sup>-1</sup> dyn <sup>-1</sup> V <sup>-2</sup> )
I	0.96	1.13	1.10	6.60	-20.2	3.64	2.12
II	1.27	0.94	0.92	10.60	-19.1	3.26	2.28
III	0.92	0.72	0.70	9.60	-17.7	2.80	3.00
IV	1.10	1.07	1.03	10.70	-13.1	0.70	6.68
V	1.06	0.97	0.98	12.00	-12.1	1.40	9.96

<sup>a</sup> For membranes I–III, values of phenomenological coefficients are calculated from  $J_{\text{total}}$  measurements, and for membranes IV and V, values of phenomenological coefficients are calculated from electroosmotic pressure measurements. <sup>b</sup> Estimated from streaming potential measurements. <sup>c</sup> Taken from ref 56 (from the data on Pyrex sinter membrane/acetone system).

of acetone through Pyrex sinter membranes. They tested the domain of validity of the nonlinear phenomenological equations and estimated the value of the second-order coefficients. When  $\Delta\varphi = 0$ ,  $J_v$  is given by

$$(J_v)_{\Delta\varphi=0} = L_{11}(\Delta P/T) + \frac{1}{2}L_{111}(\Delta P/T)^2 + \dots \quad (126)$$

and when  $\Delta P = 0$

$$(J_v)_{\Delta P=0} = L_{12}(\Delta\varphi/T) + \frac{1}{2}L_{122}(\Delta\varphi/T)^2 + \dots \quad (127)$$

Thus from eqs 124, 126, and 127 one can write

$$(J_v)_{\text{total}} = (J_v)_{\Delta P=0} + (J_v)_{\Delta\varphi=0} + L_{112}(\Delta P\Delta\varphi/T^2) \quad (128)$$

Similarly for electroosmotic pressure difference one can write from eq 124.

$$\left(\frac{\Delta P}{\Delta\varphi}\right)_{J_v=0} = -\frac{L_{12}}{L_{11}} - \frac{L_{112}}{2L_{11}} \frac{\Delta P}{T} - \frac{L_{122}}{2L_{11}} \frac{\Delta\varphi}{T} - \frac{L_{111}(\Delta P)^2}{2L_{11}T\Delta\varphi} + \dots \quad (129)$$

Similar information can be obtained from the measurement of the streaming potential and current:

$$\left(\frac{\Delta\varphi}{\Delta P}\right)_{I=0} = -\frac{L_{21}}{L_{22}} - \frac{L_{211}}{2L_{22}} \frac{\Delta P}{T} - \frac{L_{212}}{L_{22}} \frac{\Delta\varphi}{T} - \frac{L_{222}(\Delta\varphi)^2}{2L_{22}T\Delta P} + \dots \quad (130)$$

and

$$(I/\Delta P)_{\Delta\varphi=0} = \frac{L_{21}}{T} + \frac{1}{2} \frac{L_{211}}{T^2} \frac{\Delta P}{T} + \dots \quad (131)$$

When second-order terms are negligible, eqs 130 and 131 reduce to

$$\left(\frac{\Delta\varphi}{\Delta P}\right)_{I=0} = -\frac{L_{21}}{L_{22}} \quad (132)$$

$$\left(\frac{I}{\Delta P}\right)_{\Delta\varphi=0} = \frac{L_{21}}{T} \quad (133)$$

The mathematical stratagem as given by eqs 126–133 was utilized by Rastogi and Jha<sup>261</sup> to evaluate the first- and second-order phenomenological coefficients in an acetone/Pyrex sinter G4 membrane system. The second-order coefficient  $L_{112}$  was evaluated using eqs 128 and 129. It was found that the range of validity of Poiseuille's law was so large that the coefficient  $L_{111}$  was zero. It was also discovered that up to  $\Delta\varphi = 440$  V the coefficient  $(L_{122}/T^2)$  was 0. Imposing these conditions and using eqs 128 and 129,  $(L_{112}/T^2)$  was evaluated. The streaming potential measurement showed that up to  $\Delta P = 100$  cm of acetone no

**Table XIII. Phenomenological Coefficients from Streaming Current and Streaming Potential Data (Zeokarb 225 (Na<sup>+</sup> Form) Membrane/Aqueous Methanol Systems)<sup>a</sup>**

mole fraction of water	$(L_{21}/T) \times 10^6$ (cm <sup>3</sup> s <sup>-1</sup> V <sup>-1</sup> )	$(L_{22}/T) \times 10^6$ (ohm <sup>-1</sup> )	$(L_{211}/T^2) \times 10^{10}$ (cm <sup>5</sup> s <sup>-1</sup> dyn <sup>-1</sup> V <sup>-1</sup> )	$L_{212}/T^2$ (cm <sup>3</sup> s <sup>-1</sup> V <sup>-1</sup> )
0.00	6.20 <sup>b</sup>		1.20 <sup>b</sup>	0 <sup>b</sup>
	6.30 <sup>c</sup>	0.105 <sup>c</sup>	1.26 <sup>c</sup>	0 <sup>c</sup>
0.60	0.60 <sup>b</sup>		1.60 <sup>b</sup>	0 <sup>b</sup>
	0.64 <sup>c</sup>	0.160 <sup>c</sup>	1.92 <sup>c</sup>	0 <sup>c</sup>
1.00	4.60 <sup>b</sup>		-0.60	0 <sup>b</sup>
	4.68 <sup>c</sup>	0.260 <sup>c</sup>	-0.52	0 <sup>c</sup>

<sup>a</sup> Taken from ref 263. <sup>b</sup> Streaming current. <sup>c</sup> Streaming potential.

nonlinearity arose. The values of the coefficients  $L_{12}$  and  $L_{21}$  were found to be equal, confirming Onsager's relations. The nonlinear phenomenological equations were also tested by comparing the experimentally determined values of  $(J_v)_{\text{total}}$  with those computed with the use of eq 128, utilizing the experimentally determined values of  $(J_v)_{\Delta P=0}$  and  $(J_v)_{\Delta\varphi=0}$ . Rastogi, Singh, and Srivastava<sup>56</sup> further refined their experiments on the electroosmosis of acetone through a Pyrex sinter G4 membrane and tested the precision of the expansion given by eq 120. Data on electroosmotic flow  $(J_v)_{\Delta P=0}$  was shown to be represented by eq 127. The total flow  $J_v$  was however represented by the equation

$$J_v = L_{11} \frac{\Delta P}{T} + L_{12} \frac{\Delta\varphi}{T} + L_{112} \frac{\Delta P\Delta\varphi}{T^2} + \frac{1}{2}L_{122} \left(\frac{\Delta\varphi}{T}\right)^2 + \frac{1}{2}L_{1112} \frac{(\Delta P)^2\Delta\varphi}{T^3} + \frac{1}{2}L_{1122} \frac{\Delta P(\Delta\varphi)^2}{T^3} \quad (134)$$

The various phenomenological coefficients occurring in these equations were also evaluated. From streaming potential data for which the linear terms in eq 125 were found to be a good enough representation (up to  $\Delta P = 100$  cm of acetone), the value of the coefficient  $L_{21}$  was estimated. From the coefficient values given in Table XII, the validity of Onsager's relations is obvious. Rastogi et al.<sup>262</sup> extended their studies to the electroosmosis of methanol through a porous plug made of compressed quartz powder. They examined the validity of the truncated form of the  $L_i$ 's equation in the nonlinear region. These authors also provided a more thorough test of second-order symmetry relations through their data on electroosmosis, streaming potential, and current on Zeokarb 225 (Na<sup>+</sup> form) membrane/methanol or membrane/methanol–water mixture systems.<sup>263</sup> It was found that  $L_{112} \neq L_{211}$  and  $L_{122} \neq L_{212}$  as Tables XIII and XIV show Onsager's symmetry is, however, obeyed. The recent data by Shukla et al.<sup>264</sup> also shows that second-order symmetries do not hold.

**Table XIV. Transport Coefficients Obtained from Electroosmotic Data (Zeokarb 225 (Na<sup>+</sup> Form) Membrane/Aqueous Methanol Solution)<sup>a</sup>**

mole fraction of water	$(L_{11}/T) \times 10^7$ (cm <sup>5</sup> s <sup>-1</sup> dyn <sup>-1</sup> )	$(L_{12}/T) \times 10^6$ (cm <sup>3</sup> s <sup>-1</sup> V <sup>-1</sup> )	$(1/2 L_{122}/T^2) \times 10^8$ (cm <sup>3</sup> s <sup>-1</sup> V <sup>-2</sup> )	$(L_{112}/T^2) \times 10^9$ (cm <sup>5</sup> s <sup>-1</sup> dyn <sup>-1</sup> V <sup>-1</sup> )	$(L_{1112}/T^3) \times 10^{13}$ (cm <sup>7</sup> s <sup>-1</sup> dyn <sup>-2</sup> V <sup>-1</sup> )	$(L_{1122}/T^3) \times 10^{11}$ (cm <sup>5</sup> s <sup>-1</sup> dyn <sup>-1</sup> V <sup>-2</sup> )
0.00	2.80	6.20	-0.80	0.26	-0.17	0.52
0.60	0.44	0.62	0.33	-0.05	0.05	-0.04
1.00	0.28	4.30	0.00	0.00	0.00	0.04

<sup>a</sup> Taken from ref 263.**Table XV. Phenomenological Coefficients for Isotropic Membrane (Pyrex) (Temperature 35 ± 0.01 °C)**

liquid	mem-brane	direction of flow				direction of flow			
		$(L_{12}/T) \times 10^5$ (cm <sup>3</sup> s <sup>-1</sup> V <sup>-1</sup> )	$(L_{21}/T) \times 10^5$ (cm <sup>3</sup> s <sup>-1</sup> V <sup>-1</sup> )	$(L_{122}/T^2) \times 10^8$ (cm <sup>3</sup> s <sup>-1</sup> V <sup>-2</sup> )	$(L_{21}/L_{22}) \times 10^7$ (cm <sup>3</sup> s <sup>-1</sup> ohm <sup>-1</sup> )	$(L_{12}/T) \times 10^5$ (cm <sup>3</sup> s <sup>-1</sup> V <sup>-1</sup> )	$(L_{21}/T) \times 10^5$ (cm <sup>3</sup> s <sup>-1</sup> V <sup>-1</sup> )	$(L_{122}/T^2) \times 10^8$ (cm <sup>3</sup> s <sup>-1</sup> V <sup>-2</sup> )	$(L_{21}/L_{22}) \times 10^7$ (cm <sup>3</sup> s <sup>-1</sup> ohm <sup>-1</sup> )
acetone	I	9.5	9.0	6.6		9.0	9.1	5.5	
	II	9.4	9.1	5.7		8.9	8.8	5.4	
	III	7.7	7.6	6.3	15.4	7.4	8.2	6.2	14.6
methanol	IV	3.8	4.0	2.7		4.1	4.2	2.7	
	V	4.0	3.4	2.7	2.4	3.8	3.3	3.0	2.5
	VI	5.3	5.2	3.9		5.1	5.5	4.3	
ethyl methyl ketone	VII	2.4	2.4	1.3	6.2	2.4	2.6	1.4	6.4
	VIII	2.6	2.8	1.4	8.4	2.6	2.6	1.4	8.1

<sup>a</sup> Taken from ref 265.**Table XVI. Phenomenological Coefficients for Anisotropic Membrane (Quartz) (Temperature 40 ± 0.01 °C)**

liquid	mem-brane	direction of flow				direction of flow			
		$(L_{12}/T) \times 10^5$ (cm <sup>3</sup> s <sup>-1</sup> V <sup>-1</sup> )	$(L_{21}/T) \times 10^5$ (cm <sup>3</sup> s <sup>-1</sup> V <sup>-1</sup> )	$(L_{122}/T^2) \times 10^8$ (cm <sup>3</sup> s <sup>-1</sup> V <sup>-2</sup> )	$(L_{21}/L_{22}) \times 10^7$ (cm <sup>3</sup> s <sup>-1</sup> ohm <sup>-1</sup> )	$(L_{12}/T) \times 10^5$ (cm <sup>3</sup> s <sup>-1</sup> V <sup>-1</sup> )	$(L_{21}/T) \times 10^5$ (cm <sup>3</sup> s <sup>-1</sup> V <sup>-1</sup> )	$(L_{122}/T^2) \times 10^8$ (cm <sup>3</sup> s <sup>-1</sup> V <sup>-2</sup> )	$(L_{21}/L_{22}) \times 10^7$ (cm <sup>3</sup> s <sup>-1</sup> ohm <sup>-1</sup> )
ethyl methyl ketone	I	0.61	0.64	1.83	1.30	0.79	0.83	1.81	1.49
	II	0.72	0.68			0.76	0.80		
acetone	III	0.74	0.70			0.82	0.84		
	IV	0.64	0.61			0.70	0.72		
	V	1.06	1.12		0.91	1.36	1.42		
methanol	VI	1.04	1.08	2.90		1.28	1.34	2.87	
	VII	1.05	1.10			1.32	1.38		
	VIII	1.63	1.70	1.77	0.70	1.84	1.96	1.80	0.83
	IX	1.66	1.72			1.87	1.92		
	X	1.66	1.68			1.86	1.94		

<sup>a</sup> Taken from ref 265.

It has to be noted that there is no justification from the theoretical viewpoint based on physical consideration for second-order and higher symmetries.

Studies on the directional characteristics of electroosmotic transport<sup>265</sup> in a Pyrex and quartz membrane are quite interesting since membranes in living systems are usually anisotropic. The concept of the vectorial character of phenomenological coefficients is contained in the well-known Curie-Prigogine principle<sup>1,3,18,266</sup> which has important biological implications in the context of active transport and leads to the generalization that living membranes of necessity, have to be anisotropic membranes. Since  $\mathbf{J}$ ,  $\mathbf{I}(\Delta\varphi/T)$ , and  $(\Delta P/T)$  are vectors, the higher coefficients are of different ranks.

The directional characteristics of the electroosmotic transport of acetone, methanol, and ethyl methyl ketone through both quartz and Pyrex membranes were investigated.<sup>265</sup> The former membrane was found to be anisotropic, whereas the latter was found to behave as an isotropic membrane. The magnitude of solvodynamic flow through both membranes, Pyrex sinter G-4 and quartz plug, was found to be independent of the direction of flow and proportional to the pressure difference showing that the coefficient  $L_{11}$  is scalar.

The electroosmotic data were shown to be represented by the equation

$$\vec{J}_v = L_{12} \left( \frac{\vec{\Delta\varphi}}{T} \right) + 1/2 L_{122} \left( \frac{\vec{\Delta\varphi}}{T} \right)^2 \quad (135)$$

The data on streaming potential and current was shown to be adequately represented by the linear phenomenological relation (eq 28) for I. It is clear that the second-order symmetry is not obeyed, i.e.  $L_{211} \neq L_{112}$ . The experimentally determined values of the phenomenological coefficients for both Pyrex and quartz membrane are reproduced in Tables XV and XVI. The invariance of the phenomenological coefficient with the direction of flow in the case of Pyrex membrane demonstrates its isotropic character. However, for quartz membranes the values of the coefficients  $L_{12}/T$  and  $L_{21}/T$  differ appreciably on reversal of the direction of flow although, for the same direction of flow, Onsager's relations remain valid. The coefficient  $L_{122}/T^2$  remains unaltered even on reversing the direction of flow. A summary of the qualitative results is given in Table XVII. The membranes have a three-dimensional network of capillaries and the flows  $\mathbf{J}_v$  or  $\mathbf{I}$  normal to a particular plane would be made up of relative contributions along the three axes. In real anisotropic media each spatial component of  $\Delta\varphi$  and each spatial component of  $\Delta P$  would couple to produce each spatial component of  $\mathbf{J}_v$  and each spatial component of  $\mathbf{I}$ . This would result in a common second-order tensor repre-

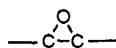
**Table XVII. Directional Dependence of Phenomenological Coefficients<sup>a</sup>**

quartz plug	Pyrex sinter
$\vec{L}_{11} = \overleftarrow{L}_{11}$	$\vec{L}_{11} = \overleftarrow{L}_{11}$
$\vec{L}_{12} \neq \overleftarrow{L}_{12}$	$\vec{L}_{12} = \overleftarrow{L}_{12}$
$\vec{L}_{21} \neq \overleftarrow{L}_{21}$	$\vec{L}_{21} = \overleftarrow{L}_{21}$
$\vec{L}_{122} = \overleftarrow{L}_{122}$	$\vec{L}_{122} = \overleftarrow{L}_{122}$
$\vec{L}_{21} = \overleftarrow{L}_{21}$	$\vec{L}_{21} = \overleftarrow{L}_{21}$
$\vec{L}_{22} = \overleftarrow{L}_{22}$	$\vec{L}_{22} = \overleftarrow{L}_{22}$

<sup>a</sup> Taken from ref 265.

sented by  $6 \times 6$  numbers (phenomenological coefficients) in a given coordinate system. In physical terms, the difference may arise because in a solvodynamic flow the radial velocity gradient is maximum in the central region of the capillary, whereas in electroosmosis and streaming current, the flow is initiated at the walls of the capillary. Naturally the surface characteristics of the capillary at the entrance and exit would affect the electroosmotic flow rather than the solvodynamic flow.

Rastogi et al.<sup>265</sup> have tried to suggest the reason for asymmetric behavior in the case of a quartz membrane. The asymmetry in the behavior of electroosmosis and streaming current has to arise on account of the difference in molecular character of the surface at the entrance and at the exit sides of the capillary. Quartz, a polymeric form of  $\text{SiO}_2$ , is known to have a three-dimensional network in which every oxygen atom is common to two tetrahedral ( $\text{SiO}_4$ ) groups. The structure is largely based on the formation of large anions arranged about small cations. The regular arrangement is distorted to some extent so that spirals of  $-\text{O}-\text{Si}-\text{O}-\text{Si}-$  chain lie around the trigonal screw axis of symmetry. Such a structure cannot lead to asymmetry. The asymmetry of the quartz membrane might, in their opinion, be due to the nonuniform coating of araldite on the quartz particles. Araldite was used for fixing up the quartz membrane and contains an epoxy resin<sup>267</sup> with the group



Because of the negative charge on the oxygen atom the character of the surface would be similar to quartz although the potential may not be the same at all the points in the quartz membrane. The isotropic character of the Pyrex sinter is to be expected in view of the absence of symmetry in the atomic network<sup>268</sup> which will be statistically the same in all directions. However, the random network theory has been questioned by later workers who believe that Pyrex glasses are inhomogeneous systems comprising both ordered, crystallite and disordered, vitreous zones.

## B. Ion-Exchange Membranes

Electrokinetic studies on highly charged membranes have proven quite revealing. Lakshminarayanan et al.<sup>269,270</sup> and Tombalakian et al.<sup>271</sup> have examined the dependence of the transport numbers of water in aqueous solutions on current density using ion-exchange

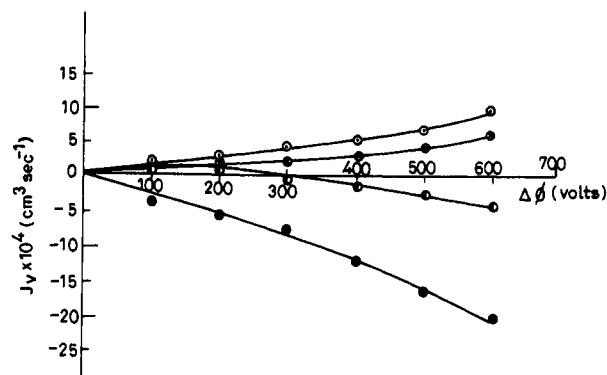


**Figure 19.** Dependence of electroosmotic flux  $J_v$  on potential difference  $\Delta\phi$  in case of a water-methanol/Zeokarb 226 system: (●) 0% water; (◐) 10% water; (⊙) 20% water; and (○) 30% water. A positive  $J_v$  indicates flow from the positive electrode. A negative  $J_v$  indicates flow from the negative electrode.<sup>272</sup>

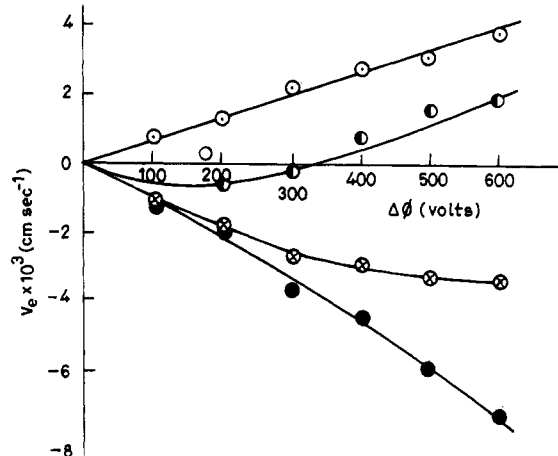


**Figure 20.** Dependence of electrophoretic velocity  $V_e$  on potential difference  $\Delta\phi$  for water-methanol/Zeokarb 226 system: (○) 5% water; (◐) 10% water; (⊙) 20% water; (●) 30% water. A positive  $V_e$  indicates migration of the particles toward the negative electrode. A negative  $V_e$  indicates migration of the particles toward the positive electrode.<sup>272</sup>

membranes. The electrokinetic ion-exchange studies from the viewpoint of nonequilibrium thermodynamics are from Rastogi and his group. These authors<sup>272</sup> have studied the electroosmosis of ethanol, methanol, and their mixtures with water through the porous plugs made from Zeokarb 226. They also conducted electrophoretic velocity measurements on suspensions of the ion exchanger in water, methanol, ethanol, and their mixtures. The electroosmotic flux and electroosmotic pressure were found to vary with the electrical potential difference in a nonlinear manner. The sign of these effects was found to depend on the composition of the mixture. Reversal of the direction and nonlinearity were also observed for the electrophoretic velocity. For 10% aqueous methanol and aqueous ethanol, the electroosmotic flux changed its sign beyond  $\Delta\phi = 300$  and 200 V, respectively. Two typical results showing sign reversal and nonlinearity are reproduced in Figures 19 and 20.

For the electroosmotic flux and electrophoretic velocity  $V_e$ , the following equations were shown to adequately represent the data:

$$J_v = L_{12}(\Delta\phi/T) + \frac{1}{2}L_{122}(\Delta\phi/T)^2 \quad (136)$$

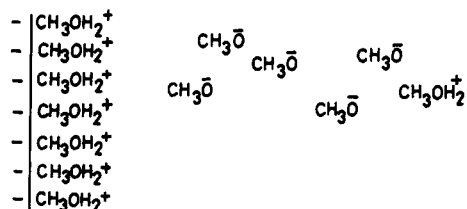


**Figure 21.** Double layer at a cation exchanger-methanol interface.

$$V_s = L'_{12}\Delta\varphi + 1/2L'_{122}(\Delta\varphi)^2 \quad (137)$$

The transport phenomena at  $\Delta\varphi$ , at which sign reversal takes place, merits a deeper investigation. Among other things it is likely that a separation of components of the mixture might be taking place.

Hadermann et al.<sup>273</sup> have investigated electroosmosis in the  $\gamma$ -alumina-2-propanol system. They suspected that the nonlinearity in this case may arise due to a dissociation field effect.<sup>274</sup> By using Onsager's theory,<sup>275</sup> a linear dependence of electroosmotic pressure difference  $(\Delta P/\Delta\phi)_{J_v=0}$ , on  $\Delta\phi$  is predicted which of course was not observed by Rastogi et al.<sup>272</sup>

Although similar nonlinear relations, eqs 136 and 137, represent the data on electroosmotic and electrophoretic velocities, no correlation between  $L_{12}$  and  $L'_{12}$  could be discovered.<sup>272</sup> However, it follows that the nonlinear terms in the transport equation do not arise as a result of hydrodynamic factors. This is evident because no sign reversal for aqueous methanol or ethanol was observed for unchanged membranes.<sup>273</sup> The nonlinear terms may be due to a change in the double-layer characteristic (Figure 21) at high values of  $\Delta\varphi$  in the case of highly charged membranes remembering that the autoprotolysis equilibria involving the hydroxyl protons of the alcohol.

Rastogi et al.<sup>278</sup> have also studied the streaming potentials developed during the streaming of methanol, water, and methanol-water mixtures through porous plugs prepared by the mechanical compression of Zeokarb 225. The resin used was in various forms, e.g.  $H^+$ ,  $Na^+$ ,  $Ba^{2+}$ , and  $Al^{3+}$ . The streaming potential changed its sign at  $\Delta P > 30$  cm of the liquid column. Multiple sign reversals were observed in ion exchangers of different forms, e.g.  $Ba^{2+}$ . A few typical results are shown in Figures 22 and 23. To check the internal consistency of the data, corresponding electroosmotic experiments were also conducted and the validity of Onsager's relations demonstrated. The trends observed (e.g. Figures 22 and 23) are well reproduced. There are difficulties in explaining the multiple sign reversal in terms of the existence of multiple steady state related to the exotic phenomena in far from equilibrium situations because the values of  $\Delta P$  at which multiple sign reversal occurs is not high enough. These may be connected with the slow-release kinetics of doubly or triply charged cations bound to fixed negative charges on the ion exchanger as was observed recently in the case of cellulose acetate membranes.<sup>126</sup> (We thank one of the referees for drawing our attention to this point.) However, it has to be noted that multiple charge reversals are observed both in the case of doubly charged cations and monovalent cations.

Rastogi and Shabad<sup>279</sup> attempted to decipher the nature of the second-order phenomenological coefficient

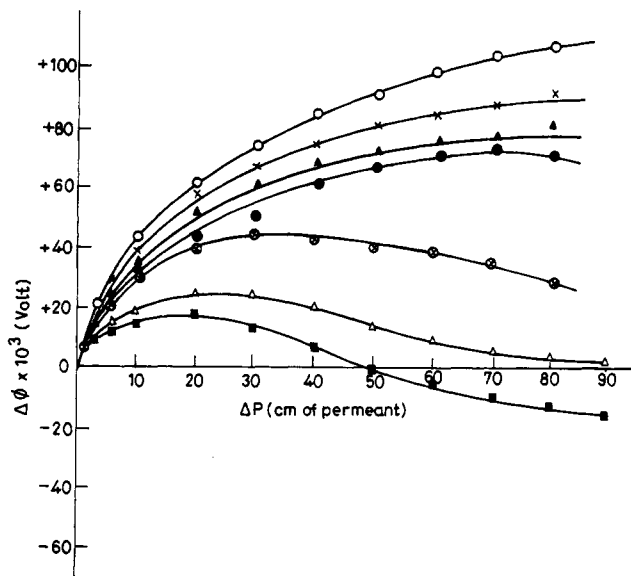


**Figure 22.** Dependence of streaming potential ( $\Delta\phi$ ) on pressure difference ( $\Delta P$ ) for Zeokarb 225 ( $H^+$  form)/methanol-water system at different mole fractions of water: ( $\odot$ ) 0.00 mol fraction of water; ( $\times$ ) 0.20 mol fraction of water; ( $\blacktriangle$ ) 0.40 mol fraction of water; ( $\bullet$ ) 0.6 mol fraction of water; ( $\oplus$ ) 0.8 mol fraction of water; ( $\triangle$ ) 0.95 mol fraction of water; ( $\blacksquare$ ) 1.0 mol fraction of water.<sup>278</sup>

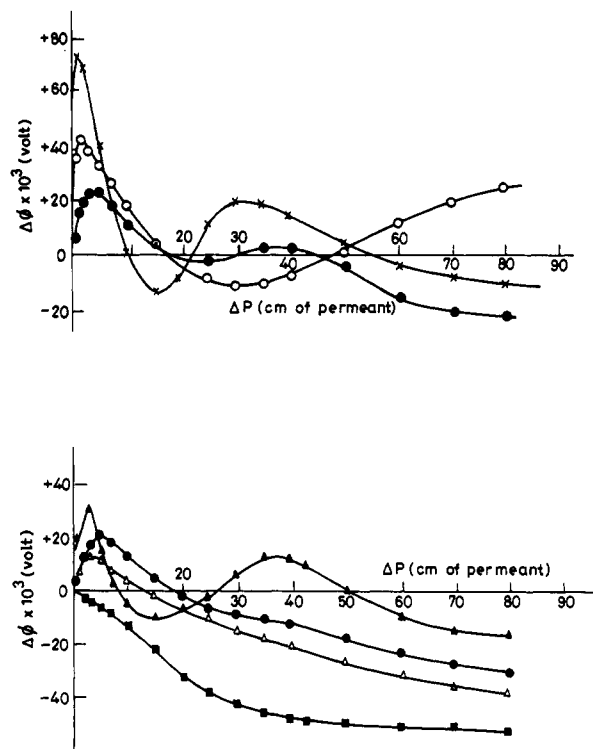


**Figure 23.** Dependence of streaming potential ( $\Delta\phi$ ) on pressure difference ( $\Delta P$ ) for Zeokarb 225 ( $\text{Ba}^{2+}$  form)/methanol-water system at different mole fractions of water: (○) 0.00 mol fraction of water; (×) 0.20 mol fraction of water; (▲) 0.40 mol fraction of water; (●) 0.6 mol fraction of water; (⊗) 0.8 mol fraction of water; (⊙) 0.95 mol fraction of water; (■) 1.00 mol fraction of water.<sup>278</sup>

$L_{122}$  occurring in the nonlinear electroosmotic transport (eq 136). By using double-layer model and the dipole moment vector associated with the permeant molecules, the vectorial character by the second-order phenomenological coefficient  $L_{122}$  in eq 136 was examined. The analysis was along the following lines:

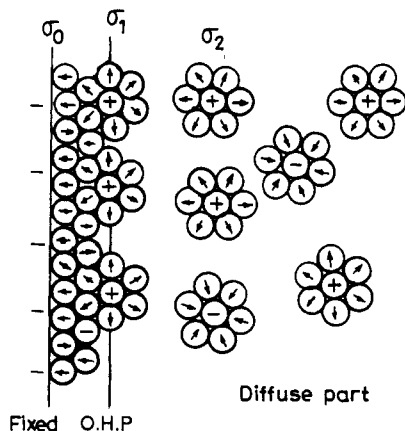


**Figure 24.** Structure of electrical double layer for the Zeokarb 226 (H<sup>+</sup> form)/water system.<sup>279</sup>

Consider that a membrane whose surface has a fixed negative charge is in contact with a dipolar permeant, say water. The solvent dipoles in the neighborhood of the interface are largely oriented, i.e. dielectric saturation occurs.<sup>280</sup> The electrical double layer may appropriately be represented as in Figure 24. Let the charge density of the solid be  $\sigma_0$  and  $\sigma_1$  and  $\sigma_2$  the corresponding values on the solution side of the fixed and diffused layers, respectively. For a membrane water system (Figure 24) "+" denotes a hydronium ion. The circles in Figure 24 denote dipolar molecules and the arrows indicate the direction of the dipole vector. Dipoles of the type  $\uparrow$  are called "flip up" and those of the type  $\downarrow$  are called "flop down" dipoles.<sup>281</sup> Obviously the effective zeta potential  $\zeta_{\text{eff}}$  will be composed of the charge contribution potential  $\Delta\psi$  and the dipolar potential  $\Delta\chi$  so that

$$\zeta_{\text{eff}} = \Delta\psi \text{ (charge contribution)} + \Delta\chi \text{ (dipolar contribution)} \quad (138)$$

The potential at point *P* due to a dipole AB will be given by<sup>282</sup>

$$\chi = \frac{\vec{\mu} \cdot \vec{r}}{4\pi\epsilon r^3} = \frac{\mu \cos \theta}{4\pi\epsilon r^2} \quad (139)$$

where  $\theta$  is the angle between the radius vector and the dipole moment vector,  $\mu$  is the dipole moment, and  $\epsilon$  is the dielectric constant of the medium. The potential difference in the dipole layer is given by

$$\Delta\chi = \chi(\uparrow) + \chi(\downarrow) \quad (140)$$

where  $\chi(\uparrow)$  is the dipole potential due to the flip-up dipole and  $\chi(\downarrow)$  is potential due to the flop-down dipole. Since  $\cos \theta = 1$  in the vicinity of the interface it follows from eq 139 that

$$\Delta\chi = \frac{\mu N}{4\pi\epsilon r^2} \quad (141)$$

where  $N$  is defined by

$$N = N(\uparrow) - N(\downarrow) \quad (142)$$

In eq. (142)  $N(\uparrow)$  is the number of flip-up dipoles per unit area and  $N(\downarrow)$  is the number flop-down dipoles per unit area on the interface.  $N(\uparrow)$  and  $N(\downarrow)$  are given by the equations,<sup>281</sup>

$$N(\uparrow) = N_{11}(e^{-\Delta G^\circ_c(\uparrow)/RT})e^{-x} \quad (143)$$

$$N(\downarrow) = N_{11}(e^{-\Delta G^\circ_c(\downarrow)/RT})e^{-x} \quad (144)$$

where  $N_{11}$  are the number of free sites per unit area of the interface and  $\Delta G^\circ_c(\uparrow)$  and  $\Delta G^\circ_c(\downarrow)$  are the standard free energy change associated with the adsorption of water in the flip-up and flop-down states, and  $x$  is given by

$$x = \frac{\vec{\mu} \cdot \vec{X}}{kT} - \frac{Uc}{kT} (\theta(\uparrow) - \theta(\downarrow)) \quad (145)$$

where  $U$  is the interaction energy between dipoles,  $X$  is the electric field strength,  $c$  is the number of dipoles which interact with a particular dipole, and  $k$  is the Boltzmann constant. It should be noted that all the  $c$  dipoles do not have the same orientation. The fractions  $\theta(\uparrow)$  of flip-up and  $\theta(\downarrow)$  of flop-down dipoles are given as follows

$$\theta(\uparrow) = \frac{N(\uparrow)}{N_T}$$

and

$$\theta(\downarrow) = \frac{N(\downarrow)}{N_T} \quad (146)$$

where  $N_T$  is the total number of dipoles on the interface including flip-up and flop-down states at the charge concerned. We know that

$$\frac{N(\uparrow) - N(\downarrow)}{N_T} = \tanh x \quad (147)$$

and

$$\tanh x = \frac{e^x - e^{-x}}{e^x + e^{-x}} = x \quad (148)$$

when  $x \ll 1$ . In such a situation

$$N(\uparrow) - N(\downarrow) = N_T x \quad (149)$$

Combining eqs 141 and 149 one can write

$$\Delta\chi = \frac{\mu N_T}{4\pi\epsilon r^2} \left[ \frac{\vec{\mu} \cdot \vec{X}}{kT} - \frac{Uc}{kT} + \frac{Uc\theta}{kT} \right] \quad (150)$$

Since the interaction energy between the flip-up dipoles is  $\vec{\mu} \cdot \vec{X}$  and that between the flop-down dipoles is  $-\vec{\mu} \cdot \vec{X}$  we have

$$\Delta\chi = \frac{\mu N_T}{4\pi\epsilon r^2} \left[ \frac{\vec{\mu} \cdot \vec{X}}{kT} - \frac{\vec{\mu} \cdot \vec{X} c \theta(\uparrow)}{kT} - \frac{\vec{\mu} \cdot \vec{X} c \theta(\downarrow)}{kT} \right] \quad (151)$$

or

$$\Delta\chi = \frac{\mu N_T}{4\pi\epsilon r^2} \left[ \frac{\vec{\mu} \cdot \vec{X} (1 - c)}{kT} \right] \quad (152)$$

because  $\theta(\uparrow) + \theta(\downarrow) = 1$ . In view of eq 152, eq 138 can be rewritten as

$$\zeta_{\text{eff}} = \Delta\psi + \frac{N_T \mu \cdot \bar{X}(1-c)}{4\pi\epsilon r^2 kT} \quad (153)$$

Thus it can be seen that the resultant field in the double layer will be due to charges in the double layer and dipoles adsorbed at the interface. Equation 145 describes a Hamiltonian based on a two-dimensional Ising-type model with a two-state Langevin dipole-field interaction. In order to avoid inconsistent results from eq 153 in the limit when  $c = 1$ , it could be better replaced by a mean field treatment.<sup>283</sup> (Thanks are due to one of the referees for drawing our attention to this point.) Considering the  $y$  component of the resultant electric field the Poisson equation can be written as

$$\frac{dE_y}{dy} = \frac{4\pi\rho}{\epsilon} \quad (154)$$

where  $E_y$  is the  $y$  component of the resultant electric field and  $\rho$  is charge density. Equation 154 can be rewritten as

$$\frac{d^2\Phi}{dy^2} = -\frac{4\pi\rho}{\epsilon} \quad (155)$$

where  $\Phi$  is the potential in the double layer. When the electric field  $\bar{X}$  is applied, electroosmosis ensues and the electrical force is balanced by the viscous force in the stationary state. Thus

$$\bar{X} \cdot \rho \, dy = \eta \frac{d^2\bar{v}}{dy^2} \, dy \quad (156)$$

where  $\bar{v}$  is the electroosmotic velocity and  $\eta$  is the viscosity of the medium. Inserting eq 155 into eq 156 and integrating the resulting equation between  $y = a$  and  $y =$  distance of the slipping plane, one obtains

$$\bar{v} = \frac{\epsilon \bar{X}}{4\pi\eta} \zeta_{\text{eff}} \quad (157)$$

Hence the volume flow per second through a capillary of radius  $a$  and length  $l$  is given by

$$J_v = \pi a^2 \bar{v} \quad (158)$$

so that

$$J_v = \frac{a^2 \epsilon \bar{X}}{4\eta} \zeta_{\text{eff}} \quad (159)$$

substituting the values of  $\zeta_{\text{eff}}$ , from eq 153 into eq 159 and rearranging the terms one can write

$$J_v = \left[ \frac{a^2 \epsilon \Delta\psi}{4\eta} \right] \bar{X} + \left[ \frac{a^2 N_T \mu (1-c) \bar{\mu}}{16\pi\eta r^2 k} \right] \frac{(\bar{X} \cdot \bar{X})}{T} \quad (160)$$

Comparison of eq 160 with eq 136 justifies the vectorial character of the coefficient  $L_{122}$ .

In the light of their theory, based on the realistic double-layer model (Figure 24), Rastogi and Shabad<sup>279</sup> have attempted to rationalize the phenomenon of sign reversal observed in the case of the electroosmosis of a methanol-water mixture and an ethanol-water mixture through Zeokarb 226 membranes. For example, in the case of the methanol-water mixture, the double layer picture shown in Figure 24 will remain unchanged except that there will be oriented dipoles of both permeants in the flip-up and flop-down position. In this case, in Figure 24 the encircled plus sign would

continue to denote the hydronium ion but the encircled negative ions would denote methoxide ions. In the system containing aqueous methanol, two possibilities exist: (i) both water and methanol dipoles are adsorbed or (ii) only one type of dipole is adsorbed. The second one is a remote possibility. The effective dipole potential and the effective zeta potential for the system would therefore, be

$$\Delta\chi_{\text{eff}} = \Delta\chi_{\text{H}_2\text{O}} + \Delta\chi_{\text{CH}_3\text{OH}} \quad (161)$$

and

$$\zeta_{\text{eff}} = \Delta\psi + [\Delta\chi_{\text{H}_2\text{O}} + \Delta\chi_{\text{CH}_3\text{OH}}] \quad (162)$$

where

$$\Delta\chi_{\text{H}_2\text{O}} = \frac{N_1 \mu_1 \bar{\mu}_1 \cdot \bar{X}(1-c)}{4\epsilon_1 r_1^2 kT} \quad (163)$$

and

$$\Delta\chi_{\text{CH}_3\text{OH}} = \frac{N_2 \mu_2 \bar{\mu}_2 \cdot \bar{X}(1-c)}{4\epsilon_2 r_2^2 kT} \quad (164)$$

In eqs 163 and 164 the subscript 1 and 2 represent water and methanol. In eq 162 both  $\Delta\chi_{\text{H}_2\text{O}}$  and  $\Delta\chi_{\text{CH}_3\text{OH}}$  may have signs opposite to that of  $\Delta\psi$ , and therefore, the sign of  $\zeta_{\text{eff}}$  would depend on the magnitude of these. Since  $\Delta\chi_{\text{H}_2\text{O}}$  and  $\Delta\chi_{\text{CH}_3\text{OH}}$  also depend on the field strength,  $\zeta_{\text{eff}}$  can be zero or undergo sign reversal depending on the circumstances. This may explain the observation on sign reversal in the electroosmotic experiments on alcohol water mixtures through ion exchange membranes.<sup>272</sup> Changes in the zeta potential would also be influenced by dissociation of the ion exchanger. The greater the dissociation of the membrane the greater the extent of adsorption of the dipoles.

It should be pointed out that the explanation given above in the case of electroosmosis has not been extended to account for the phenomenon of multiple sign reversal observed in the case of streaming potentials.<sup>278</sup> This would be a worthwhile exercise. By using the same logic as in the case of electroosmosis, it would appear that dipole orientation in the double layer should be affected by the streaming pressures.

Several studies have been conducted<sup>284-291</sup> on different ion exchange membranes. All these studies substantiate the validity of the truncated form of eq 120 in electroosmotic and electrophoretic transport data and show the usefulness of the theoretical frame given by Rastogi et al.<sup>279</sup>

Lorimer<sup>292-294</sup> considered the various approaches<sup>21,259,294-299</sup> and developed a general theory<sup>293</sup> to provide a thermodynamic explanation for nonequilibrium phenomena for discontinuous systems. Irmay<sup>298</sup> included the inertial terms, involving accelerations, in the equations of motion for a fluid permeating a porous diaphragm. Irmay's theory although purely hydrodynamic in nature, reveals the dependence of hydraulic permeability on the applied pressure at low Reynolds numbers. Mickulecky and Caplan<sup>21</sup> argued that the average viscous contribution to isothermal dissipation function are negligible.

Lorimer's approach<sup>292,293</sup> differs from that of deGroot and Mazur<sup>1</sup> by including the spatial acceleration, the kinetic energy of diffusion, and the nonconservative

**Table XVIII. Variation of Measured Particle Velocity ( $v_e$ ) with Electrical Gradients ( $E$ ) in the Case of Sodium Bentonite Particles/Sodium Chloride System**

concentration of NaCl (N)	$v_e = a + bE + cE^2$ ( $a, b, c$ are constants)
$10^{-4}$	$v_e = -1.795 + 2.577E + 0.0080E^2$
$5 \times 10^{-4}$	$v_e = -0.244 + 2.207E + 0.0049E^2$
$10^{-3}$	$v_e = -0.689 + 2.274E + 0.0017E^2$
$2 \times 10^{-3}$	$v_e = 0.08 + 2.184E - 0.0003E^2$
$5 \times 10^{-3}$	$v_e = 0.08 + 2.201E - 0.0014E^2$

<sup>a</sup> Taken from ref 303.

polarization in the equation for the rate of entropy production. In the resulting equation for entropy production, contributions from the kinetic energy of diffusion, barycentric kinetic energy, polarization forces, work done by viscous forces, etc. appear. It has been shown that the first contribution gives a term in square of mass flows, the second and third contributions give terms in the square of the volume flux and the square of the electrical potential difference, while the fourth is incorporated in the volume flow, and the fifth is in general negligible. In order that the range of validity of these equations may be investigated experimentally, Lorimer<sup>294</sup> formulated functional phenomenological equations for the flows of matter, volume, charge, and heat for a discontinuous system in which the inertial terms in the viscous equations of motion are not considered negligible.

We will now pass on to the studies on electrokinetic phenomenon in soil systems in the nonlinear region of nonequilibrium thermodynamics. The knowledge of electrokinetic properties of soil–water system helps in explaining several phenomena. Electroosmosis has been applied to several engineering problems<sup>300</sup> such as soil stabilization, reduction of friction between soil and metal implements, etc. Similarly, knowledge of the electrokinetic properties of clay–water systems is important in several fields of clay technology<sup>301</sup> such as the interpretation of electrical resistivity and potential logs in boreholes, the electrical effects accompanying ground water flow etc.

### C. Studies on Soil Systems

Ravina and Zaslavsky's review<sup>156</sup> covers the early work on nonlinear electroosmotic flux and hydraulic flux. They<sup>302</sup> also developed a differential formulation of nonlinear flow equations similar to Li's approach<sup>259</sup> with one main difference. In Li's approach the function is expanded by using Taylor's series around zero values of  $J_i$  and  $X_j$  by taking  $\Delta X_j$  of any size. The derivatives ( $\partial J_i / \partial X_j$ ) are then taken at the same zero or at equilibrium. In the differential formulation<sup>302</sup> it is suggested the total differential of  $J_i$  be expressed at any set of values  $X_j$ . The first electrokinetic quantitative studies of the electrophoresis of clay particles in the nonlinear region of soil systems are due to these workers.<sup>303</sup> Their data on the electrophoretic velocity of sodium bentonite particles in sodium chloride solutions at different concentrations, are summarized in Table XVIII. The electrical gradients used to obtain the data in Table XVIII were, in each case, in the range of 2–20 V cm<sup>-1</sup>. A regression analysis was used to get an estimate of the coefficients and their significance.

The nonlinear equations obtained in this case (Table XVIII) are not consistent with eq 120 or eq 137. The coefficient "b" in the equations in Table XVIII may be viewed as the electrophoretic mobility in the linear range and the coefficient "a" as the deviation from a homogeneous linear equation. According to the equation in Table XVIII even when the applied electrical gradient  $E$  is 0,  $V_e$  has a finite value. The question arises as to what can be the driving force for this residual value of  $V_e$ . Ravina and Zaslavsky<sup>303</sup> have not provided an answer to this question. The whole thing may just as well be a statistical artifact.

Electroosmotic studies in the nonlinear region, through clay membranes, have been conducted on a kaolinite–water system.<sup>304</sup> Experiments on electroosmotic pressure, electroosmotic velocity, streaming potential, and current have also been conducted. Analysis of the data revealed that the cross coefficients  $L_{12}$  and  $L_{21}$  remain constant for a larger region in comparison to the straight coefficients particularly  $L_{11}$ . Equation 28 was found to have a much larger validity range, e.g. the streaming potential, and also the streaming current was found to vary proportionally throughout the range studied, i.e. upto  $\Delta P = 24$  cm of Hg. The electroosmotic velocity also varied proportionally with the applied electrical potential difference throughout the range studied i.e. up to  $\Delta \phi = 50$  V. However, the electroosmotic pressure difference showed a departure from the proportional relationship with  $\Delta \phi$ . Beyond  $\Delta \phi = 35$  V, it became less than proportional. Thus the nonlinearity of electroosmotic effects in the kaolinite–water system arose primarily as a result of nonconstancy of the coefficient  $L_{11}$ . The equation

$$J_v = L_{11}\Delta P + L_{12}\Delta \phi + \frac{1}{2}L_{111}(\Delta P)^2 \quad (165)$$

was shown to adequately describe the water flux data in the nonlinear region. The data also showed the validity of Onsager's relations indicating its internal consistency. Studies on the bentonite–water system, however, call for more critical scrutiny. Michaels and Lin's<sup>162</sup> studied on streaming potential in the case of the kaolinite–water system and those of Kemper<sup>305</sup> in the case of bentonite indicated that the coefficients  $L_{22}$ ,  $L_{21}$ ,  $L_{21}$  in eqs 27 and 28 remain constant up to quite reasonable limits in the case of clays. Although the proportional relationship (Darcy's law)

$$(J_v)_{\Delta \phi=0} = L_{11}\Delta P \quad (166)$$

adequately describes the experimental data for the flow of water through coarse soils,<sup>306</sup> Swartzendruber<sup>307</sup> suspected that it may not hold for clays particularly for bentonite-like clays. He suggested empirically that the following equation

$$(J_v)_{\Delta \phi=0} = \alpha[\Delta P - \Delta P_0\{1 - \exp(-\Delta P/\Delta P_0)\}] \quad (167)$$

should hold instead<sup>307</sup> where  $\alpha$  is some constant. Equation 167 reduces to

$$(J_v)_{\Delta \phi=0} = \alpha(\Delta P)^2 \quad (168)$$

which ignores the linear regime. The actual experimental data as well as its analysis therefore need a fresh look.

### D. Studies on Systems of Biological Relevance

Not many studies are available where conclusions of biological significance have been drawn from nonequi-



librium thermodynamic studies on electrokinetic phenomena in the nonlinear region. Studies conducted by Rastogi et al.<sup>308,309</sup> on electrokinetic phenomena, both electroosmotic and electrophoretic, on cholesterol, estrone/electrolyte, and nonelectrolyte systems were conducted from the point of view of examining their earlier theoretical framework.<sup>279</sup> These studies involving quantification of the electrical properties of their interfaces do have biological relevance. Cholesterol is involved in many diseases from atherosclerosis to xanthomatosis. Before deposition in arteries and as stones in the gallbladder, the first stage which occurs is coagulation which is influenced by the properties of the cholesterol/solution interfaces. Similarly the female sex hormone estrone is believed to act as one of the physiological regulatory agents by affecting the cellular membranes. Thus the study of the estrone/electrolyte–nonelectrolyte interface becomes relevant.

In the case of cholesterol where studies were confined to the linear region, the values of the zeta potential estimated from electroosmotic and electrophoretic measurements were found to disagree.<sup>309</sup> The main reason for this appears to be the fact that in the equation used for the calculation of the zeta potential from electroosmotic data, the values for the specific conductivity and viscosity are for the liquid inside the pore, whereas the experimental values substituted are for the bulk liquid. Comparison of the zeta potential for the cholesterol/electrolyte–nonelectrolyte systems show that the magnitude of the zeta potential is much higher in the former case. This might be due to the effective charge being higher in the former case. For the same reason the values of the zeta potential estimated from electroosmotic measurements did not agree with those estimated for electrophoretic measurements in the case of estrone.<sup>308</sup> In the case of the estrone/nonelectrolyte systems nonlinear flux equations were experimentally substantiated for electroosmotic transport, whereas, when electrolyte solutions were used as permeants, linear equations were found to be sufficient. This was explained on the basis of the possibility of formation of a dipolar layer in the case of nonelectrolyte solution as permeants. This is in accordance with the formalism of Rastogi and Shabad.<sup>279</sup> Electrophoretic data<sup>308</sup> were again represented by linear equations.

Shukla and coworkers have carried out studies where conclusions of physiological significance have been obtained.<sup>264,310–314</sup> They have experimented with mammalian (goat) urinary bladder membrane and used aqueous solutions of mixtures of constituent of urine as permeants, under both normal and pathological conditions. The data on hydraulic permeability revealed<sup>310</sup> that the membrane is anisotropic. In the case of an aqueous solution of urea–glucose mixture it was observed that with increasing urea concentration at constant glucose concentration, the hydraulic permeability first increased and then decreased. It was also observed that if the urea concentration is held constant, the hydraulic permeability first decreased and then increased with increasing glucose concentration.

Shukla and Mishra<sup>311</sup> have extended their studies and measured the hydraulic permeability, electroosmotic permeability, streaming potential, and current across urinary bladder membranes using aqueous solutions of urea, thiourea, glucose, and creatinine. They

showed that nonlinear relations exist between fluxes and forces. Onsager's and higher order phenomenological coefficients have been estimated. They argued that the nonlinear equations appear reasonable because in the urinary bladder system, although the initial filling of urine in the bladder does not result in a significant change of pressure the accumulation more urine causes the pressure to rise rapidly.<sup>315</sup> Therefore, nonlinear relationships are not unlikely. Using the stability criterion<sup>11,12,316</sup>

$$\sum \delta J_i \delta X_i > 0 \quad (169)$$

Shukla et al.<sup>312</sup> showed that the nonlinear steady states in their system were quite stable. These authors,<sup>311</sup> on the basis of the trends observed in their data, have attempted to correlate micturition with electrokinetic phenomena as follows:

Urine is collected through the kidney by ureters which are tubes consisting of smooth muscle. They also prevent back-flow of urine when pressure builds up in the bladder during micturition. When there is no urine in the bladder the intravesical pressure is very low. As urine collects in the pelvis the increased pressure stretches the bladder. During micturition, the detrusor muscle contracts to empty the bladder. The micturition reflex occurs on account of micturition waves and is self-regenerative. Shukla and associates<sup>310–314</sup> have tried to correlate micturition waves with streaming potentials/currents.

Their observations need further corroboration. In addition it has to be noted that the in vitro system chosen for the studies cannot be expected to retain all the characteristics of an in vivo membrane system and hence it is uncertain as to what extent their results can be extrapolated to in vivo systems.

In the next section we propose to discuss exotic phenomena, e.g. bistability and electrokinetic oscillations which occur in the far-from-equilibrium region. This may appear to be out of place in the first instance in this review since there exists a justifiably strong reservation about the application of nonequilibrium thermodynamics in this region. Furthermore, in the case of chemical reactions, the ideas of nonequilibrium thermodynamics<sup>6,7,210</sup> cannot be profitably extrapolated to the nonlinear region or far-from-equilibrium region. This is exemplified in the case of oscillatory reactions where nonlinear dynamics rather than thermodynamics has been established as the effective basic tool. However, the case of electrokinetic phenomena is different. Fluxes and forces as defined by linear thermodynamics have neat physical significance and are measurable and need not be subjected to artificial linear transformation. Even in the case of nonlinear flux equations, the first-order terms obey Onsager's symmetry. The case of chemical reactions is complicated on account of the need to search for elementary and coupled reactions. These may be too many, and the only viable course of action is to fall back on mass-action kinetics. The utility or otherwise of ideas of the nonlinear region or far-from-equilibrium region has to be investigated and hence a discussion of nonlinear phenomena should be in order.

## V. Far-from-Equilibrium Region

### A. Electrokinetic Oscillations—Introductory

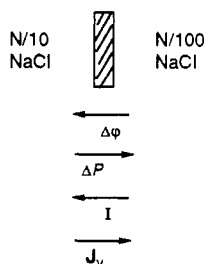
While this article was being written, a review by Raima Larter on oscillations and spatial nonuniformities in membranes appeared<sup>317</sup> and included a brief survey of the literature on oscillatory phenomena. In this section, attention will be focused on some more relevant aspects.

At equilibrium, the thermodynamic forces,  $\Delta P$ ,  $\Delta\phi$ ,  $\Delta C$ , etc. are zero and the consequent fluxes  $J_v$ ,  $I$ , etc. are also zero. For finite values but not large values of the differences, the linear thermodynamics of irreversible process using linear phenomenological equations adequately describes the electrokinetic phenomena. When the magnitude of the thermodynamic forces further increases, the nonlinear phenomenological equations become significant (see the discussion on the nonlinear region) and even third-order terms as in the case of the urinary bladder have to be taken into account.<sup>310,311</sup> Even in such nonlinear situations a monotonic buildup of the steady state is obtained and no dynamic instability is observed. However, under specific conditions, when a difference in the concentration of an electrolyte (say sodium chloride) is maintained across the membrane, bistability and temporal oscillations in volume flow, pressure difference, potential difference, and resistance have been observed. There are a few interesting studies reported. Experimental, as well as theoretical, papers have appeared: Teorell,<sup>14,15</sup> Meares and Page,<sup>318,319</sup> and Kobatake and Fujita.<sup>20,320</sup> Now that the gross features and principles of oscillatory chemical reactions are well understood there is a need to understand the dynamic instability in membrane processes governed by electrokinetic principles. Dynamic instability in such cases can be successfully studied from the experimental angle because the system can be maintained in the far-from-equilibrium region to any desired extent by controlling the variables, as in the case of a continuously stirred tank reactor (CSTR).

Before a discussion of the Teorell-type oscillator is considered a brief introduction to bistability is needed.

### B. Bistability

The following type of system has been used by several groups to demonstrate bistability in electrokinetic phenomena.<sup>20a,318,321,322</sup>



Typical N-shaped curves, which have also been referred to as the flip-flop type, between current  $I$  and electrical potential difference  $\Delta\phi$  are obtained. The nature of  $I$  versus  $\Delta\phi$  plots obtained from such studies is depicted in Figure 25 which show that within a narrow range of

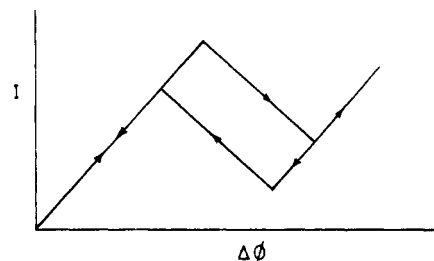


Figure 25. The nature of  $I$  versus  $\Delta\phi$  plots.

$\Delta\phi$ , the system can exist in two steady states i.e. for the same value of  $\Delta\phi$  it can have two values of  $I$ . In other words the membrane system exists in two steady states, one with a lower resistance and the other with a higher resistance. The former is due to the filling of membrane pores with concentrated solution while the latter corresponds to the situation when the membrane pores are filled with dilute solution. Rastogi and associates<sup>322</sup> found similar results. However, they found that within the range of bistability, the electroosmotic flux is highly nonlinear and is given by the equation

$$J = L_{12}\Delta\phi e^{b\Delta\phi} \quad (170)$$

where  $b$  is another constant.

Kobatake and Fujita<sup>20a</sup> developed a theory of the phenomenon by deducing continuity equations for electricity and mass flow by combining the Navier-Stokes equation for the mass movement and the concepts of thermodynamics of irreversible processes. The steady-state solution of the resulting equations yielded the characteristic N-shaped relation between the electric current  $I$  and the transmembrane potential  $\Delta\phi$  which involved hysteresis between the transition points. The features of the curves predicted by Kobatake and Fujita's theories<sup>20a</sup> compared well with Franck's experimental results<sup>321</sup> on a sintered glass membrane separating 0.01 and 0.1 N NaCl solutions with the only difference being that no hysteresis was observed. However, in later experiments, Meares and Page<sup>318</sup> observed both bistability and hysteresis. Kobatake<sup>320</sup> also attempted to study the phenomenon in terms of generalized entropy production as proposed by Glandsdorff and Prigogine<sup>323-326</sup> and has tried to show that the transition between two steady states takes place when the generalized entropy productions of the two states corresponding to the high and low electric resistances of the membrane have the same value. However, a general proof is difficult to provide.

The possibility of multiple steady states in the streaming potential is seen in the experiments conducted by Rastogi et al.<sup>278</sup> on a Zeokarb 225 ( $\text{Ba}^{2+}$  form)/methanol-water system. The results are plotted in Figure 23. These are reproducible experiments, and the data are internally consistent. Reproducibility of the data was checked through a number of observations made for increasing as well as for decreasing magnitudes of  $\Delta P$  for the same direction of flow. The internal consistency was also checked by releasing the pressure occasionally so that  $\Delta P = 0$ . The streaming potential returned to zero value. For the  $\text{Ba}^{2+}$  form and also the  $\text{Al}^{3+}$  form of the resin multiple sign reversals were observed. The possibility of multiplicity of steady states can be understood if one examines the characteristic

nonlinear flux equation for the  $H^+$  form of the resin,<sup>278</sup> i.e.

$$I = L_{21}(\Delta P/T) + L_{22}(\Delta \phi/T) + \frac{1}{2}L_{211}(\Delta P/T)^2 + L_{212}(\Delta \phi/T)(\Delta P/T) \quad (171)$$

when  $I = 0$  one gets a quadratic equation in  $\Delta P$  and consequently two values of  $\Delta P$  for the same value of  $\Delta \phi$ . It should be noted that  $\Delta P$  is the independent variable and  $\Delta \phi$  is the dependent variable in the experiment, and further steady states are obtained continuously on varying the pressure and hence no instability is involved.

### C. Indications of Electrokinetic Mechanism in Cellular Excitability

The phenomenon of nerve conduction appears to be an electrokinetic phenomenon whereby it is possible to envisage channels in the membrane which are used as pathways for ion transport. Attempts have been made to mimic the excitation behavior on artificial bilayer lipid membranes (BLM systems) in the presence of channel-forming proteinaceous substances.<sup>327,328</sup> Only BLMs did not show any excitability. However, when an excitability-inducing material (EIM), like the proteinaceous substance, isolated from egg white,<sup>329</sup> which is yet to be completely characterized, was introduced, action potentials similar to those in some excitable cells were produced<sup>330,331</sup> under certain conditions. Bean et al.<sup>332</sup> attribute this to the formation of discrete proteinaceous trans-membrane channels which have two or more well-defined conductance states. Several groups have attempted to establish the characteristics of these channels.<sup>333-335</sup> Hoffman et al.<sup>336</sup> reported observations of voltage-clamped oxidized cholesterol BLMs with EIM which have several rather than two conductance states at a given voltage polarity. Mueller and Rudin<sup>337</sup> mimicked the excitation behavior on BLMs formed from *Sphingomyelin* in tocopherol and modified by alamethacin. There is some evidence of channel formation and discrete steps in conductance.<sup>335,338</sup> Similar observations were made by Mauro et al.<sup>339</sup> in the case of monazomycin.

Pant and Rosenberg<sup>340</sup> reproduced sustained coupled electrical and mechanical oscillations across BLM systems containing no EIM or other channel formers when the BLM separated KCl solutions containing a redox couple. Sustained oscillations in both voltage mode and in current mode, for several hours were obtained. It was found that on increasing the applied voltage, the amplitude of the oscillation is increased but not the frequency. The oscillations observed by Pant and Rosenberg<sup>340</sup> cannot be compared with those obtained with Teorell's oscillator (to be described later) since the medium on the two sides of the membrane in the former case is quite complex. It was also observed that when electrical oscillations begin the position of the circumference of the membrane also begins to oscillate, thus further complicating the issue. It appears that the electrical and mechanical oscillations are coupled. The question whether or not these oscillations are related to the streaming potential, osmotic pressure or fundamental electromechanical instabilities in the electrified bilayer lipid membrane calls for further investigation. Monnier et al.<sup>341-344</sup> developed lipid-like

membranes through the polymerization of oils which show, in the absence at any channel former, some excitability properties including action potential and regular oscillations in voltage when a constant current is applied. Botre et al.<sup>345</sup> have also mimicked excitability in the absence of any channel formers. Shashoua's experiments<sup>346,347</sup> are even more revealing. He showed that polyelectrolyte bipolar membranes containing no lipids or proteins, under a dc. electric field, can spontaneously generate transients with time constants and amplitudes analogous to the spike potentials of neuronal membranes. Several other studies where excitability characteristics could be mimicked in the absence of channel formers are documented. For example, studies on a filter whose pores were filled with dioleoyl phosphate (DOPH) were conducted by Kamo et al.<sup>348</sup> The mechanism of oscillation in these systems was explained on the basis of an earlier observed hysteresis of membrane permeability with concentration.<sup>349-351</sup> Ishii et al.<sup>352</sup> studied the oscillation of electrical potential in porous membranes doped with triolein induced by  $Na^+/H^+$  concentration gradient. Yoshida et al.<sup>353</sup> and Arisawa and Furukawa<sup>354</sup> studied nitrocellulose membranes doped with glycerol  $\alpha$ -monooleate and filters containing varying amounts of lipids.

Oscillations in membrane potential have been observed when pancreatic islet cells are placed in a medium containing glucose.<sup>355</sup> It is found that: (i) the potential across the membrane remains of the order of  $-40$  to  $-50$  mV (inside to outside) as long as the extracellular glucose concentration is maintained at a low basal level, e.g. 2.8 mM; (ii) in the total absence of glucose, the cell polarizes to values in excess of this and may reach potentials  $\geq -60$  mV; (iii) when the concentration of extracellular glucose reaches 4 mM, typical patterns of spike discharge are obtained; and (iv) when the concentration is  $\sim 28$  mM, the spike discharge becomes continuous. The electrical oscillations observed in the above case could be due to (i) simple membrane oscillations, (ii) oscillations due to coupling of the glycolytic reaction and membrane transport of glucose, and (iii) oscillations due to development of the streaming potential. Further studies are needed to clarify the exact nature of the oscillations.

The pumilion toxin- $\beta$  (PTX- $\beta$ ) which induces repetitive activity of the electrically excitable membrane of frog sartorius muscle has been investigated by Rao et al.<sup>356</sup> The role of calcium and sodium ions in nerve and skeletal muscle activity has also been examined. Here again, there is a possibility of electrical oscillation triggered by the streaming potential.

It was observed<sup>354,357</sup> that, when a constant direct current and static pressure are simultaneously applied, the resistance of a Millipore membrane, on which a synthetic lipid analogue—dioleoyl phosphate (DOPH)—is absorbed and  $Ca^{2+}$  ions are allowed to combine with it, undergoes undamped oscillations for several hours when the current stimulus was kept below  $0.1 \mu A$  and the pressure stimulus ranges between 15 and 35 mmHg. It has been suggested<sup>358</sup> that this behavior is related to conformational changes of DOPH in the presence of the ions of the bathing electrolyte. Kim and Larter<sup>359</sup> suggested a different mechanism based on coupling between the externally driven flow and the electroosmotic flow.

## D. Teorell's Oscillator

In view of the studies cited in the above paragraphs particularly those where excitability behavior has been mimicked, even in the absence of channel formers, Teorell's work<sup>14,15,360</sup> on systems consisting of porous glass or ion exchange membranes separating two electrolyte solutions of differing concentration assumes great significance. Since the occurrence of oscillatory phenomena could be demonstrated in these systems, Teorell's experiments point toward the possibility of developing a physical theory of transport phenomena observed in several excitable cells. On driving a constant current through the membrane, oscillations are observed in the membrane potential as well as resistance and hydrostatic pressure. It was found that there exists a certain threshold value of applied current below which only damped oscillations were obtained. Above this threshold value, undamped and sustained oscillations were obtained. Similar results were obtained by Meares et al.<sup>318,319</sup> It should be mentioned that Forgacs<sup>362</sup> independently reported oscillations in membrane potential on passing a constant current through a cation exchange membrane separating identical solutions of silver nitrate. However, the mechanism of oscillation generation is still not clear.

Electrokinetic experiments are difficult. As pointed out by Meares and Page,<sup>318</sup> a number of conditions have to be satisfied in order to achieve undamped oscillations. These are as follows: (i) The maximum area of membrane should be  $\sim 38.5 \text{ mm}^2$ , with the best results obtained for 12.6 or 7.1  $\text{mm}^2$  of membrane exposed. (ii) There should be no restriction on the cross section of vertical capillaries, which could range from 0.5 to 10 mm. (iii) A stirring rate  $> 100 \text{ rpm}$  and fluid circulation rate  $> 500 \text{ mL/h}$  are adequate for getting undamped oscillations. (iv) The absolute concentration of the electrolytes and their ratio were found to be necessary for regular periodic oscillations. (v) A critical current density was required for each experimental configuration above which undamped oscillations could be obtained.

For Teorell's oscillator the following membrane characteristics hold: pore diameter  $\approx 1 \mu\text{m}$ ; porosity  $\approx 70\text{--}80\%$ ; thickness  $\approx 1 \text{ mm}$ . The half-time for the relaxation of the pressure head is  $\approx 5 \text{ min}$ . Evidently some of the requirements are governed by the necessity of having appropriate relaxation time magnitudes. Furthermore, it is obvious that the proper choice of (i) material, (ii) porosity, (iii) thickness, and (iv) electrical charge of the membrane is necessary. Silver-silver chloride electrodes to be used in such experiments have to be heavily chlorodized.

In the above context it is worthwhile to draw attention to bistability studies in systems similar to those for which steady-state current voltage relationships at fixed pressures were found to be N-shaped. The ratio of the conductances in the two steady states are compared in Table XIX. A sudden discontinuity was found around  $\Delta\phi \approx 10 \text{ V}$ . Three steady state multiplicity types are usually observed: (i) multiplicity without hysteresis and no sudden change in state, (ii) multiplicity with hysteresis but no sudden change in state, (iii) multiplicity without hysteresis but with a sudden change in the state—a characteristic N-shaped relationship. The N-shaped relationship seems to be due to an interplay

**Table XIX. Ratio of Conductance in the Two Steady States**

membrane system	approximate ratio of conductance in the two steady state	ref
0.5 N NaCl/Pyrex sinter/ 0.05 N NaCl	2:1	Tasaki's unpublished data cited in ref 20
0.1 N NaCl/Pyrex sinter/ 0.01 N NaCl	3:1	361
0.1 N NaCl/millipore filter/ 0.01 N NaCl	7.5	318
0.1 N NaCl/Pyrex sinter/ 0.01 N NaCl	2:1	322
0.1 N KCl/Pyrex sinter/ 0.01 N KCl	4:1	322

of the hydrostatic flux and the electroosmotic flux. Initially, the hydrostatic flux predominates and the membrane pores are filled with concentrated solutions but at the crossover point, there is a sudden increase in electroosmotic flux and the membrane pores are filled with dilute solution. The reverse behavior is observed when we move from the higher to the lower potential side. However, complete flushing of the membrane with either concentrated or dilute solution seldom occurs. Hence the ratio of conductances, along the branches representing two steady states in the N-shaped curve, does not compare with the case when complete flushing would have occurred.

The Teorell type of membrane oscillations has been theoretically examined by several authors, e.g., Arnou,<sup>363</sup> Kobatake et al.,<sup>20</sup> Meares and Page,<sup>319</sup> as well as Teorell himself.<sup>15</sup> Arnou's analysis showed that oscillations observed in the Teorell system were hydrodynamic in origin and a consequence of the boundary condition effect on the hydrodynamic stability. Larter<sup>317</sup> believes that this conclusion need not be universally true for all membrane oscillations. We will now discuss Kobatake et al.'s<sup>20,320</sup> and Meares and Page's<sup>319</sup> analysis of the Teorell oscillator.

To review the earlier theoretical developments let us consider the phenomenological eqs 1–3 for the membrane system shown in Figure 2. Let us consider the case when  $\Delta\Pi_i = 0$ . In the linear range the Onsager's relation  $L_{ij} = L_{ji}$  holds among the phenomenological coefficients, and the steady state is characterized by the minimum of entropy production.

A little beyond the linear range when the fluxes and the relation between the fluxes and forces is nonlinear, we can have  $d\Psi = \sum J_i dX_i$ , where  $\Psi$  is a sort of potential. In the nonlinear range, one may have two steady states which may have the same value<sup>320</sup> of  $\Psi$ . This may give rise to the phenomenon of bistability. Beyond the bifurcation point, the system may exist in two steady states. An exchange of stability may take place at this point.<sup>11,12</sup> Unstable states can also occur beyond the bifurcation point, leading to oscillatory behavior.

It should be noted that the phenomenological coefficients, in eqs 1–3, are constants when  $\Delta C = 0$ , i.e. when solutions of the same concentration are on both sides of membrane. When  $\Delta C \neq 0$ ,  $L_{12}$ ,  $L_{21}$ , and  $L_{22}$  are complex functions of concentrations and in turn volume flux and electroosmotic flux functions. Thus, these

equations become nonlinear and under specific conditions can give rise to exotic nonequilibrium phenomena.

Thermodynamic considerations give an insight into the broad general features of nonequilibrium phenomena. For a detailed quantitative understanding of instability and oscillatory features, kinetic and other theoretical methods have to be considered. Two approaches have been suggested in the literature. The first is Teorell's semiempirical approach<sup>15</sup> and a second more refined one due to Kobatake et al.<sup>20</sup> and Meras and Page.<sup>319</sup>

The essential features of Teorell's theory are as follows. The contributions of  $\Delta C$  in influencing flow processes in the oscillator are ignored except its contribution which affects membrane resistance. Thus, in equations

$$J_v = L_{11}\Delta P + L_{12}\Delta\phi \quad (27)$$

$$I = L_{21}\Delta P + L_{22}\Delta\phi \quad (28)$$

on account of the membrane set up  $L_{12}$  has a negative value and  $L_{22} = 1/\mathcal{R}$  where  $\mathcal{R}$  is the resistance. It is assumed that  $L_{22}$  depends on the volume flow. When one writes

$$\dot{\mathcal{R}} = -k(\mathcal{R} - \mathcal{R}_{J_v}^\infty) = -k[\mathcal{R} - f(J_v)] \quad (172)$$

where  $\mathcal{R}_{J_v}^\infty$  = steady-state value of the resistance, nonlinearity is implicitly introduced. Equation 172 can be written as

$$\Delta\dot{\phi} = k[I(f(J_v) - \Delta\phi)] \quad (173)$$

since  $\Delta\phi = I\mathcal{R}$ . Two other assumptions are made. First,  $L_{12}$  is assumed to be constant, which is doubtful. Second, the streaming current  $L_{21}\Delta P$  is supposed to be negligible compared to the ohmic current<sup>21</sup> which, of course, is not an unreasonable approximation. It has been suggested from theoretical considerations that  $L_{12}$  is inversely proportional to  $C^{1/2}$  but the actual relationship may be quite complex.

Taking the time derivative of eq 27 under the above conditions, we have:

$$\dot{J}_v = L_{11}\Delta\dot{P} + L_{12}\Delta\dot{\phi} \quad (174)$$

or

$$\dot{J}_v = L_{11}(J_v/q) + L_{12}k[I(f(J_v) - \Delta\phi)] \quad (175)$$

when we substitute the value  $J_v = q \, d\Delta P/dt$  and  $\Delta\dot{\phi}$  from eq 173,  $q$  being a geometrical factor as defined by Teorell.<sup>15</sup>

Now, for small excursions in the region where the curve of the function  $\mathcal{R}_{J_v}^\infty = f(J_v)$  is linear (i.e. around  $J_v = 0$ )<sup>14,15</sup> with a slope  $r$  so that in this range  $\mathcal{R}_{J_v}^\infty = rJ_v + \mathcal{R}_0^\infty$ , from eqs 173 and 174, we can write

$$dx/dt = a_{11}x + a_{12}y \quad (176)$$

$$dy/dt = a_{21}x + a_{22}y \quad (177)$$

where  $x = J_v$ ,  $y = (\Delta\phi - (\Delta\phi)_0)^\infty$ . The coefficients  $a_{11}$ ,  $a_{12}$ ,  $a_{21}$ , and  $a_{22}$  in eqs 176 and 177 are defined as

$$a_{11} = klir - s/q \quad (178)$$

$$a_{12} = (-kl) \quad (179)$$

$$a_{21} = kir \quad (180)$$

$$a_{22} = -k \quad (181)$$

where  $k$  is the membrane coefficient,  $s$  is the hydrostatic permeability (the porosity),  $l$  is the electroosmotic permeability,  $q$  is the geometrical factor, and  $i$  is the current strength as defined in Teorell's theoretical treatment.<sup>14,15</sup>

Equations 176 and 177 are of the form which can permit oscillations<sup>12</sup> provided (i)  $a_{11} + a_{22} = 0$ , i.e.  $k(lir - 1) = s/q$  and (ii)  $(a_{11}a_{22} - a_{12}a_{21}) > 0$ , i.e.  $ks/q > 0$ . Both these conditions are possible.

Kobatake's treatment is more elaborate. Using a capillary model of the membrane and the concept of an electrical double layer, they obtain for the flux of the electrolyte component  $(J_s)_c$  and for the electric current  $(I)_c$ , both relative to the capillary wall:

$$(J_s)_c = -D(\partial c/\partial x) + D'c(\partial\phi/\partial x) + cu_m \quad (182)$$

$$(I)_c = -\lambda c(\partial\phi/\partial x) - \lambda'(\partial c/\partial x) \quad (183)$$

where  $u_m$  is the velocity of the local center of mass at a particular position. The other constants are the same as defined in the Kobatake and Fujita's work.<sup>20</sup>  $J_s$  is the average flux of the salt,  $I$  is the average intensity of the current. This approach is related to deGroot and Mazur's thermodynamic-hydrodynamic treatment of similar irreversible processes.<sup>1</sup>

Defining the average rate of mass flow  $U_m$ , over the cross section of the capillary as

$$U_m = \frac{(\int 2\pi r \rho u_m dr)}{(\int 2\pi r dr)} \quad (184)$$

$$J_s = \frac{(\int 2\pi r (J_s)_c c dr)}{\int 2\pi r dr} \quad (185)$$

$$I = \frac{(\int 2\pi r (I)_c dr)}{(\int 2\pi r dr)} \quad (186)$$

Now when we replace the density  $\rho$  with  $\rho_0$  of water, we can write,

$$J_s = -D(\partial c/\partial x) + D'c(\partial\phi/\partial x) + cu_m \quad (187)$$

$$I = -\lambda c(\partial\phi/\partial x) - \lambda'(\partial c/\partial x) \quad (188)$$

However, it can be shown that

$$U_m = -A(\partial\phi/\partial x) - (B/C)^{1/2}(\partial\phi/\partial x) \quad (189)$$

where  $A$  and  $B$  are as defined by Kobatake and Fujita.<sup>20</sup> It should be noted that  $U_m$ , and in turn  $J_s$ , depend on the pressure and potential gradients. The coefficient of the second term is the electroosmotic coefficient. For the steady flow inside the capillary, the conservation of mass and electricity yield the equations:

$$dU_m/dx = 0 \quad dJ_s/dx = 0 \quad dI/dx = 0 \quad (190)$$

These equations are sufficient to determine the three variables  $\rho$ ,  $\phi$ , and  $c$  inside the membrane as a function of  $x$ . These equations have been exactly solved by Kobatake and Fujita by assuming boundary conditions and that all the coefficients are constant. The results yield a characteristic  $I$  versus  $\Delta\phi$  curve which agrees with the bistability observed in similar systems.

In treating oscillations, Kobatake and Fujita<sup>20</sup> essentially used an equation of the following type:

$$h(d^2h/dt^2) + f(dh/dt) + \rho gh = 0 \quad (191)$$

where  $h$  denotes the position of the meniscus,  $g$  is the acceleration due to gravity;  $\rho$  is the density while  $f(dh/dt)$  is of such a form that the above equation represents the behavior of a self-excited system which can produce oscillations. The term  $f(dh/dt)$  is related to the pressure difference on the two sides of the membrane which in turn is related to  $U_m$  and thus the mechanism of oscillations can be related to the volume flux and the electroosmotic flux.

Kobatake and Fujita's approach has been critically examined by Caplan and Mikulecky.<sup>364</sup> First, the contribution of pressure to flow relative to the center of mass was neglected. Second, the local phenomenological equations relating to a streamline within a pore are not symmetrical when referred to a membrane. It should be noted that from the point of view of irreversible thermodynamics, whatever the structure of the membrane, it is necessary that any changes in reference frames must preserve Onsager's symmetry. Third, the integral phenomenological coefficients depend on the concentration and cannot be explicitly obtained unless the variable concentrations are replaced by average values. Evidently this is not the case for the membrane oscillator.

With respect to the second point, Caplan and Mikulecky have shown that a correct averaging procedure yields symmetrical relations,<sup>21</sup> if the local forces and flows are chosen so as to form a set of conjugate pairs.

Meares and Page<sup>319</sup> developed a theory of the stationary states on the basis of a broad pore model similar to that used by Kobatake and Fujita<sup>20</sup> but they used the conjugate set of fluxes and forces as recommended by Mikulecky and Caplan.<sup>21</sup> In their theory they also considered the concentration dependence of the surface charge within the pores and took into account the presence of unstirred diffusion layers in the solutions adjacent to the membrane surface.

For analyzing the periodic behavior of a membrane oscillator both Kobatake and Fujita<sup>20</sup> and Meares and Page<sup>319</sup> assumed that the salt and water fluxes in the membrane did not depart from the stationary fluxes which would prevail under instantaneous conditions. However, nonstationary effects arising from the momentum of the fluid flowing in the chambers of the membrane cell were considered.

In addition to the above mentioned theoretical problems, the physical understanding of the oscillatory phenomena is still not very clear. As indicated in the previous subsections nonequilibrium steady states are obtained in the linear range when  $\Delta C = 0$ . Similar steady states are obtained when nonlinear flux equations have to be taken into account. The foregoing theoretical discussion shows that exotic nonequilibrium states can arise when  $\Delta C \neq 0$  and when the phenomenological coefficients are not constants but depend upon the concentration in a complex manner.

When the membrane is saturated with concentrated solution, electroosmotic flux increases very rapidly at the applied current on account of the high potential difference. The flux is much higher than the corre-

sponding flux for the dilute solution (positive) to concentrated (negative) solution side, and in due course the membrane is filled with dilute solution. Now the higher electroosmotic pressure built up on the concentrated solution side relaxes to the lower electroosmotic pressure required for lower electroosmotic velocity (for a dilute solution). Hence, a backflow occurs from the concentrated solution side. A certain time lag is necessarily involved. The cycle repeats over and over again. Electroosmotic flux provides the positive feedback while hydrostatic flux provides the negative feedback.

## VI. Concluding Remarks and Future Projections

Linear thermodynamics of irreversible processes provides a base for exploring the nonequilibrium region. The power of linear thermodynamics lies in identifying the fluxes and forces and predicting the steady-state relations. Thermodynamic consistency of experimental results in this range can be tested by using Onsager's reciprocal relation. In the linear range, steady states are stable. Out of a number of cross phenomena such as thermosmosis, electrophoretic phenomena, the Dufour and Soret effects, and thermoelectric phenomena, only electroosmosis and streaming effects are the most appropriate for studying incursions in linear, nonlinear, and far-from-equilibrium phenomena from an experimental angle. These cases can be investigated under controlled conditions and extended systematically to the nonequilibrium region. The stability of steady states and the approach to the steady state can also be conveniently investigated.

From a conceptual angle, it has to be understood how electroosmosis of neutral species in a mixture of ionic species such as in iontophoresis occurs. A formal thermodynamic treatment of the phenomena is imperative in view of its importance in transdermal drug delivery.

So far, most of the experimental studies cited in this review have been limited to cases where concentration differences on the two sides of the membrane were zero and thus exotic nonlinear phenomena were largely masked. Systematic studies in situations where  $\Delta C \neq 0$  are needed since the coefficients in flux equations are known to be concentration dependent. In other words, the gradual transition from smooth steady-state behavior to exotic behavior, where bistability and oscillations are observed, deserves to be investigated in depth. It is true that thermodynamics as such cannot be the tool for investigating such situations, but it would still provide a basis for correlations. There is no doubt that dynamic theories based on electrohydrodynamics can successfully provide the bridge which should be the subject for future studies.

Although oscillations in electroosmotically driven systems have been described as stated above, there is a distinct possibility of a similar type of oscillations in systems driven by streaming effects. These are likely to be physiologically important. First of all the experiments have to be designed in a way to elucidate the physics of nonlinear exotic effects. Efforts have to be made to predict such effects in experimental situations once the physical conditions are controlled and understood. These studies need to be extended to situations parallel to physiological conditions.



All biological membranes, e.g. plasma membranes, are under the influence of very high electric field across them ( $\sim 10^7$  V m $^{-1}$ ), 100 mV across the membrane of thickness around 100 Å. It is also well known that the passive permeability of water through plasma membranes is quite high, indicating the presence of hydrophilic pathways in them. Thus it appears on a priori grounds that electroosmosis may have a role in physiology. Save for the few attempts made by Fensom, Dainty, Spanner, etc. reviewed in this article, this point has not been investigated in full detail. Such investigations should prove rewarding.

Electrokinetic studies in the far-from-equilibrium region are expected to be intimately related to the physiology of excitable cells/membranes. This assertion has been made very clearly by Teorell in his papers.<sup>14,15</sup> Although the theoretical approach of Kobatake<sup>20,320</sup> and Meares and Page<sup>319</sup> are quite illuminating and shed light on the nature of electrokinetic phenomena in the far-from-equilibrium region, as yet no direct connection with the physiology of excitable cells has been established although the latter may also be linked to the dipole-orienting gate protein phenomena. This appears to be a worthwhile future task for physical biologists.

The phenomenon of photoelectroosmosis is a new class of electrokinetic effect which is relatively less explored particularly from the point of view of nonequilibrium thermodynamics. Since this phenomenon is fascinating from several angles, e.g. bioenergetics, solar energy transduction, it merits a fuller investigation particularly from the point of view of nonequilibrium thermodynamics of electrokinetic energy conversion.

## VII. List of Symbols

$A$	pore area
$a_s$	activity of the solute
bio	figure of merit for the i, o, conversion mode
$\bar{C}_s$	mean concentration of the solute
$C$	concentration of the component indicated by the subscript
$\bar{C}$	capacitance
$E$	electric field strength
$F_k$	external force acting on component $k$
$F$	Faraday
$f_{kl}$	molar frictional coefficients between the components indicated by the subscripts
$g$	acceleration due to gravity
$h_\infty$	height level corresponding to the steady state of electroosmotic pressure
$h$	height level corresponding to electroosmotic pressure at any time $t$
$h_0$	height level corresponding to electroosmotic pressure at $t = 0$
$I$	flow of current
$J_v$	flow of volume
$J_s$	flow of solute
$J_w$	flow of water
$J_i$	flow of the species $i$ , $i = 1, 2$
$k$	specific conductance of the liquid
$L_{ik}$	phenomenological coefficient relating the $i$ th flow to $k$ th force, similarly $L_{ij}$
$L_{ik}^E$	excess phenomenological coefficient
$L_{ijk, \text{etc.}}$	second-order and higher phenomenological coefficient

$l$	length of the capillary
$N(\uparrow)$	number of flip-up dipoles
$N(\downarrow)$	number of flop-down dipoles
$N_T$	total number of dipoles
$\Delta P$	pressure differences
$\mathbf{P}^a$	axial vector representing the antisymmetric part of the total pressure tensor $\mathbf{P}$
$R$	gas constant
$\mathcal{R}$	electrical resistance
$R_{ij, \text{etc.}}$	phenomenological coefficients in the phenomenological equations written in the inverted matrix form
$r$	radius of the capillary
$S_r$	salt rejection parameter
$T$	temperature
$V$	volume
$\bar{V}_w$	partial molar volume of water
$\bar{\mathbf{v}}$	average barycentric velocity
$\mathbf{v}$	average velocity of the component indicated by the subscript
$\bar{V}$	partial molar volume of the component indicated by the subscript
$X$	generalized thermodynamic force
$Z_i$	charge number of the $i$ th species
$\beta$	efficiency of energy conversion
$\beta_e$	efficiency of energy conversion for electroosmosis
$\beta_s$	efficiency of energy conversion for streaming potential
$\eta$	coefficient of viscosity
$\epsilon$	dielectric constant
$\zeta$	zeta potential
$\Delta\phi$	potential difference
$\Delta\Pi_i$	osmotic pressure difference of the impermeable solute
$\Delta\Pi$	osmotic pressure difference
$\Delta\Pi_s$	osmotic pressure difference of the permeable solute
$\tilde{\mu}_i$	electrochemical potential of the species $i$ , $i = 1, 2$
$\pi$	transposed viscous pressure tensor
$\mu_w$	chemical potential of water
$\mu_s$	chemical potential of the solute
$\omega$	mean angular velocity of the constituent particles
$\rho_k$	mass per unit volume of component $k$
$\varphi$	dissipation function
$\bar{\varphi}_x$	average local dissipation function at a depth $x$ within the membrane
$\tau_e$	relaxation time in case of electroosmotic pressure
$\tau_s$	relaxation time in case of streaming potential
$\sigma$	entropy production ( $= \sum J_i X_i$ )
$\bar{\mu}$	dipole moment vector
$\bar{v}$	partial molar volumes

## VIII. Acknowledgments

Thanks are due to The Council of Scientific and Industrial Research, New Delhi, for support. Thanks are due to some of the referees of the *Chemical Reviews* for making highly constructive comments. Thanks are also due to Sri Ambika Pd. Singh for typing the manuscript.

## IX. References

- (1) deGroot, S. R.; Mazur, P. *Non-equilibrium Thermodynamics*; North Holland: Amsterdam, 1962.
- (2) Haase, R. *Thermodynamics of Irreversible Processes*; Addison Wesley: Reading, MA, 1969.
- (3) Fitts, D. D. *Non-equilibrium Thermodynamics*; McGraw Hill: New York, 1962.



- (4) Prigogine, I. *Introduction to Thermodynamics of Irreversible Processes*; Wiley: New York, 1968.
- (5) Onsager, L. *Phys. Rev.* **1931**, *37*, 405; **1932**, *38*, 2265.
- (6) Meixner, J. *Ann. Phys.* **1941**, *39*, 333; **1942**, *40*, 165; **1943**, *41*, 409; **1945**, *43*, 244.
- (7) Casimir, H. B. G. *Rev. Mod. Phys.* **1945**, *17*, 343.
- (8) DeGroot, S. R. *L'Effect Soret (The Soret Effect)*; North Holland: Amsterdam, 1945. See also: *J. Phys. Radium* **1947**, *8*, 188; 193.
- (9) Prigogine, I. *Etude Thermodynamique des Processus Irreversibles (Thermodynamic Study of Irreversible Processes)*; Desoer: Liege, 1947.
- (10) Prigogine, I. *J. Phys. Colloid Chem.* **1951**, *55*, 765.
- (11) Glandorff, P.; Prigogine, I. *Thermodynamic Theory of Structure, Stability and Fluctuation*; Wiley Interscience: New York, 1971.
- (12) Nicolis, G.; Prigogine, I. *Self Organization in Non-equilibrium Systems*; Wiley Interscience: New York, 1977.
- (13) Volkenstein, M. V. *Biophysics*; Mir Publication: Moscow, 1983.
- (14) Teorell, T. *J. Gen. Physiol.* **1959**, *42*, 831.
- (15) Teorell, T. *J. Gen. Physiol.* **1959**, *42*, 847.
- (16) Katchalsky, A.; Curran, P. F. *Non-equilibrium Thermodynamics in Biophysics*; Harvard University Press: Cambridge, MA, 1967.
- (17) Kedem, O.; Katchalsky, A. *Trans. Faraday Soc.* **1963**, *59*, 1918.
- (18) Kirkwood, J. G.; Baldwin, R. L.; Dunlop, P. J.; Gosting, L. G.; Kegeles, G. J. *Chem. Phys.* **1960**, *33*, 1505.
- (19) Schlögl, R. *Discuss. Faraday Soc.* **1956**, *21*, 46.
- (20) (a) Kobatake, Y.; Fujita, H. *J. Chem. Phys.* **1964**, *40*, 2212; (b) **1964**, *40*, 2219.
- (21) Caplan, S. R.; Mikulecky, D. C. *J. Phys. Chem.* **1966**, *70*, 3049.
- (22) Boronowski, B. *J. Membr. Sci.* **1991**, *57*, 119.
- (23) Juo, D.; Casas-Vazquez, J.; Lebon, G. *Rep. Prog. Phys.* **1988**, *51*, 1105.
- (24) Castello, L. F. del; Rodriguez, J. *Non-Equilib. Thermodyn.* **1989**, *14*, 127.
- (25) Rastogi, R. P. *J. Sci. Ind. Res.* **1969**, *28*, 284.
- (26) Srivastava, R. C.; Pal, Raj, J. *J. Sci. Ind. Res.* **1971**, *30*, 267.
- (27) Saxen, U. *Ann. Phys.* **1892**, *47*, 46.
- (28) Mazur, P.; Overbeek, J. Th. G. *Recl. Trav. Chim. Pays-Bas* **1951**, *70*, 83.
- (29) Rastogi, R. P.; Srivastava, R. C. *Physica* **1961**, *27*, 265.
- (30) Staverman, A. J. *Trans. Faraday Soc.* **1952**, *48*, 176.
- (31) Staverman, A. J.; Smit, J. A. M. *Thermodynamics of Irreversible Processes Membrane Theory: Osmosis Electrokinetics, Membrane Potentials*. In *Physical Chemistry enriching topics from Colloid and Surface Science*; Van Olphen, H., Mysels, K. J., Eds.; IUPAC commission 1.6 Colloid and Surface Chemistry, LaJolla, CA, 1975.
- (32) Skalak, R.; Chien, S., Eds.; *Handbook of Bioengineering*; McGraw Hill: New York, 1987.
- (33) Copenhaver, W. M.; Kelly, D. E.; Wood, R. L. *Bailey's Textbook of Histology*; Williams and Wilkins: Baltimore, MD, 1979.
- (34) Urelins, B.; Garele, G. *Acta Physiol. Scand.* **1980**, *110*, 257.
- (35) Kedem, O.; Katchalsky, A. *Trans. Faraday Soc.* **1963**, *59*, 1931.
- (36) Kedem, O.; Katchalsky, A. *Trans. Faraday Soc.* **1963**, *59*, 1941.
- (37) Kirkwood, J. G. *Ion Transport Across Membranes*; Academic Press: New York, 1954; p 119.
- (38) Oster, G.; Perelson, A.; Katchalsky, A. *Nature* **1971**, *234*, 393.
- (39) Oster, G.; Perelson, A.; Katchalsky, A. *Q. Rev. Biophys.* **1973**, *6*, 1.
- (40) Srivastava, R. C.; Chacko, P. V.; Srivastava, S.; Yadav, S. *J. Membr. Sci.* **1978**, *3*, 39.
- (41) Helmholtz, H. *Wied Ann. N.F.* **1879**, *1*, 339.
- (42) Gouy, G. *J. Phys.* **1910**, *9*, 457.
- (43) Chapman, D. L. *Philos. Mag.* **1913**, *25*, 475.
- (44) Stern, G. *Z. Electrochem.* **1924**, *30*, 508.
- (45) Overbeek, J. Th. G. *J. Colloid Sci.* **1953**, *8*, 420.
- (46) Sørensen, T. S.; Koefoed, J. *J. Chem. Soc., Faraday Trans. 2* **1974**, *70*, 665.
- (47) Debye, P.; Huckel, E. *Phys. Z.* **1923**, *28*, 185.
- (48) Dainty, J.; Croghan, P. C.; Fensom, D. S. *Can. J. Bot.* **1963**, *41*, 953.
- (49) Schmid, G. S. *Z. Electrochem.* **1950**, *54*, 424.
- (50) Schmid, G. S.; Schwarz, H. *Z. Electrochem.* **1952**, *56*, 35.
- (51) Schmid, G. S. *Z. Electrochem.* **1952**, *56*, 181.
- (52) Rastogi, R. P.; Singh, K.; Singh, S. N. *Indian J. Chem.* **1968**, *6*, 466.
- (53) Lakshminarayanaiah, N. *Chem. Rev.* **1965**, *65*, 539.
- (54) Solomon, A. K. *J. Gen. Physiol.* **1968**, *51*, 335.S.
- (55) Lakshminarayanaiah, N. *J. Phys. Chem.* **1969**, *73*, 4428.
- (56) Rastogi, R. P.; Singh, K.; Srivastava, M. L. *J. Phys. Chem.* **1969**, *73*, 46.
- (57) Overbeek, J. Th. G. *Colloid Science*; Kryut, H. R., Ed.; Elsevier: Amsterdam, 1952; Vol. I, p 224.
- (58) Vink Hans. *J. Chem. Soc., Faraday Trans. 1* **1982**, *78*, 3115.
- (59) Vink Hans. *J. Chem. Soc., Faraday Trans. 1* **1983**, *79*, 2355, 2359.
- (60) Lamm, O. *Ark. Kemi. Mineral. Geol.* **1944**, *18A*, no. 2.
- (61) Lamm, O. *Adv. Chem. Phys.* **1964**, *6*, 291.
- (62) Spiegler, K. S. *Trans. Faraday Soc.* **1958**, *54*, 1408.
- (63) Kedem, O.; Katchalsky, A. *J. Gen. Physiol.* **1961**, *45*, 143.
- (64) Vink Hans. *J. Chem. Soc., Faraday Trans. 1* **1988**, *84*, 133.
- (65) Haase, R. *Z. Phys. Chem. N.F.* **1976**, *103*, 235.
- (66) Blokhra, R. L.; Parmar, M. L.; Agarwal, S. K. *J. Electroanal. Chem.* **1978**, *89*, 417.
- (67) Blokhra, R. L.; Kumar, S.; Kumar, R.; Upadhyay, N. *J. Chem. Eng. Data* **1988**, *33*, 347.
- (68) Kumar, R.; Singh, K. *Indian J. Chem.* **1980**, *19A*, 511.
- (69) Singh, K.; Srivastava, V. N. *Indian J. Chem.* **1979**, *18A*, 395.
- (70) Tasaka, M.; Miyahara, N. *Maku (Membrane)* **1988**, *14*, 71.
- (71) Tasaka, M.; Sekiguchi, O.; Urahama, M.; Matsubara, T.; Kiyon, R.; Suski, S. *J. Membr. Sci.* **1990**, *48*, 91.
- (72) (a) Sekiguchi, O.; Kiyono, R.; Matsubara, T.; Tasaka, M. *J. Membr. Sci.* **1990**, *48*, 309. (b) See also: *J. Membr. Sci.* **1991**, *58*, 59.
- (73) Brun, T. S.; Vaula, D. *Ber. Bunsen-Ges. Phys. Chem.* **1967**, *71*, 825.
- (74) Reynard, J. M.; Larchet, C.; Bulvestre, G.; Anclair, B. *J. Membr. Sci.* **1992**, *67*, 57.
- (75) Ibanez, J. A.; Forte, J.; Harnandez, A.; Tejerina, F. *J. Membr. Sci.* **1988**, *36*, 45.
- (76) Oda, Y.; Yawataya, T. *Bull. Chem. Soc. Jpn.* **1955**, *28*, 263.
- (77) Brydges, T. G.; Lorimer, J. W. *J. Membr. Sci.* **1983**, *13*, 291.
- (78) Bary, P. H.; Hope, A. B. *Biophys. J.* **1969**, *9*, 700, 729.
- (79) Osterle, J. F. *Electrokinetic Energy Conversion*. Paper presented at the Winter Annual Meeting of the American Society of Mechanical Engineers, Philadelphia, Nov. 17-22, 1963; paper no. 63-WA-68 Applied Mechanics Division.
- (80) Osterle, J. F. *J. Appl. Mech.* **1964**, *31*, 161.
- (81) Morrison, F. A.; Osterle, J. F. *J. Chem. Phys.* **1965**, *43*, 2111.
- (82) Osterle, J. F. *J. Appl. Sci. Res.* **1964**, *12A*, 425.
- (83) Kedem, O.; Caplan, S. R. *Trans. Faraday Soc.* **1965**, *61*, 1897.
- (84) Paterson, R. In *Membrane and Ion Transport*; Bittar, E. D., Ed.; John Wiley & Sons: New York, 1970; Vol. I, p 123-164.
- (85) Srivastava, R. C.; Jain, A. K. *J. Polym. Sci. (Polymer Physics Edition)* **1975**, *13*, 1603.
- (86) Srivastava, R. C.; Jain, A. K. *J. Hydrol.* **1975**, *25*, 339.
- (87) Gross, R. J.; Osterle, J. F. *J. Chem. Phys.* **1968**, *49*, 176.
- (88) Staverman, A. J. *Trans. Faraday Soc.* **1952**, *48*, 176.
- (89) Schlögl, R. *Material Transport through Membranes*. Dr Dietrich Steinkopff Verlag, Darmstadt, Germany, 1964.
- (90) Osterle, J. F. *Membranes as Energy Converters. Proc. Symp. Eng. Signif. Biol. Sci.*, Carnegie Institute of Technology, Pittsburgh, PA, 25-27 Jan 1967; San Francisco Press: San Francisco, CA, 1967.
- (91) Dresner, L. *J. Phys. Chem.* **1963**, *67*, 1635.
- (92) Martinez, L.; Gigoso, M. A.; Hernandez, A.; Terneja, F. *J. Membr. Sci.* **1987**, *35*, 1.
- (93) Fair, J. C.; Osterle, J. F. *J. Chem. Phys.* **1971**, *54*, 3307.
- (94) Koh, W. H.; Silverman, P. J. *J. Membr. Sci.* **1983**, *13*, 279.
- (95) Narebska, A.; Koter, S. *J. Membr. Sci.* **1987**, *30*, 141.
- (96) Srivastava, M. L.; Rastogi, S. C. *Indian J. Technol.* **1971**, *9*, 70.
- (97) Phillips, R. W.; Mastrangelo, S. V. R. *J. Appl. Phys.* **1972**, *43*, 387.
- (98) Miller, D. G. *Chem. Rev.* **1960**, *60*, 15.
- (99) Hanley, H. J. M. *Transport Phenomena in Fluids*; Marcel Dekker: New York, 1969; Chapter 11.
- (100) Dubois, R.; Roberts, A. H. *J. Phys. Chem.* **1936**, *40*, 543.
- (101) Lorenz, P. B. *J. Phys. Chem.* **1953**, *57*, 430.
- (102) Cooke, C. E., Jr. *J. Chem. Phys.* **1955**, *23*, 2299.
- (103) Bull, H. B. *J. Phys. Chem.* **1933**, *39*, 577.
- (104) Rutgers, A. J.; desMet, M. *Trans. Faraday Soc.* **1952**, *48*, 635.
- (105) Rastogi, R. P.; Jha, K. M. *J. Phys. Chem.* **1966**, *70*, 1017.
- (106) Blokhra, R. L.; Kaul, C. L. *Electrochim. Acta* **1966**, *11*, 1391.
- (107) Blokhra, R. L.; Kaul, C. L.; Soni, B. R.; Jalota, S. K. *Electrochim. Acta* **1967**, *12*, 773.
- (108) Blokhra, R. L.; Parmar, M. L.; Sharma, V. P. *Colloid and Interface Science*; Karker, M., Ed.; Academic Press: New York, 1976; Vol. IV (Hydrosols and Rheology), pp 259-279.
- (109) Blokhra, R. L.; Singhal, T. C. *J. Electroanal. Chem.* **1973**, *48*, 353.
- (110) Blokhra, R. L.; Singhal, T. C. *J. Electroanal. Chem.* **1974**, *57*, 19.
- (111) Blokhra, R. L.; Singhal, T. C. *Indian J. Chem.* **1975**, *13*, 913.
- (112) Blokhra, R. L.; Singhal, T. C. *J. Phys. Chem.* **1974**, *78*, 2302.
- (113) Blokhra, R. L.; Parmar, M. L. *Indian J. Chem.* **1977**, *15A*, 384.
- (114) Blokhra, R. L.; Agarwal, S. K.; Arora, N. J. *Colloid Interface Sci.* **1980**, *73*, 88.
- (115) Blokhra, R. L.; Kohli, S. J. *Non-equilib. Thermodyn.* **1981**, *6*, 311.
- (116) Blokhra, R. L.; Thakur, S. S. *J. Non-equilib. Thermodyn.* **1982**, *7*, 145.
- (117) Blokhra, R. L.; Parmar, M. L.; Chauhan, S. C. *J. Membr. Sci.* **1983**, *14*, 67.
- (118) Blokhra, R. L.; Parmar, M. L.; Thakur, S. S. *J. Membr. Sci.* **1984**, *21*, 123.
- (119) Blokhra, R. L.; Kumar, S. *J. Membr. Sci.* **1989**, *43*, 31.
- (120) See ref 67.
- (121) Glansdorff, P.; Prigogine, I. *Physica* **1954**, *20*, 773.
- (122) Haase, R. *Z. Phys. Chem. N.F.* **1976**, *103*, 247.
- (123) Manjikian, S. *Ind. Eng. Chem. Proc. Res. Dev.* **1967**, *6*, 23.
- (124) Helmcke, J. G. *Kolloid Z.* **1954**, *135*, 29.
- (125) Hansen, B. M.; Sørensen, T. S.; Jensen, J. B.; Henenberg, M. *J. Colloid Interface Sci.* **1989**, *130*, 359.
- (126) Sørensen, T. S.; Jensen, J. B.; Hansen, B. M. *Desalination* **1991**, *80*, 293.
- (127) Srivastava, R. C.; Mehta, A. J. *Non-equilib. Thermodyn.* **1980**, *5*, 255.
- (128) Benavente, J.; Fernandez-Pineda, C. *J. Membr. Sci.* **1985**, *23*, 121.
- (129) Haase, R.; Horff, K. *J. Membr. Sci.* **1983**, *22*, 279.
- (130) Fernandez-Pineda, C.; Mengual, J. J. *Colloid Interface Sci.* **1977**, *61*, 102.
- (131) Aizawa, M.; Tomono, S.; Suzuki, S. *J. Membr. Sci.* **1980**, *6*, 235.

- (132) Srivastava, R. C.; Abraham, M. G. *J. Colloid Interface Sci.* 1976, 57, 58.
- (133) Srivastava, R. C.; Abraham, M. G. *J. Chem. Soc., Faraday Trans. 1* 1976, 72, 2631.
- (134) Srivastava, R. C.; Abraham, M. G.; Jain, A. K. *J. Phys. Chem.* 1977, 81, 906.
- (135) Vinogradov, S. N.; Linnel, R. H. *Hydrogen Bonding*; Van-Nostrand Reinhold: London, 1971; p 277.
- (136) Hasted, J. B. In *Water—A Comprehensive Treatise*; Franks, F., Ed.; Plenum Press: New York, 1973; Vol. 2, pp 205–458.
- (137) Singh, K.; Shabad, R. *Indian J. Chem.* 1979, 17A, 283.
- (138) Jain, A. K.; Tewari, R. K. *J. Colloid Interface Sci.* 1979, 72, 358.
- (139) Singh, K.; Shabad, R.; Kumar, R.; Pande, M. M. *Indian J. Chem.* 1980, 19A, 1062.
- (140) Knozinger, H. In *The Hydrogen Bond: III Dynamics Thermodynamics and special System*; Schuster, P.; Zundel, G.; Sandorfy, C., Eds.; North Holland: Amsterdam, 1976; p 1329.
- (141) Sourirajan, S.; Matsura, T. *Reverse Osmosis—Process and Principles*, National Research Council of Canada, Ottawa, 1985.
- (142) Johnson, J. S.; Dreoner, L.; Kraus, K. A. *Hyperfiltration (Reverse Osmosis)*. In *Principles of Desalination*; Spiegler, K. S., Ed.; Academic Press: New York, 1966; Chapter 8.
- (143) McKelvey, J. G.; Spiegler, K. S.; Wyllie, M. R. *J. Chem. Eng. Progr. Symp. Ser.* 1959, 55, 199.
- (144) Tanny, G.; Hoffer, E.; Kedem, O. *Experientia Suppl.* 1971, 18, 619.
- (145) Tanny, G.; Kedem, O. *J. Colloid Interface Sci.* 1975, 51, 177.
- (146) Tanny, G.; Hoffer, E. *J. Colloid Interface Sci.* 1973, 44, 21.
- (147) Merten, U., Ed. *Reverse Osmosis*; Addison Wesley: Reading, MA, 1966.
- (148) Spiegler, K. S.; Kedem, O. *Desalination* 1966, 1, 311.
- (149) Hoffer, E.; Kedem, O. *Desalination* 1967, 2, 125.
- (150) Tanny, G. *Nature* 1973, 242, 474.
- (151) Drost-Hansen, W. *Chemistry of the Cell Interface, Part B*; Brown, H. D., Ed.; Academic Press: New York, 1971; Chapter VI.
- (152) Winterkorn, H. F. In *Water and its Conduction in Soils*. Intern. Symp. Highway Res. Board Spl. Report 40, 1958; Highway Research Board: Washington, DC, 1960; pp 324–338.
- (153) Taylor, S. A.; Cary, J. W. *Trans. Int. Congr. Soil Sci.* 1960, 7, 80–90 (Madison, WI; Aug 14–24, 1960).
- (154) Russel, M. B. *Soil Sci. Soc. Am. Proc.* 1960, 24, 439.
- (155) Philip, J. R. *Soil Sci.* 1960, 89, 132.
- (156) Ravina, I.; Zaslavsky, D. *Soil Sci.* 1968, 106, 60.
- (157) Srivastava, R. C.; Abrol, I. P. *Trans. Int. Congr. Soil Sci.* 1968, 9, 253–262 (Adelaide).
- (158) Groenevelt, P. H.; Bolt, G. H. *J. Hydrol.* 1969, 7, 358.
- (159) Srivastava, R. C.; Pal, Raj J. *Sci. Ind. Res.* 1971, 30, 267.
- (160) Groenevelt, P. H.; Bolt, G. H. In *Ecological Studies—Analysis and Synthesis*; Hadas, A., Ed.; Springer-Verlag: Berlin, 1973; Vol. 4, pp 43–48.
- (161) Srivastava, R. C.; Pal, Raj *Non-equilibrium Thermodynamics in Soil Physics*; Oxford and IBH: New Delhi, 1973.
- (162) Michaels, A. S.; Lin, C. S. *Ind. Eng. Chem.* 1954, 47, 1249.
- (163) Winterkorn, H. F. *Am. Soc. Testing Materials. Spec. Tech. Publ.* 1955, 163, 27.
- (164) Swartzendruber, D. *Adv. Agron.* 1966, 18, 327.
- (165) Bolt, G. H.; Groenevelt, P. H. *Bull. Intern. Assoc. Scient. Hydrol.* 1969, 14, 17.
- (166) Gairon, S.; Swartzendruber, D. In *Ecological Studies—Analysis and Synthesis*; Hadas, A., Ed.; Springer-Verlag: Berlin, 1973; Vol. 4, pp 141–151.
- (167) Kemper, W. D.; Shainberg, I.; Quirk, J. P. *Soil Sci. Soc. Am. Proc.* 1972, 36, 229.
- (168) Gairon, S.; Swartzendruber, D. *Soil Sci. Soc. Am. Proc.* 1975, 39, 811.
- (169) Olsen, H. W. *Soil Sci. Soc. Am. Proc.* 1969, 33, 338.
- (170) Srivastava, R. C.; Abraham, M. G. *J. Non-Equilib. Thermodyn.* 1979, 4, 107.
- (171) Tien, H. T. *Bilayer Lipid Membranes—Theory and Practice*; Marcel Dekker: New York, 1974.
- (172) Jain, M. K. *The Bimolecular Lipid Membranes A System*; Van Nostrand Reinhold Company: New York, 1972.
- (173) Ting, H. P.; Tien, H. T. *Light Induced Water Permeation Through BLM*. In *First Cell Biology—Biophysics Mid-West Meeting*, Chicago, IL. March 14–15, 1969.
- (174) Srivastava, R. C.; Jakhari, R. P. S. *J. Phys. Chem.* 1981, 85, 1457.
- (175) Srivastava, R. C.; Jakhari, R. P. S. *J. Phys. Chem.* 1982, 86, 1441.
- (176) Srivastava, R. C.; Tandon, A.; Sharma, R. K.; Bhise, S. B. *J. Colloid Interface Sci.* 1983, 93, 568.
- (177) Srivastava, R. C.; Tandon, A.; Sharma, R. K.; Bhise, S. B. *J. Colloid Interface Sci.* 1984, 99, 71.
- (178) Srivastava, R. C.; Sharma, R. K.; Tandon, A.; Bhise, S. B. *J. Colloid Interface Sci.* 1985, 108, 249.
- (179) Srivastava, R. C.; Tandon, A.; Kurup, S.; Bhise, S. B.; Sharma, R. K. *J. Electroanal. Chem.* 1985, 187, 325.
- (180) Srivastava, R. C.; Tandon, A.; Sharma, R. K.; Bhise, S. B.; Madamwar, D. B. *Indian J. Chem.* 1985, 24A, 918.
- (181) Tandon, A.; Nagappa, A. N.; Srivastava, R. C. *Int. J. Pharm.* 1986, 32, 39.
- (182) Srivastava, R. C.; Tandon, A. *Biotech. Bioeng.* 1988, 31, 511.
- (183) Vyas, V. V.; Nagrath, R.; Srivastava, R. C. *J. Colloid Interface Sci.* 1989, 130, 311.
- (184) Srivastava, R. C. In *Surfactants in Solution*; Mittal, K. L., Ed.; Plenum Press: New York, 1989; Vol. 8, pp 179–194.
- (185) Singh, V.; Raju, D. B.; Ravindran, C.; Srivastava, R. C. *J. Colloid Interface Sci.* 1990, 139, 337.
- (186) Srivastava, R. C. In *Trends in Bioenergetics and Biotechnological Processes*; Singhal, G. S.; Rama Sarma, T., Eds.; Today and Tomorrow's Publishers: New Delhi, 1991; pp 211–240.
- (187) Kesting, R. E.; Vincent, A.; Ebarlin, J. *Office of Saline Water, Research and Development*, Aug 1964, No. 117, Aug 1964.
- (188) Kesting, R. E. *Reverse Osmosis Process Using Surfactants Feed Additions*, OSW Patent Applications, SAL-830, Nov 3, 1965.
- (189) Kesting, R. E.; Subcasky, J. W.; Paton, J. D. *J. Colloid Interface Sci.* 1968, 28, 156.
- (190) Srivastava, R. C.; Yadav, S. J. *J. Colloid Interface Sci.* 1979, 69, 280.
- (191) Sherwood, T. K.; Brian, P. L. T.; Fisher, R. E. *Ind. Eng. Chem. Fundam.* 1967, 6, 2.
- (192) Harris, F. L.; Humphreys, G. B.; Spiegler, K. S. In *Membrane Separation Processes*; Meares, P., Ed.; Elsevier: Amsterdam, 1976.
- (193) Jain, A. K.; Tewari, R. K.; Srivastava, R. K. *J. Membr. Sci.* 1987, 31, 195.
- (194) Jain, A. K.; Srivastava, R. K. *J. Membr. Sci.* 1990, 51, 337.
- (195) Gershfield, N. L. In *Methods in Membrane Biology*; Korn, E. D., Ed.; Plenum Press: New York, 1974; Vol. I, Chapter 20.
- (196) Gershfield, N. L.; Pagano, R. E. *J. Phys. Chem.* 1972, 76, 1244.
- (197) Haberland, M. E.; Reynolds, J. A. *Proc. Natl. Acad. Sci. U.S.A.* 1973, 70, 2313.
- (198) Jain, M. K. *Curr. Top. Membr. Transp.* 1975, 6, 1.
- (199) Katchalsky, A.; Kedem, O. *Biophys. J.* 1962, 2, 53.
- (200) Singh, K.; Tiwari, A. K. *J. Colloid Interface Sci.* 1987, 116, 42.
- (201) Singh, K.; Tiwari, A. K. *J. Membr. Sci.* 1987, 34, 155.
- (202) Singh, K.; Tiwari, A. K. *Indian J. Chem.* 1988, 27A, 565.
- (203) Rizvi, S. A.; Zaidi, S. B. *J. Colloid Interface Sci.* 1984, 97, 536.
- (204) Rizvi, S. A.; Zaidi, S. B. *Z. Phys. Chem.* 1983, 136, 163.
- (205) Rizvi, S. A.; Zaidi, S. B. *J. Non-Equilib. Thermodyn.* 1984, 9, 245.
- (206) Rizvi, S. A.; Zaidi, S. B. *J. Membr. Sci.* 1986, 29, 259.
- (207) Rastogi, R. P.; Shabad, R.; Upadhyay, B. M.; Singh, S. B.; Pandey, P. C. *J. Membr. Sci.* 1984, 19, 51.
- (208) Stocking, C. R.; Franceschi, V. R. *Am. J. Bot.* 1981, 68, 1008.
- (209) Elbaum, D.; Harrington, J.; Nagel, R. L. *Prog. Clin. Biol. Res.* 1975, 1, 311.
- (210) Nelson, R. C. *J. Chem. Phys.* 1963, 39, 112.
- (211) OKamoto, Y.; Brenner, W. *Organic Semiconductors*; Reinhold/Chapman and Hall: London, 1964; p 160.
- (212) Tien, H. T.; Karvaly, B. In *Solar Power and Fuels*; Bolton, J. R., Ed.; Academic Press: New York, 1977; Chapter 7.
- (213) Tien, H. T.; Chen, V. K. In *Progress in Surface and Membrane Science*; Cadenhead, D. A.; Danielli, J. F.; Rosenberg, M. D., Eds.; Academic Press: New York, 1974; Vol. 8, pp 119–157.
- (214) Marks, G. S. *Heme and Chlorophyll*; Van Nostrand: London, 1969; pp 94–98.
- (215) Remington, C. *Biochem. J.* 1960, 75, 622.
- (216) Fensom, D. S. *Can. J. Bot.* 1957, 35, 573.
- (217) Fensom, D. S. *Can. J. Bot.* 1958, 36, 367.
- (218) Fensom, D. S. *Can. J. Bot.* 1959, 37, 1003.
- (219) Spanner, D. C. *J. Exp. Bot.* 1958, 9, 332.
- (220) Spanner, D. C. *Encyclopedia of Plant Physiology*; Springer-Verlag: Berlin, 1975; Vol. I, pp 301–327.
- (221) Fensom, D. S.; Dainty, J. *Can. J. Bot.* 1963, 41, 685.
- (222) Dainty, J.; Croghan, P. C.; Fensom, D. S. *Can. J. Bot.* 1963, 41, 953.
- (223) Fensom, D. S.; Meylan, S.; Pilet, P.-E. *Can. J. Bot.* 1965, 43, 453.
- (224) Pilet, P. E.; Meylan, S. *Bull. Soc. Bot. Suisse* 1953, 63, 43.
- (225) Scott, B. L.; McAuley, A. L.; Jeyes, P. *Aust. J. Biol. Sci.* 1955, 8, 36.
- (226) Fensom, D. S.; Wanless, I. R. *J. Exp. Bot.* 1967, 18, 563.
- (227) Ursino, D. J.; Fensom, D. S. *Can. J. Bot.* 1970, 48, 1289.
- (228) Tyree, M. T.; Fensom, D. S. *J. Exp. Bot.* 1970, 21, 304.
- (229) Spanner, D. C. *J. Exp. Bot.* 1970, 21, 325.
- (230) Tyree, M. T.; Spanner, D. C. *Can. J. Bot.* 1969, 47, 1493.
- (231) Spanner, D. C. *Plant Cell Environ.* 1978, 1, 7.
- (232) Spanner, D. C. *Ann. Bot.* 1978, 42, 485.
- (233) Fensom, D. S. *Can. J. Bot.* 1972, 50, 479.
- (234) Wanless, I. R.; Bryniak, N.; Fensom, D. S. *Can. J. Bot.* 1973, 51, 1055.
- (235) Williams, E. J.; Munro, C.; Fensom, D. S. *Can. J. Bot.* 1972, 50, 2255.
- (236) Fensom, D. S.; Williams, E. J. *Nature* 1974, 250, 490.
- (237) Stallworthy, W. B.; Fensom, D. S. *Can. J. Physiol. Pharmacol.* 1966, 44, 866.
- (238) Wedner, H. J.; Diamond, J. M. *J. Membr. Biol.* 1969, 1, 92.
- (239) Hill, A. E. *Proc. R. Soc. London, Ser. B* 1975, 190, 99, 115.
- (240) Miyamoto, M.; Nakahari, T.; Yoshida, H.; Imai, Y. *Membrane* 1987, 12, 223.
- (241) Imai, Y.; Miyamoto, M.; Nakahari, T.; Murakami, M.; Yoshida, H. *Jpn. J. Physiol.* 1986, 36, 397.
- (242) Imai, Y.; Miyamoto, M.; Nakahari, T.; Tanaka, H.; Soma, Y. *Biomed. Res. Suppl.* 1986, 2, 213.
- (243) Miyamoto, M.; Nakahari, T.; Yoshida, H.; Imai, Y. *J. Membr. Sci.* 1989, 41, 377.

- (244) Gustin, M. C. *Science* **1991**, *253*, 100.
- (245) Langer, R. *Science* **1990**, *249*, 1527.
- (246) Pikal, M. J.; Shah, S. *Pharm. Res.* **1990**, *7*, 213.
- (247) Pikal, M. J.; Shah, S. *Pharm. Res.* **1990**, *7*, 222.
- (248) Green, P. G.; Hinz, R. S.; Cullander, C.; Yamne, G.; Guy, R. H. *Pharm. Res.* **1991**, *8*, 1113.
- (249) Green, P. G.; Hinz, R. S.; Kim, A.; Szoka, F. C.; Guy, R. H. *Pharm. Res.* **1991**, *8*, 1121.
- (250) Kasting, G. B.; Merritt Keister, J. C. *J. Membr. Sci.* **1988**, *35*, 137.
- (251) Gangarosa, L.; Park, N.; Wiggins, C.; Hill, J. J. *Pharmacol. Exp. Ther.* **1980**, *212*, 377.
- (252) Burnette, R.; Marrero, D. *J. Pharm. Sci.* **1986**, *75*, 738.
- (253) Burnette, R.; Ongpipattanakul, B. *J. Pharm. Sci.* **1987**, *76*, 765.
- (254) Rastogi, R. P.; Misra, B. M. *Trans. Faraday Soc.* **1967**, *63*, 584.
- (255) Rastogi, R. P.; Misra, B. M. *Trans. Faraday Soc.* **1967**, *63*, 2926.
- (256) Rastogi, R. P.; Singh, K.; Misra, B. M. *Desalination* **1967**, *3*, 32.
- (257) deGroot, S. R.; Overbeek, J. Th. G.; Mazur, P. *J. Chem. Phys.* **1952**, *20*, 1825.
- (258) Krut, H. R. *Colloid Science*; Elsevier: Amsterdam, 1952; Vol. I, pp 207-221.
- (259) Li, J. C. M. *J. Appl. Phys.* **1962**, *33*, 616.
- (260) Rastogi, R. P.; Singh, K. *Trans. Faraday Soc.* **1967**, *63*, 2917.
- (261) Rastogi, R. P.; Jha, K. M. *Trans. Faraday Soc.* **1966**, *62*, 585.
- (262) Rastogi, R. P.; Singh, K.; Singh, S. N. *J. Phys. Chem.* **1969**, *73*, 1593.
- (263) Rastogi, R. P.; Shabad, R.; Upadhyay, B. M.; Khan, S. A. *J. Non-equilib. Thermodyn.* **1981**, *6*, 273.
- (264) Shukla, P. C.; Misra, G. *Langmuir* **1992**, *8*, 1149.
- (265) Rastogi, R. P.; Srivastava, M. I.; Singh, S. N. *J. Phys. Chem.* **1970**, *74*, 2960.
- (266) Curie, P. *Oeuvres, Gauthier-Villars* **1908**, 129.
- (267) Golding, B. *Polymers and Resins*; Van Nostrand-Reinhold: Princeton, NJ, 1959; p 355.
- (268) Zachariassen, W. H. *J. Chem. Phys.* **1935**, *3*, 162.
- (269) Lakshminarayanaiah, N. *J. Phys. Chem.* **1970**, *74*, 2385.
- (270) Lakshminarayanaiah, N.; Subrahmanyam, V. *J. Phys. Chem.* **1968**, *72*, 1253.
- (271) Tombalakian, A. S.; Barton, H. J.; Graydon, W. F. *J. Phys. Chem.* **1974**, *78*, 65.
- (272) Rastogi, R. P.; Singh, K.; Singh, J. J. *J. Phys. Chem.* **1975**, *79*, 2574.
- (273) Hadermann, A. F.; Waters, P. F.; Woo, J. W. *J. Phys. Chem.* **1974**, *78*, 65.
- (274) Harned, H. S.; Owen, B. B. *The Physical Chemistry of Electrolyte Solutions*; Reinhold: New York, 1958; p 216.
- (275) Onsager, L. *J. Chem. Phys.* **1934**, *2*, 599.
- (276) Singh, K.; Singh, J. *Colloid Polym. Sci.* **1977**, *255*, 379.
- (277) Roberts, J. D.; Caserio, M. C. *Modern Organic Chemistry*; W. A. Benjamin: New York, 1967; p 384.
- (278) Rastogi, R. P.; Singh, K.; Kumar, R.; Khan, S. A. *J. Phys. Chem.* **1977**, *81*, 2114.
- (279) Rastogi, R. P.; Shabad, R. *J. Phys. Chem.* **1977**, *81*, 1953.
- (280) Bockris, J. O'M.; Parsons, R. *Trans. Faraday Soc.* **1949**, *45*, 916.
- (281) Bockris, J. O'M.; Reddy, A. K. N. *Modern Electrochemistry*; Plenum Press: New York, 1970; Part II, pp 781-788.
- (282) Halliday, D.; Resnick, R. *Physics*; Wiley: New York, 1966; Part II, International Edition, p 719.
- (283) Chandler, D. *Introduction to Modern Statistical Mechanics*; Oxford University Press: New York, 1987; Chapter V, pp 119-154.
- (284) Rastogi, R. P.; Singh, K.; Kumar, R.; Shabad, R. *J. Membr. Sci.* **1977**, *2*, 317.
- (285) Singh, K.; Kumar, R. *Indian J. Chem.* **1979**, *17A*, 539.
- (286) Kumar, R. *J. Membr. Sci.* **1979**, *5*, 51.
- (287) Kumar, R. *Colloid Polym. Sci.* **1979**, *257*, 550.
- (288) Singh, K.; Kumar, R. *Indian J. Chem.* **1979**, *18A*, 10.
- (289) Kumar, R. *J. Non-equilib. Thermodyn.* **1980**, *5*, 259.
- (290) Singh, K.; Srivastava, V. N. *J. Non-equilib. Thermodyn.* **1981**, *6*, 195.
- (291) Rastogi, R. P.; Shabad, R. *Indian J. Chem.* **1982**, *21A*, 859.
- (292) Lorimer, J. W. *J. Membr. Sci.* **1983**, *14*, 275.
- (293) Lorimer, J. W. *J. Membr. Sci.* **1985**, *25*, 181.
- (294) Lorimer, J. W. *J. Membr. Sci.* **1985**, *25*, 211.
- (295) Bataille, J.; Kestin, J. *J. Non-equilib. Thermodyn.* **1979**, *4*, 229.
- (296) Nonnenmacher, T. F. *J. Non-equilib. Thermodyn.* **1980**, *5*, 361.
- (297) Perez-Garcia, G.; Jou, C. *J. Non-equilib. Thermodyn.* **1982**, *7*, 191.
- (298) Irmay, S. *Trans. Am. Geophys. Union* **1958**, *39*, 702.
- (299) Hubbert, M. K. *Trans. Amer. Inst. Min. Metall. Pet. Eng.* **1956**, *207*, 222.
- (300) Zaslavsky, D.; Ravina, I. In *Moisture Equilibria and Moisture Changes in Soils Beneath Covered Areas*; Aitchison, G. D. A., Ed.; Butterworths: London, 1965; p 55.
- (301) Olphen, H. V. *Clay Colloid Chemistry*; Interscience: New York, 1963; p 188.
- (302) Zaslavsky, D.; Ravina, I. *Soil Sci.* **1968**, *107*, 1.
- (303) Ravina, I.; Zaslavsky, D. *Soil Sci.* **1968**, *106*, 94.
- (304) Srivastava, R. C.; Avasthi, P. K. *Kolloid Z. U. Z. Polym.* **1972**, *250*, 353.
- (305) Kemper, W. D. *Soil Sci. Soc. Am. Proc.* **1960**, *24*, 10.
- (306) Musket, M. *The Flow of Homogeneous Fluids Through Porous Media*; J. W. Edwards, Inc.: Ann Arbor, MI, 1946.
- (307) Swartzendruber, D. *Soil Sci.* **1962**, *93*, 22.
- (308) Rastogi, R. P.; Shabad, R.; Upadhyay, B. M. *J. Colloid Interface Sci.* **1981**, *83*, 41.
- (309) Rastogi, R. P.; Singh, K.; Shabad, R.; Upadhyay, B. M. *J. Colloid Interface Sci.* **1981**, *80*, 402.
- (310) Shukla, P. C.; Misra, G. *J. Membr. Sci.* **1986**, *26*, 277.
- (311) Shukla, P. C.; Misra, G. *J. Membr. Sci.* **1987**, *31*, 157.
- (312) Shukla, P. C.; Misra, G. *Indian J. Biochem. Biophys.* **1987**, *24*, 287.
- (313) Shukla, P. C.; Misra, G.; Misra, J. P. *J. Colloid Interface Sci.* **1989**, *129*, 53.
- (314) Shukla, P. C.; Misra, G.; Misra, J. P. *Biophys. Chem.* **1989**, *33*, 31.
- (315) Guyton, A. C. *Text Book of Medical Physiology*; W. B. Saunders: Philadelphia, PA, 1981; p 226; p 473.
- (316) Rastogi, R. P.; Shabad, R. *J. Chem. Educ.* **1983**, *60*, 540.
- (317) Larter, R. *Chem. Rev.* **1990**, *90*, 355.
- (318) Meares, P.; Page, K. R. *Philos. Trans. R. Soc. London* **1972**, *A272*, 1.
- (319) Meares, P.; Page, K. R. *Proc. R. Soc. London* **1974**, *A339*, 513.
- (320) Kobatake, Y. *Physica* **1970**, *48*, 301.
- (321) Franck, U. F. *Electrochemistry* **1963**, *67*, 657.
- (322) Rastogi, R. P.; Srivastava, R. C.; Singh, A. R.; Misra, A. P.; Pandey, P. C. Manuscript in preparation.
- (323) Prigogine, I. In *Non-equilibrium Thermodynamics—Variational Techniques and Stability*; Donnelly, R. J., Herman, R., Prigogine, I., Eds.; University of Chicago Press: Chicago, 1965; p 3.
- (324) Glansdorff, P. *Mol. Phys.* **1960**, *3*, 277.
- (325) Glansdorff, P.; Prigogine, I.; Hays, D. *Phys. Fluids* **1962**, *5*, 144.
- (326) Glansdorff, P.; Prigogine, I. *Physica* **1964**, *30*, 351.
- (327) Siddiqui, F. A.; Tien, H. T. *Electrochemistry of Bilayer Lipid Membranes*. In *Topics of Bioelectrochemistry and Bioenergetics*; Milazzo, G., Ed.; John Wiley and Sons: New York, 1983; Vol. 5, p 157.
- (328) Ehrenstein, G.; Lecar, H.; Nossal, R. *J. Gen. Physiol.* **1970**, *55*, 119.
- (329) Kushmir, L. D. *Biochim. Biophys. Acta* **1968**, *150*, 285.
- (330) Mueller, P.; Rudin, D. O.; Tien, H. T.; Wescott, W. C. *Nature* **1962**, *194*, 979.
- (331) Mueller, P.; Rudin, D. O. *J. Theor. Biol.* **1968**, *18*, 222.
- (332) Bean, R. C.; Shephert, W. C.; Eichner, J. T. In *The Role of Biogenic Amines and Physiological Membranes in Modern Drug Therapy*; Biel, J. H., Abood, L. G., Eds.; Marcel Dekker, Inc.: New York, 1971; p 124.
- (333) Latorre, R.; Ehrenstein, G.; Lecar, H. *J. Gen. Physiol.* **1972**, *70*, 72.
- (334) Ehrenstein, G.; Blumenthal, R.; Latorre, R. *J. Gen. Physiol.* **1974**, *63*, 707.
- (335) Robinson, R. L.; Strickholm, A. *Biochim. Biophys. Acta* **1978**, *509*, 9.
- (336) Hoffman, R. A.; Long, D. D.; Arndt, R. A.; Roper, L. D. *Biochim. Biophys. Acta* **1976**, *455*, 780.
- (337) Mueller, P.; Rudin, D. O. *Nature* **1965**, *217*, 713.
- (338) Gordon, L. G. M.; Haydon, D. A. *Biochim. Biophys. Acta* **1972**, *255*, 1014.
- (339) Mauro, A.; Nanavati, R. P.; Heyer, E. *Proc. Natl. Acad. Sci. U.S.A.* **1972**, *69*, 3742.
- (340) Pant, H. C.; Rosenberg, B. *Biochim. Biophys. Acta* **1971**, *225*, 379.
- (341) Monnier, A. M. *Comparative Biochemistry and Physiology of Transport*; North Holland: Amsterdam, 1974; p 205.
- (342) Monnier, A. M. *Adv. Chem. Phys.* **1975**, *29*, 341.
- (343) Monnier, A. M. *J. Membr. Sci.* **1977**, *2*, 49.
- (344) Monnier, A. M. *J. Membr. Sci.* **1977**, *2*, 67.
- (345) Botre, C.; Drost, W.; Marchetti, M.; Memoli, A.; Scarpelli, E. M. *Biochim. Biophys. Acta* **1970**, *219*, 283.
- (346) Shashoua, V. E. *Nature* **1967**, *215*, 846.
- (347) Shashoua, V. E. In *The Molecular Basis of Membrane Functions*; Josteson, D. E., Ed.; Prentice Hall: Englewood Cliffs: New Jersey, 1968; p 147.
- (348) Kamo, N.; Yoshioka, T.; Yoshida, M.; Sugita, T. *J. Membr. Biol.* **1973**, *12*, 193.
- (349) Yoshida, M.; Kamo, N.; Kobatake, Y. *J. Membr. Biol.* **1972**, *8*, 389.
- (350) Kobatake, Y.; Irimagiri, A.; Matsumoto, N. *Biophys. J.* **1970**, *10*, 728.
- (351) Yoshida, M.; Kobatake, Y.; Hashimoto, M.; Moitra, S. *J. Membr. Biol.* **1971**, *5*, 185.
- (352) Ishii, T.; Kuroda, Y.; Yoshikawa, K.; Sakabe, K.; Matsubara, Y.; Iriyama, K. *Biochem. Biophys. Res. Commun.* **1984**, *123*, 792.
- (353) Yoshida, T.; Ogura, S.; Okuyama, M. *Bull. Chem. Soc. Jpn.* **1975**, *48*, 2775.
- (354) Arisawa, J.; Furukawa, T. *J. Membr. Sci.* **1977**, *2*, 303.
- (355) Mathews, E. K.; O'Connor, M. D. L. *J. Exp. Biol.* **1979**, *81*, 75.
- (356) Rao, K. S.; Warmick, J. E.; Dally, J. W.; Albuquerque, E. X. *J. Pharm. Exp. Therap.* **1987**, *243*, 775.
- (357) Arisawa, J.; Misawa, K. *J. Membr. Sci.* **1987**, *32*, 223.
- (358) Arisawa, J.; Misawa, K. *J. Membr. Sci.* **1989**, *42*, 57.
- (359) Kim, J. T.; Larter, R. *J. Phys. Chem.* **1991**, *95*, 7948.
- (360) Teorell, T. *Biophys. J. Suppl.* **1962**, *2*, 27. See also: *Ark. Kemi* **1961**, *18*, 401.
- (361) Franck, U. F. *Ber. Bunsen-Ges. Phys. Chem.* **1967**, *71*, 789.
- (362) Forgacs, C. *Nature* **1961**, *190*, 339.
- (363) Aranow, R. H. *Proc. Natl. Acad. Sci. U.S.A.* **1963**, *50*, 1066.
- (364) Caplan, S. R.; Mikulecky, D. C. In *Ion Exchange*; Marnisky, J. A., Ed.; Marcel Dekker Inc.: New York, 1966; Vol. I, Chapter I.